POLSKA AKADEMIA NAUK
INSTYTUT FIZYKI

ACTA PHYSICA POLONICA

DWUMIESIĘCZNIK

Vol. XV — Fasc. 5

WARSZAWA 1956

First reprint by PWN — Polish Scientific Publishers 1969

MICROSTRUCTURE OF PHOTOCONDUCTIVE LEAD SULPHIDE LAYERS

By A. Feltynowski, I. Glass, T. Piwkowski and A. Toruń

Institute of Physics, Polish Academy of Science, Warsaw

(Received September 26, 1955)

The microstructure of PbS layers has been investigated by means of electron diffraction and electron microscopy. The PbS layers were obtained by evaporating in vacuo. The specimens to be examined were prepared by the method of formvar pseudo-replicas or directly by evaporation on thin films of formvar, collodion of aluminium. In general, the PbS layers consist of crystals 200—300 Å in size; an influence of the substratum on the size or shape of these crystals has not been observed. The diffraction patterns of layers deposited directly by evaporation correspond to a regular face-centred lattice of the NaCl type. The diffraction patterns of the pseudo-replicas show characteristic departures from this structure consisting of a decrease in the diameter of the 200 ring and an increase in the diameter of the 220 ring as compared with the diameters of the remaining rings.

We have investigated the structure of photoconductive PbS layers with the aid of an electron microscope and electron diffraction. These layers are formed in a hard glass envelope (Fig. 1) having the shape of a flat cylinder 35 mm in diameter and 15—20 mm high with two tungsten electrodes E sealed in glass. On one of the walls of the envelope are painted graphite electrodes which extend to the electrodes E. The envelope is connected with the vacuum plant by means of tube H. Photocells from which specimens for the microscope have been prepared were further provided with cylinders about 15 mm in diameter and 50 mm long, serving for introducing the specimen holders (Fig. 2). The formation process of a layer consists in two evaporations: first of lead tiosulphate, which is poured into the envelope through the tube H before the latter is connected to the vacuum plant, while the layer is condensed on wall B; the second by heating wall B with a burner, this layer is re-evaporated on wall A, which is intensely cooled with an air stream. In order to intensify the cooling of this wall, a piece of glass tube C is soldered to the envelope.

In the first series of experiments, the results of which were given in a previous work (Feltynowski *et al.* 1954), a polished glass plate 1 mm thick has been placed on the wall A, hiding half of this wall. When the photocell was made and its photoconduc-

tive properties controlled, the envelope was cut through and a 0.75% dioxan solution of formvar was poured over the plate covered with the PbS layer. The dioxan soon evaporated and the formvar film thus formed (about 100 Å thick) was detached from the glass with the help of a paper band coated with a layer of glue. The PbS layer was detached together with the formvar film, forming a so-called pseudo-replica. After being immersed in warm water, the formvar film with the PbS layer rose to the surface and was taken out on a specimen holder provided with a grid. The specimen thus prepared was examined by means of diffraction and with the aid of the microscope.

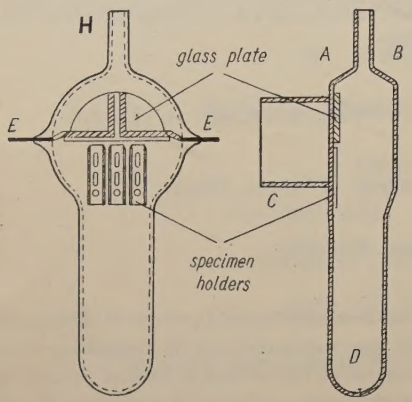

Fig. 1

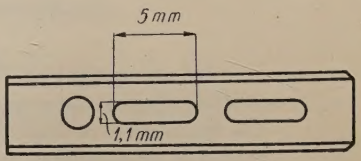

Fig. 2

PbS has a face-centred cubic structure, yet the electron diffraction pattern obtained by us (Phot. 1) shows deviations from this structure. On the basis of the data in Table 1, where the diameters of the rings, the intensity of the latter and the plane indices ascribed to them on the assumption of face-centred cubic structure are given, we find that these deviations consist in:

(1) the shifting of the ring 200 towards the middle by 5.8%,

(2) the shifting of the ring 220 outwards by 4%.

Moreover, there appear several additional rings with considerably fainter intensities, from which rings No. 3,7 and 15 could be ascribed to PbS, as their position corresponds better with the typical PbS structure. The remaining faint rings derive from admixtures. This experiment was repeated three times with three different photocells. The PbS pattern from the pseudo-replicas always showed the same characteristic deviations.

The specimens thus prepared were also examined under the microscope (Phot. 2, 3 and 4). It was found that in the layer there appear crystals which are not equally distributed, but tend to form clusters. Observations showed that the shapes and the sizes of these crystals were different for various photo-cells; for instance, in one (Phot. 2), the crystals were longitudinal, 900—3000 Å long and 250—1000 Å wide, in another (Phot. 3 and 4), however, they were considerably smaller (ca 400 Å) and tended to form chains (Phot. 3).

In the second series of experiments the layer was re-evaporated directly on specimen holders placed instead of the glass plate, and introduced there only after the first evaporation. The films on the specimen holders were of different kinds:

TABLE 1

No	D mm	Intensity	Plane indices $h\ k\ l$	$A = \frac{D}{\sqrt{h^2+k^2+l^2}}$
1	8.50	very strong	1 1 1	4.91
2	9.23	very strong	2 0 0	4.62
3	9.83	faint	(2 0 0)	(4.92)
4	10.67	faint		
5	11.21	faint		
6	12.25	faint		
7	13.39	faint	(2 2 0)	(4.74)
8	14.40	very strong	2 2 0	5.10
9	14.89	very faint		
10	16.37	strong	3 1 1	4.94
11	16.38	very faint		
12	17.20	medium	2 2 2	4.97
13	17.94	very faint		
14	18.63	faint	4 0 0	4.66
15	19.55	very faint	(4 0 0)	(4.89)
16	19.97	very faint		
17	21.38	strong	3 3 1	4.90
18	21.76	medium	4 2 0	4.87
19	22.06	very faint		
20	22.72	faint		
21	23.34	very faint		
22	23.98	medium	4 2 2	4.90
23	24.48	faint		
24	25.15	rather marked	{3 3 3} {5 1 1}	4.84
25	25.40	faint		
26	25.94	very faint		
27	26.58	faint		
28	27.52	medium	4 4 0	4.86
29	28.36	very faint		
30	29.08	faint	5 3 1	4.92
31	29.60	faint	{6 0 0} {4 4 2}	4.93
32	32.90	medium	6 2 2	4.96
33	33.70	medium	4 4 4	4.86

collodion, formvar and aluminium. The essential difficulty consisted in putting the specimen holders into the envelope after the first evaporation, without heating the condensed layer. For this purpose the envelope was provided with a large tube D and suitable glass rods for maintaining the specimen holders inside the envelope.

The diffraction patterns obtained were:

(1) quite in accordance with the PbS structure of the NaCl type (Phot. 5, Table 2);

(2) in accordance with the PbS structure but having additional rings (Phot. 6,

TABLE 2

No	D mm	Intensity	Plane indices $h\ k\ l$	$A = \frac{D}{\sqrt{h^2+k^2+l^2}}$
1	9.45	strong	1 1 1	5.45
2	10.9	very strong	2 0 0	5.45
3	15.4	very strong	2 2 0	5.45
4	18.0	strong	3 1 1	5.43
5	18.8	rather marked	2 2 2	5.43
6	21.7	rather marked	4 0 0	5.42
7	23.6	medium	3 3 1	5.42
8	24.2	very strong	4 2 0	5.41
9	26.5	strong	4 2 2	5.41
10	28.1	medium	3 3 3 5 1 1	5.41
11	30.6	faint	4 4 0	5.41
12	32.0	faint	5 3 1	5.41
13	32.4	medium	4 2 2 6 0 0	5.40
14	34.1	medium	6 2 0	5.39
15	35.9	medium	6 2 2	5.41
16	38.6	faint	7 1 1 5 5 1	5.40
17	39.0	faint	6 4 0	5.40
18	40.45	faint	6 4 2	5.40
19	41.55	very faint	5 5 3 7 3 1	5.41
20	44.55	faint	6 4 4 8 2 0	5.40
21	45.8	very faint	6 6 0 8 2 2	5.40
22	46.8	very faint	5 5 5 7 5 1	5.40
23	48.3	very faint	8 4 0	5.40
24	49.55	very faint	8 4 2	5.41

Table 3). These rings did not coincide with the additional rings appearing in the pseudo-replicas.

The PbS layer evaporated on the film is, in most cases, irrespectively of the kind of film, composed of crystals (whose sizes vary from 200 to 300 Å) which fuse into bigger crystals under the influence of illumination by an intense electron beam. Photographs 7 and 8 represent a layer not subjected to the action of the intense beam. Photographs 9 and 10 represent successive stages of formation of the bigger crystals. At first, on the layer composed mostly of crystals whose sizes vary from 200 to 300 Å there form single, widely dispersed crystals, 1000—1500 Å in size. Then in the substratum of small crystals, gaps form, the number of big crystals increases and, with a further increase in the intensity of the beam, the big crystals fuse into spheres (Phot. 11).

TABLE 3

No	D mm	Intensity	Plane indices $h\ k\ l$	$A = \frac{D}{\sqrt{h^2+k^2+l^2}}$
1	8.2	faint		
2	9.35	very faint		
3	9.6	strong		
4	10.5	faint		
5	10.7	very strong	1 1 1	6.175
6	12.35	very strong	2 0 0	6.175
7	13.2	medium		
8	14.7	medium		
9	16.3	medium		
10	17.35	very strong	2 2 0	6.13
11	18.7	faint		
12	20.4	strong	3 1 1	6.15
13	21.2	medium	2 2 2	6.12
14	22.3	very faint		
15	22.8	very faint		
16	24.5	faint	4 0 0	6.13
17	25.8	faint		
18	26.6	faint	3 3 1	6.10
19	27.35	faint	4 2 0	6.12
20	29.9	strong	4 2 2	6.10
21	31.55	medium	3 3 3 5 1 1	6.08
22	34.3	faint	4 4 0	6.06
23	35.6	medium		
24	36.5	medium	4 4 2 6 0 0	6.09
25	38.4	medium	6 2 0	6.07
26	40.4	medium	6 2 2	6.09
27	43.4	medium	5 5 1 7 1 1	6.08
28	43.6	medium	6 0 4	6.05
29	45.4	medium	6 4 2	6.07
30	46.6	medium	5 5 3 7 3 1	6.07
31	50.0	medium	6 4 4 8 2 0	6.07

Phot. 12 represents another case of changes in the layer due to illumination. On the left-hand side the layer has not yet changed and its structure is almost invisible. To the right, single crystals having the size of about 300 Å can already be seen. They are arranged in chains appearing in the middle of the photograph; finally, on the right-hand side of the photograph they form a spongy structure. According to the thickness of the layer, the changes due to illumination take different courses. Microscopic examination of the layers evaporated on the films reveal (though very seldom) places

covered with relatively large single crystals having the size of 1000 Å whose formation is not due to the action of electrons upon the layer, but results from different local conditions of condensation of the layer in the photocell (Phot. 8 and 13).

In order to make sure that the shift of the diffraction rings in the case of pseudo-replicas are due to the change of the structure during the preparation of the specimen, and not to improper photocell production, envelopes were made in which plates for the pseudo-replicas and specimen holders with the films were placed side by side (Fig. 1). These experiments confirmed the results previously obtained, i.e., that at direct evaporation on films, a layer giving the proper PbS pattern is obtained, whereas the pattern of the pseudo-replica shows characteristic deviations from the structure of the NaCl type.

In the third series of experiments in order to create conditions for which the condensation of the layer on the film will more closely resemble the normal conditions on the glass, phosphor bronze grids were fixed directly to the glass plate with the help of the formvar film covering the grid and the glass surface in its surrounding. The results of these experiments did not differ at all from the results obtained for layers evaporated on grids placed on the specimen holders.

The PbS layers evaporated directly from lead tiosulphate (without re-evaporation) from the tungsten band have been additionally examined. These layers were homogeneous, within the limits of the resolving power of our microscope. In the diffraction patterns there appeared the typical PbS pattern with diffused rings; there were no additional rings.

12 photocells were used for these experiments, from which about 40 specimens were examined and 154 photographs made.

Results

Diffraction investigations

1) All electron diffraction patterns (except those of pseudo-replicas) for layers obtained in quite different conditions have a typical PbS pattern.

2) The PbS structure is classical, regardless of whether the layer is sensitized or not (Sosnowski *et al.* 1947, Piwkowski 1953).

3) The method of pseudo-replicas seems to change the crystalline lattice of the detached layer (either by oxidation with dioxan, or in another way).

4) Diffraction patterns from pseudo-replicas with regard to the distribution of intensities and to the ring system suggest, however, that we are not dealing with another chemical substance, but with PbS whose lattice was subject to a certain deformation. This problem does not seem to be connected with the method of producing the layers, but rather with the whole method of preparation.

5) The appearance of additional rings should be ascribed to admixtures for cases where there is no shifting of the main rings, whilst in the case of pseudo-replicas, also to the method of preparation. Also the layers of the photocells gave the PbS

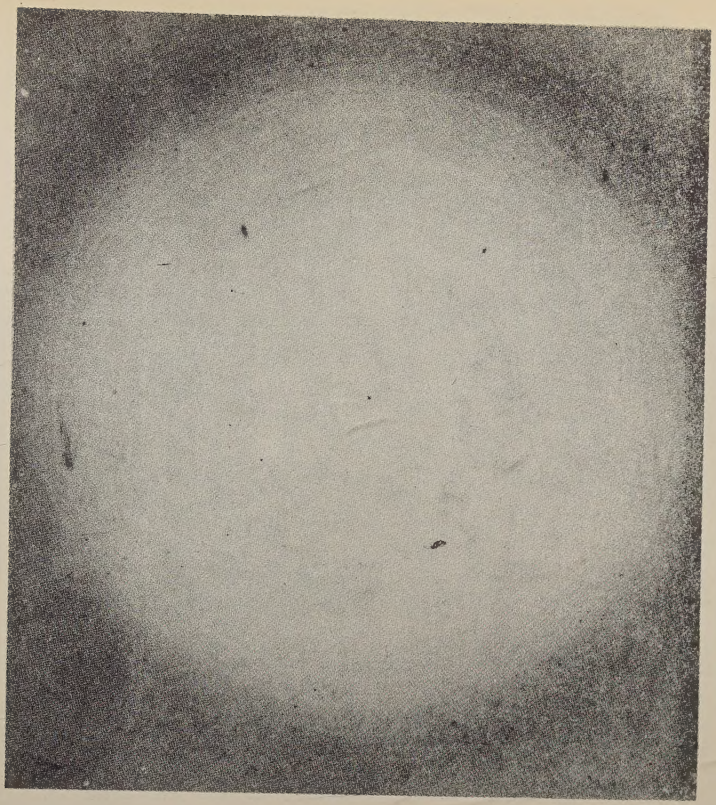

Phot. 1. Diffraction pattern obtained from the pseudo-replica of a PbS layer.

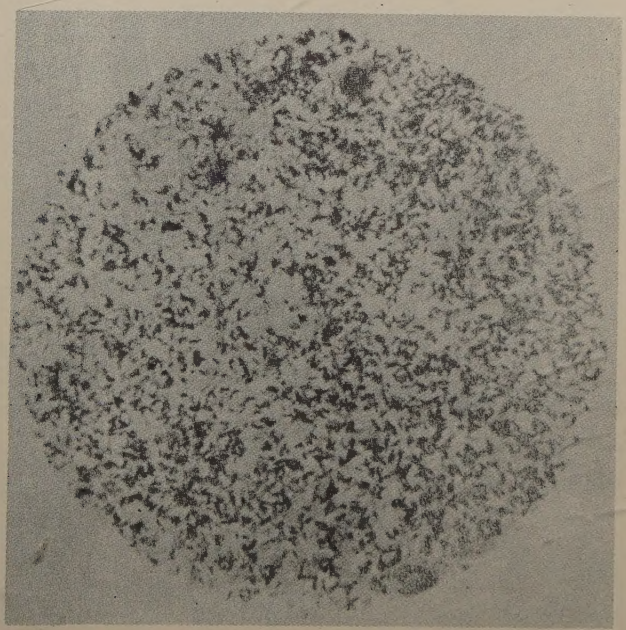

Phot. 2. Electron micrograph of the pseudo-replica of a PbS layer. Magnification 5,400 ×

Phot. 3. Electron micrograph of the pseudo-replica of another PbS layer. Magnification 5,600 ×

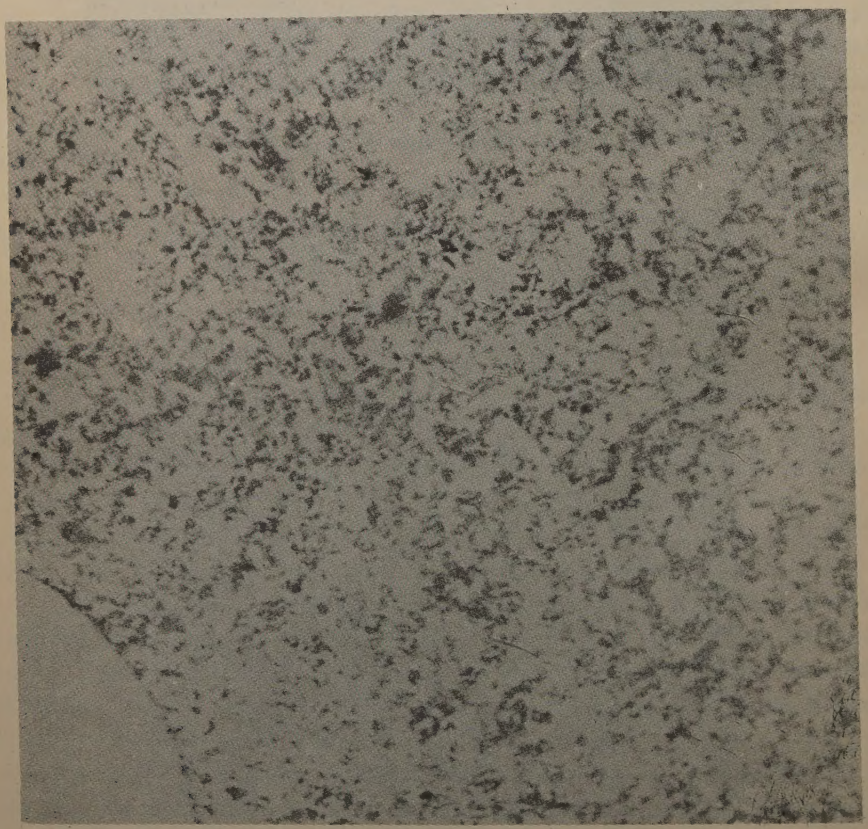

Phot. 4. Electron micrograph of the pseudo-replica of a PbS layer. Magnification 14,000 ×

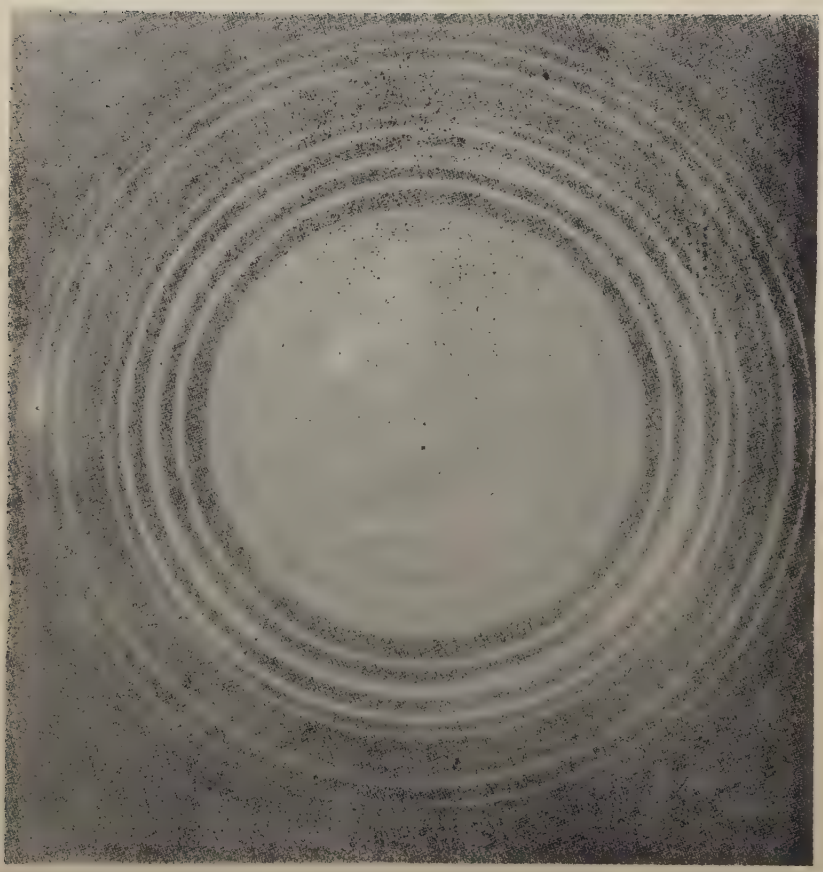

Phot. 5. Diffraction pattern of a PbS layer, evaporated directly on the collodion film. No additional rings are present.

Phot. 6. Diffraction pattern of a PbS layer, evaporated directly on the collodion film. Additional rings are present.

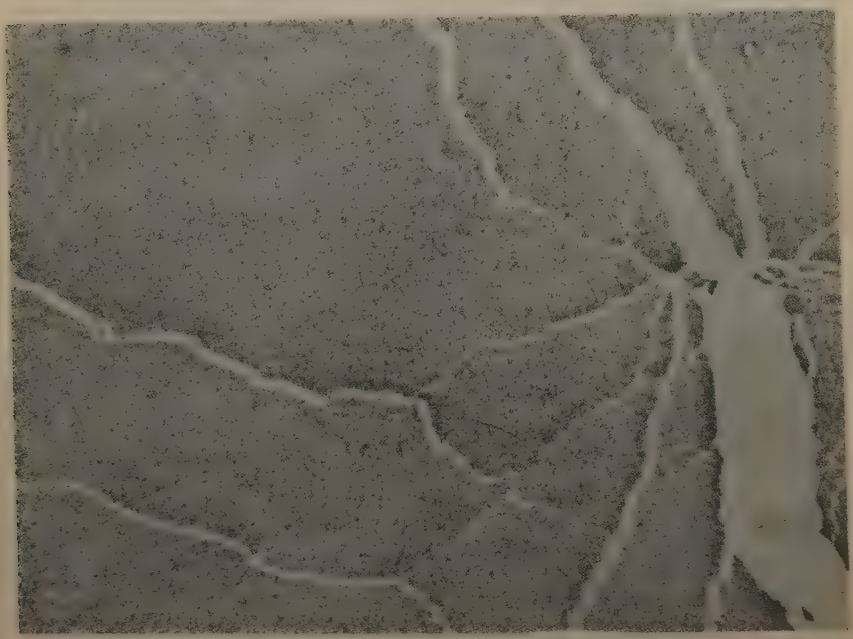

Phot. 7. Electron micrograph of a PbS layer evaporated directly on the collodion film. The layer not subjected to the action of the intense electron beam. Magnification 23,000 ×

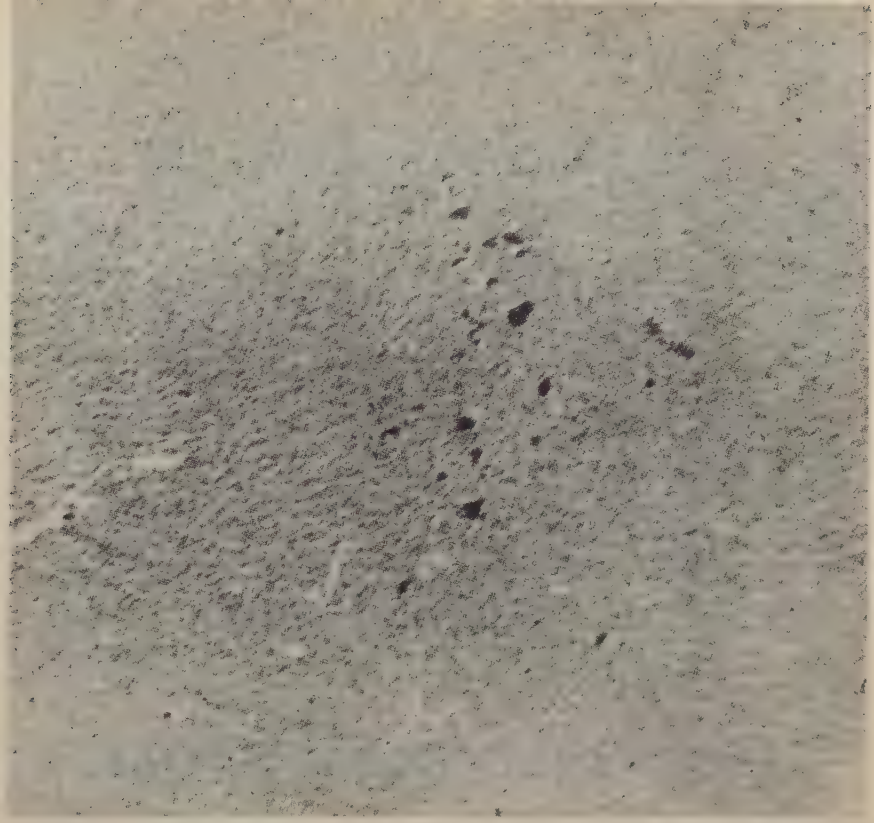

Phot. 8. Electron micrograph of a PbS layer not subjected to the action of the intense electron beam. Magnification 23,000 ×

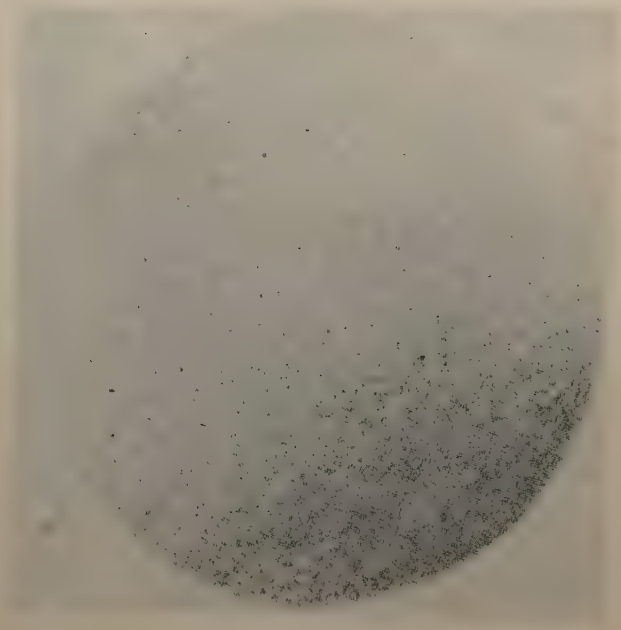

Phot. 9. Magnification 4,800 ×

Phot. 9—12. Electron micrographs of the PbS layer subjected to the action of the intense electron beam. Successive stages of formation of the bigger crystals are evident

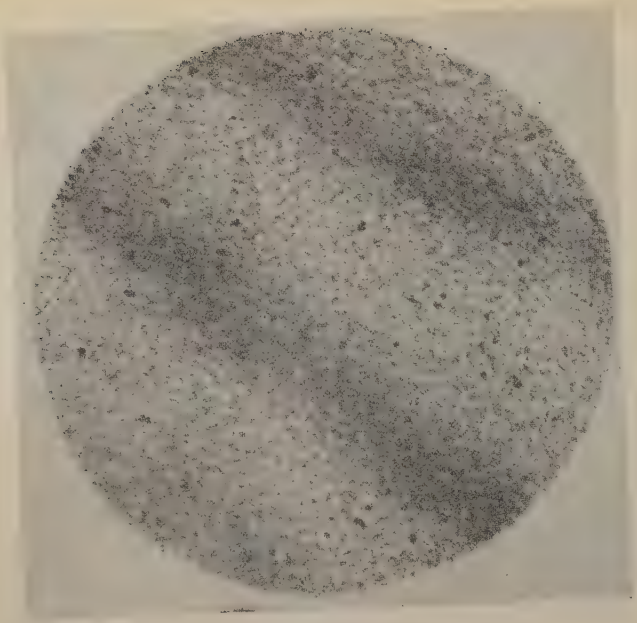

Phot. 10. Magnification 4,800 ×

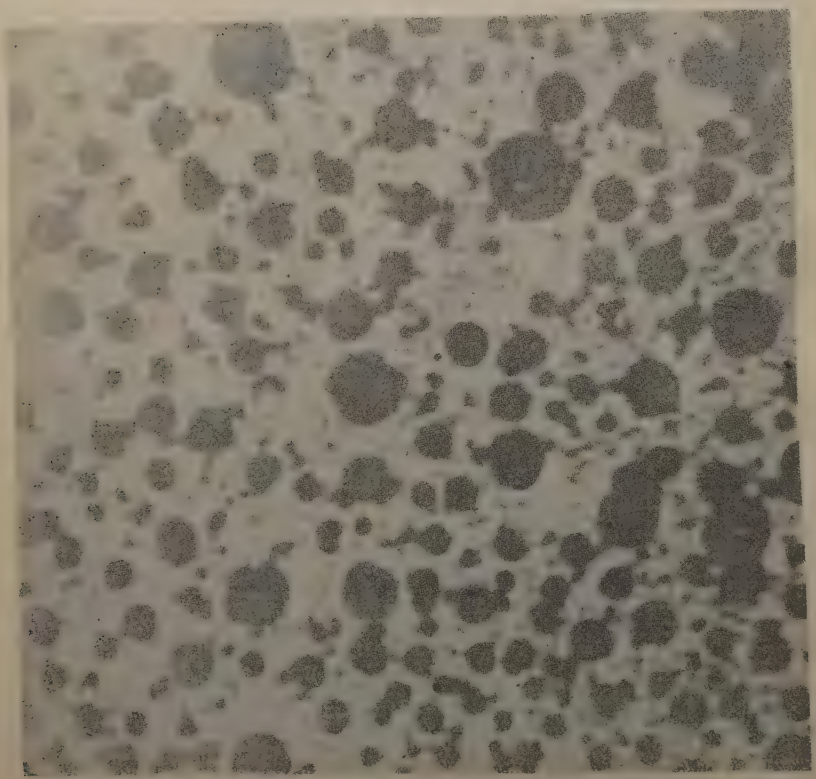

Phot. 11. Magnification 15,600 ×

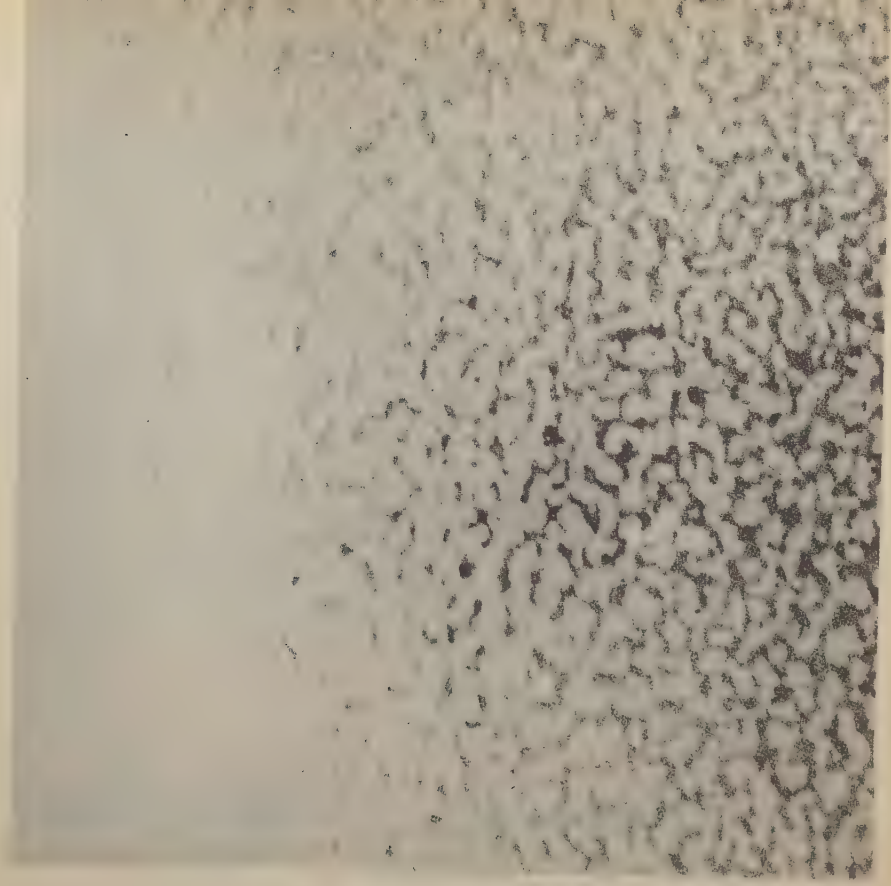

Phot. 12. Magnification 23,000 ×

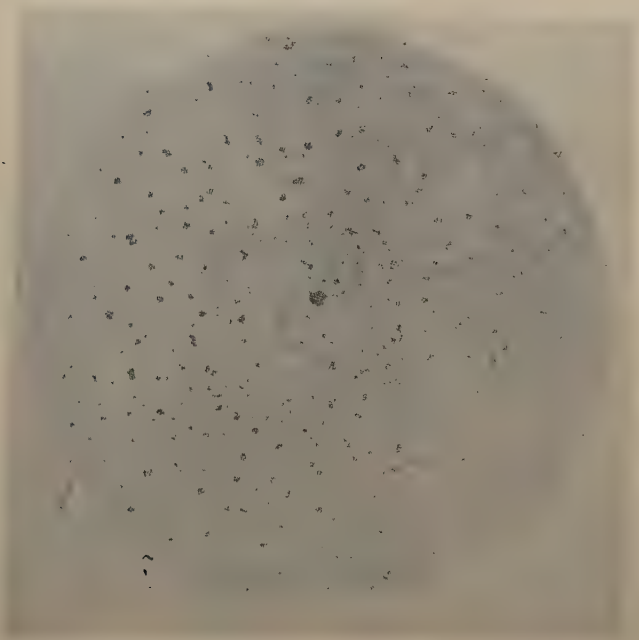

Phot. 13. Electron micrograph of the PbS layer not subjected to the action of the intense electron beam. Large crystals are also evident. Magnification 6,400 ×

pattern with different (depending on the case) additional rings, or the PbS pattern without any additional rings. Therefore, no identification of admixtures causing the appearance of these additional rings has been made.

Microscopic investigations

1) Microscopic observations allow us to assume that the structure of the layers examined under the microscope depend on the thickness of the layers, as well as on the conditions of condensation. Here it should be pointed out that even in almost identical conditions there appear quite homogeneous domains alongside others covered with well-developed, longitudinal or cubic, crystals exceeding 1000 Å in size.

2) It is known from the literature (Cario and Kallweit 1955) that the size of the crystals depends on the temperature of the surface on which they condense, on the nature of the layer, on the thickness of the evaporated layer, on the kind of substratum (physical and chemical properties, cleanliness), on the degree of vacuum, on the presence of foreign gases, on the way of obtaining the atom or molecule beam, on the intensity of the beam and on the time of evaporation.

Thus there are so many parameters affecting the size and shape of the crystals of the evaporated layer, that it is almost impossible to standardize the conditions of the experiment so as to obtain a layer of almost identical crystals.

We may of course determine the general character of the crystals which appear. For thin layers we find that the layer is quite homogeneous (the crystals lie beyond the resolving power of the microscope), for thicker layers, there appear more often bigger, well developed crystals.

3) The method of pseudo-replicas seems to be indispensable for thicker layers.

4) In layers obtained in quite different conditions (pseudo-replicas, specimen holders with films of different kinds, glass plates covered with formvar film) there occur areas where the crystals are big (of the order of 1000 Å and more).

5) The microscopic image changes decidedly due to illumination by an intense electron beam. Especially interesting is the formation of crystals from a homogeneous layer.

Changes of PbS layers due to illumination by an electron beam observed under a microscope and examined by diffraction will be the subject of a separate paper.

The authors wish to thank Professor L. Sosnowski for suggesting the subject and for valuable discussions concerning the interpretation of the results.

КРАТКОЕ СОДЕРЖАНИЕ

Фельтыновский, Глясс, Пивковский, Торунь, *Микроструктура фотопроводящих слоев сернистого свинца*

Микроструктура слоев PbS исследована при помощи электронной дифракции и электронной микроскопии. Слои получены посредством испарения в вакууме. Препараты для исследований сделаны методом формварных псевдо-реплик, а также напыляя непосредственно на формварные плёнки, коллодийные или алюминиевые. Слои PbS состоят вообще

из кристаллов размера 200—300 Å; не замечено влияния рода основания на их величину и форму. Дифракционные образы напыленных слоев соответствуют непосредственно гранецентрированной решётке типа NaCl. Дифракционные картины псевдо-реплик проявляют характерные отступления от этой структуры, заключающиеся в уменьшении диаметра кольца 200 и увеличении диаметра кольца 220 по отношению к диаметрам остальных колец.

REFERENCES

Cario, G. and Kallweit, J. H., *Z. Phys.*, **140**, 47 (1955).

Feltynowski, A., Glass, I., Piwkowski, T., and Toruń, A., *Bull. Acad. Polon. Sci.*, Cl. 3, **2**, 389 (1954).

Piwkowski, T., *Bull. Acad. Polon. Sci.*, Cl. 3, **1**, 185 (1953).

Sosnowski, L., Starkiewicz, J., and Simpson, O., *Nature* **159**, 818 (1947).

BEMERKUNGEN ÜBER DIE BERECHNUNG DES POLARISATIONSGRADES AUS DER KOMPENSATIONSEINSTELLUNG EINES GLASPLATTENSATZES

Von A. Kawski

I. Physikalisches Institut der Technischen Hochschule, Gdańsk

(Eingegangen am Januar 1956)

Es wurde gezeigt, dass man auf Grund der Neumannschen Formeln für die Intensität des Lichtes nach dem Durchgang durch einen Glasplattensatz (mit Berücksichtigung der mehrfachen Reflexionen an den Plattenoberflächen) eine allgemeine Formel für den Polarisationsgrad in der Kompensationsmethode von Arago angeben kann. Im besonderen erchält man die Formel von Gaviola und Pringsheim, ebenso wie diejenige von Sjewtschenko. Auf Grund der allgemeinen theoretischen Formel für eine beliebige Anzahl von Glasplatten, kann man also den Polarisationsgrad berechnen ohne mit dem Eichen des Satzes zu beginnen.

E. Gaviola und P. Pringsheim (1924) haben gezeigt, dass bei der Messung des Polarisationsgrades eines Lichtstrahls mit Hilfe eines kompensierenden Glasplattensatzes die einfache Formel

$$p = \frac{1 - \cos^{4k}(\alpha - \beta)}{1 + \cos^{4k}(\alpha - \beta)} \tag{1}$$

nicht angewandt werden kann. Hier bedeutet k die Zahl der Glasplatten, α und β die Einfalls- und Brechungswinkel. Die Formel (1) berücksichtigt nämlich nur den direkt durch die Platten hindruchgegangenen Anteil der auffallenden Strahlung, vernachlässigt dagegen die mehrfachen Reflexionen zwischen den einzelnen Oberflächen.

Zwecks Berechnung der Polarisationsgrade die geringer als 0,2 sind, wendet man eine kompensierende Glasplatte, dagegen im Falle der Polarisationsgrade von 0,2 bis 0,5 benutzt man meistenfalls vier Platten. Für eine einzige und für vier Platten wurden von Gaviola und Pringsheim (1924) entsprechende Formeln für den Polarisationsgrad angegeben, welche die mehrfachen Reflexionen der auffallenden Strahlung zwischen den einzelnen Oberflächen der Glasplatten berücksichtigen. Auch Sjewtschenko (s. Lewschin 1951, S. 62.) gab eine regelrechte Formel für den Polarisationsgrad für eine einzige Platte. Da es bisher keine strenge theoretische Formel für den Polari-

sationsgrad für einen kompensierenden Glassatz gab (s. Lewschin 1951, S. 62.), musste man entweder diesen Satz zunächst eichen oder auf Grund der von Gaviola und Pringsheim angegebenen Formeln und Reihen lästige Berechnungen durchführen.

Jedoch erweist es sich, dass schon im XIX Jahrhundert F. Neumann (s. G. Kirchhoff 1891, S. 166) Formeln für die Intensität des Lichtes, welches von einem System von k durchsichtiger Platten durchgelassen und reflektiert wird, abgeleitet hat, indem er gerade die mehrfachen Reflexionen zwischen den einzelnen Oberflächen des Plattensatzes berücksichtigte. Die Verifikation der Neumannschen Formeln ist von Provostaye und Desains (s. E. Verdet 1887, S. 385.) nachgewiesen. Die Übereinstimmung zwischen den Beobachtungen und der Berechnung ist ausserordentlich gut.

Im folgenden wird gezeigt, dass auf Grund der Neumannschen Formeln man eine allgemeine Formel für den Polarisationsgrad des kompensierenden Glasplattensatzes angeben und den Polarisationsgrad für eine beliebige Anzahl von Platten berechnen kann, ohne dass ein Eichen des Satzes nötig ist. Die Neumannschen Formeln für das durchgelassene Licht durch einen Satz von k Glasplatten, wenn man mit $I_{||}$ und $I_{\perp}$ die Intensitäten des parallel oder senkrecht zur Einfallsebene polarisierten Lichtes bezeichnet, lauten

$$I_{||} = \frac{d}{1 + (2k-1)(1-d)}, I_{\perp} = \frac{D}{1 + (2k-1)(1-D)}, \tag{2}$$

wobei nach den Fresnelschen Formeln

$$d = \frac{\sin 2\alpha \cdot \sin 2\beta}{\sin^2(\alpha+\beta)\cos^2(\alpha-\beta)}, D = \frac{\sin 2\alpha \sin 2\beta}{\sin^2(\alpha+\beta)} \tag{3}$$

und $\sin \alpha = n \sin \beta$, wo n der Brechungsindex ist.
Den Polarisationsgrad des Lichtes das teilweise polarisiert ist bezeichnet man, wie bekannt, durch

$$p = \frac{I_{||} - I_{\perp}}{I_{||} + I_{\perp}}. \tag{4}$$

Mit Rücksicht auf (2) folgt dann aus (4) die allgemeine Formel für den Polarisationsgrad bei k Glasplatten

$$p = \frac{k(d-D)}{k(d+D) - (2k-1)\,d \cdot D}. \tag{5}$$

Für eine einzige Glasplatte, wenn man in (5) $k = 1$ setzt, geht (5) über in

$$p = \frac{d-D}{d+D-d \cdot D} \tag{6}$$

was, wie es sich beweisen lässt, mit Gaviolas und Pringsheims Formel übereinstimmt.

Ncah (3) und (6) bekommt man

$$p = \frac{\left(1 - \frac{1}{n^2}\right)^2 \sin^2 \alpha}{\left(1 + \frac{1}{n^2}\right)\left[2 - \left(1 + \frac{1}{n^2}\right) \sin^2 \alpha\right]}, \tag{7}$$

eine mit der von Sjewtschenko identische Formel.

Für vier Platten ($k = 4$) unter Berücksichtigung von (3) lässt sich (5) wie folgt schreiben

$$p = \frac{\left(1 - \frac{1}{n^2}\right)^2 \sin^2 \alpha}{\left(1 + \frac{1}{n^2}\right)\left[2 - \left(1 + \frac{1}{n^2}\right) \sin^2 \alpha\right] - \frac{3}{n^2}\sqrt{(1 - \sin^2 \alpha)\,(n^2 - \sin^2 \alpha)}}. \tag{8}$$

Wenn man die Formel (8) mit Gaviolas und Pringsheims Formel für vier Platten vergleicht, so sieht man, dass die obige Formel viel einfacher ist. Zur Veranschaulichung der Abhängigkeit des Polarisationsgrades vom Winkel α der Glasplatteneinstellung für vier Platten ($n = 1{,}52$) seien hier die diese Abhängigkeit darstellenden Kurven angeführt (Fig. 1.).

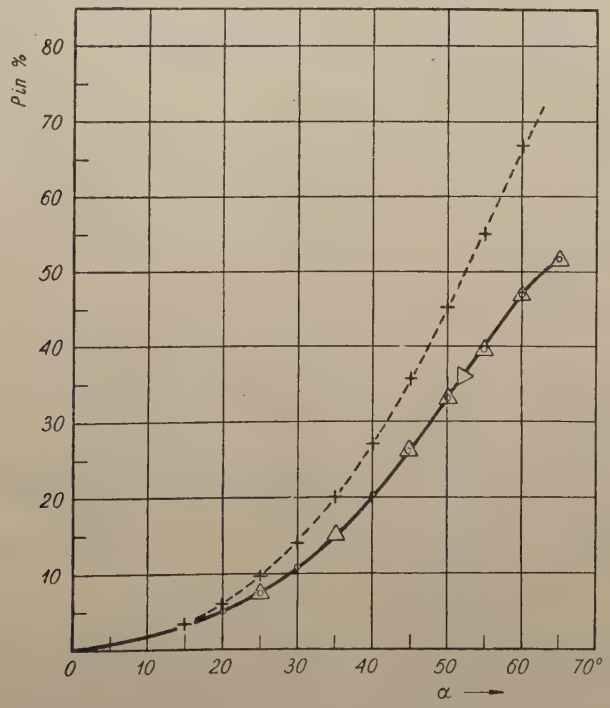

Fig. 1. Polarisationsgrad p als Funktion des Winkels α der Glasplatteneinstellung
+ berechnet nach der einfachen Formel (1)
○ berechnet nach der Formel von Gaviola und Pringsheim
△ berechnet nach der Formel (8)

Die auf Grund von (8) berechneten Polarisationsgrade liegen sehr nahe bzw. sind gleich denjenigen, welche man mit Hilfe Gaviolas und Pringsheims Formel erhält.

КРАТКОЕ СОДЕРЖАНИЕ

А. Кавский, *Заметки на тему вычисления степени поляризации в случае компенсационного установления стеклянных пластинок*

Основываясь на формулах Неймана на силу света, проходящего через систему нескольких прозрачных пластинок, учитывающих многократное отражение от поверхности пластинок, получено общую формулу, определяющую степень поляризации в компенсационном методе для *к* стеклянных пластинок. В частных случаях получено формулу Гавиоли и Принсгейма, а также формулу Севченко.

Следовательно, при помощи полученной теоретической формулы для любого количества стеклянных пластинок, можно вычислить степень поляризации, не прибегая к предварительной градуировке компенсационного прибора.

LITERATURHINWEISE

Gaviola E. u. Pringsheim P., Z. f. Phys. **24**, 24, (1924).

Kirchhoff G., Vorlesungen über Mathematische Optik Bd. II herausgegeben von Hensel K., Leipzig (1891).

Lewschin W. L. Photolumineszenz flüssiger und fester Substanzen (auf russisch) Moskau (1951).

Verdet E., Vorlesungen über die Wellentheorie des Lichtes Bd. II, deutsche Bearbeitung von Exner K., Braunschweig (1887).

TWO-CENTRE INTEGRALS IN SOLIDS

By Maciej Suffczyński

Institute of Theoretical Physics, University of Warsaw

(Received May 7, 1956)

Fletcher and Wohlfarth's method of calculating the energy two-center integrals in solids is described in detail.

Fletcher and Wohlfarth (1951) using the tight binding approximation calculated the energy band of $3d$ electrons in nickel. In this paper they calculated for the first time the necessary energy integrals in the crystal as two-centre integrals between the atomic functions centred on the central and the neighbouring atoms.

The calculation of these integrals will be described here in detail in order to point out all the integrals which should be calculated if the Fletcher-Wohlfarth idea were to be executed exactly.

The integrals will be calculated here between the $3d$ functions only, because these have sufficiently pronounced angular dependence to bring out the characteristic complexity.

Furthermore, for $3d$ electrons in transition metals, the treatment by the tight binding method may not be meaningless.

The integrals will be calculated between functions of σ, π, δ-type symmetry with respect to the axis joining the central atom with its neighbour. The tables of Slater and Koster (1954) allow the energy integrals in cubic lattices to be found in terms of these reduced two-centre integrals:

The energy integrals in the crystal have the well known form

$$\int_{\infty} \psi(\boldsymbol{r}') \left[V(\boldsymbol{r}) - U(r)\right] \psi(\boldsymbol{r})\, d_3x \tag{1}$$

The coordinate system originating in the central atom is unprimed, while the system originating in the neighbouring atom is primed.

The $3d$ functions are

$$\psi(3d\sigma) = \left(\frac{5}{16\pi}\right)^{\frac{1}{2}} \frac{3z^2 - r^2}{r^2} f(r),$$

$$\psi(3d\pi) = \left(\frac{15}{4\pi}\right)^{\frac{1}{2}} \frac{xz}{r^2} f(r), \qquad \psi(3d\bar{\pi}) = \left(\frac{15}{4\pi}\right)^{\frac{1}{2}} \frac{yz}{r^2} f(r),$$

$$\psi(3d\bar{\delta}) = \left(\frac{15}{4\pi}\right)^{\frac{1}{2}} \frac{xy}{r^2} f(r), \qquad \psi(3d\delta) = \left(\frac{15}{4\pi}\right)^{\frac{1}{2}} \frac{x^2 - y^2}{r^2} f(r). \tag{2}$$

The radial part $f(r)$ is taken in the form of a linear combination of Slater functions

$$f(r) = r^2 (A\, e^{-ar} + B\, e^{-br}) \tag{3}$$

normalized to 1, that is $(45/8)\ (A^2\, a^{-7} + B^2\, b^{-7}) + 1440\, AB\, (a+b)^{-7} = 1$.

The potential is approximated by (Z is the atomic number)

$V(r) - U(r) = -[1 + (Z-1)\, e^{-cr'}]/\, r'$ for the space outside the atomic sphere of the central atom,

$V(r) - U(r) = 0$ inside this sphere.

This is the essence of the idea put forward by Fletcher and Wohlfarth (1951, 1952). And it is at this point that the calculation of two-centre energy integrals in solids differs from the molecular case; every energy integral must be calculated as the difference of the integral over all space (∞) less the integral over the atomic sphere of the central atom (S). Such an integral will be denoted here without subscript:

$$\int = \int_\infty - \int_s, \tag{4}$$

thus $(dd\sigma) = (dd\sigma)_\infty - (dd\sigma)_s$ etc. for π, δ. The radius of the atomic sphere will always be taken equal to half the distance between the central and the neighbouring atom. Otherwise, the integration over this sphere would result in much too complicated formulas.

Therefore the assumption of Fletcher and Wohlfarth leads us to the calculation of the following integrals:

$$\left.\begin{matrix}(dd\sigma)\\(dd\pi)\\(dd\delta)\end{matrix}\right\} = \int d_3\, x\, (Ae^{-ar} + Be^{-br}) \left[-\frac{1 + (Z-1)\, e^{-cr'}}{r'}\right] (A\, e^{-ar'} + B\, e^{-br'}) \times$$

$$\times \begin{cases}(5/16\pi)\ (3z^2 - r^2)\ (3z'^2 - r'^2)\\ (15/4\pi)\ (xz)\ (x'\, z')\\ (15/4\pi)\ (xy)\ (x'\, y').\end{cases} \tag{5}$$

We introduce the spheroidal coordinates as defined by K. Rüdenberg (1951). The distance between the centres, that is, between the central atom and the neighbour is denoted here by 2R.

$$\begin{aligned} x &= x' = R\,[(\xi^2-1)\,(1-\eta^2)]^{\frac{1}{2}} \cos\varphi, && 0 \leqslant \varphi < 2\pi,\\ y &= y' = R\,[(\xi^2-1)\,(1-\eta^2)]^{\frac{1}{2}} \sin\varphi, &&\\ z &= R\,(1 - \xi\eta), && 1 \leqslant \xi < \infty,\\ z' &= R\,(1 + \xi\eta), && -1 \leqslant \eta \leqslant 1. \end{aligned} \tag{6}$$

We then have

$$r = R(\xi - \eta)$$
$$r' = R(\xi + \eta)$$
$$z' = 2R - z, \qquad d_3x = R^3(\xi^2 - \eta^2)\, d\xi\, d\eta\, d\varphi.$$

Since in (5) we have to do with linear combinations of Slater functions, we label the coefficients

$$\begin{aligned} N_0 &= A^2 \\ N_1 &= AB = N_4, & N_5 &= B^2, \\ N_2 &= A^2(Z-1), & N_7 &= B^2(Z-1). \\ N_3 &= AB(Z-1) = N_6, \end{aligned} \tag{7}$$

and the exponents

$$\begin{aligned} ar + ar' &= \alpha_0 \xi, \\ ar + br' &= \alpha_1 \xi + \beta_1 \eta, \\ ar + (a+c) r' &= \alpha_2 \xi + \beta_2 \eta, \\ ar + (b+c) r' &= \alpha_3 \xi + \beta_3 \eta, \\ br + ar' &= \alpha_4 \xi + \beta_4 \eta, \\ br + br' &= \alpha_5 \xi + \beta_5 \eta, \\ br + (a+c) r' &= \alpha_6 \xi + \beta_6 \eta, \\ br + (b+c) r' &= \alpha_7 \xi + \beta_7 \eta. \end{aligned} \tag{8}$$

We then have

$$\begin{aligned} \alpha_0 &= 2aR, & \beta_0 &= 0, \\ \alpha_1 &= R(a+b), & \beta_1 &= R(b-a), \\ \alpha_2 &= R(c+2a), & \beta_2 &= Rc, \\ \alpha_3 &= R(a+b+c), & \beta_3 &= R(b+c-a), \text{ etc.} \end{aligned}$$

We can now write

$$(dd\sigma) = R^6 \sum_{\nu=0}^{7} N_\nu \overset{\alpha_\nu\ \beta_\nu}{(dd\sigma)} \tag{9}$$

and identical linear combinations for the π and δ-integrals. The integrals for a particular α and β are

$$\left.\begin{matrix} \overset{\alpha\beta}{(dd\sigma)} \\ \overset{\alpha\beta}{(dd\,\pi)} \\ \overset{\alpha\beta}{(dd\delta)} \end{matrix}\right\} = \int d\eta \int d\xi\, e^{-\alpha\xi}\, e^{-\beta\eta}(\xi - \eta) \times$$

$$\times \begin{cases} (-5/8)\,[9\xi^4\eta^4 - 6(\xi^4\eta^2 + \xi^2\eta^4) + \xi^4 + \eta^4 + 4\xi^2\eta^2 - 6\,(\xi^2+\eta^2) + 9] \\ (15/4)\,[\xi^4\eta^4 - \xi^4\eta^2 - \xi^2\eta^4 + \xi^2 + \eta^2 - 1] \\ (-15/16)\,[\xi^4\eta^4 - 2(\xi^4\eta^2 + \xi^2\eta^4) + \xi^4 + \eta^4 + 4\xi^2\eta^2 - 2(\xi^2 + \eta^2) + 1]. \end{cases} \quad (10)$$

The integrals over all space are well known from molecular studies. The limits of integration are

$$\int_{\infty} = \int_{-1}^{1} d\eta \int_{1}^{\infty} d\xi$$

and the integrals can be expressed in terms of the $A_n(\alpha)$ and $B_m(\beta)$ functions of Kotani & al. (1940).

$$\overset{\alpha\beta}{(dd\sigma)}_{\infty} = -(5/8)\,[9\,(A_1B_0 - A_0B_1) - 6\,(A_3B_0 + A_1B_2 - A_2B_1 - A_0B_3) + A_5B_0 + A_1B_4 - A_4B_1 - A_0B_5 + 4\,A_3\,B_2 - 4\,A_2B_3 - 6\,(A_5B_2 + A_3B_4 - A_4B_3 - A_2B_5) + 9\,(A_5B_4 - A_4B_5)]$$

$$= -(5/8)\,[B_0(A_5 - 6A_3 + 9A_1) + B_1(-A_4 + 6A_2 - 9A_0) + B_2(-6A_5 + 4A_3 - 6A_1) + B_3(6A_4 - 4A_2 + 6A_0) + B_4(9A_5 - 6A_3 + A_1) + B_5(-9A_4 + 6A_2 - A_0)], \quad (11)$$

$$\overset{\alpha\beta}{(dd\pi)}_{\infty} = (15/4)\,[B_0(A_3 - A_1) - B_1(A_2 - A_0) - B_2(A_5 - A_1) + B_3(A_4 - A_0) + B_4(A_5 - A_3) - B_5(A_4 - A_2)], \quad (12)$$

$$\overset{\alpha\beta}{(dd\delta)}_{\infty} = -(15/16)\,[(B_0 + B_4 - 2B_2)(A_5 + A_1 - 2A_3) - (B_1 + B_5 - 2B_3)(A_4 + A_0 - 2A_2)], \quad (13)$$

$$\overset{\alpha\beta}{(dd\delta)}_{\infty} = -\frac{60}{(\alpha\beta)^3}\left\{e^{\beta-\alpha}\left[\left(1 + \frac{6}{\alpha} + \frac{15}{\alpha^2} + \frac{15}{\alpha^3}\right)\left(1 - \frac{3}{\beta} + \frac{3}{\beta^2}\right) + \left(1 + \frac{3}{\alpha} + \frac{3}{\alpha^2}\right)\left(1 - \frac{6}{\beta} + \frac{15}{\beta^2} - \frac{15}{\beta^3}\right)\right] + e^{-\alpha-\beta}\left[\left(1 + \frac{3}{\alpha} + \frac{3}{\alpha^2}\right)\left(1 + \frac{6}{\beta} + \frac{15}{\beta^2} + \frac{15}{\beta^3}\right) - \left(1 + \frac{6}{\alpha} + \frac{15}{\alpha^2} + \frac{15}{\alpha^3}\right)\left(1 + \frac{3}{\beta} + \frac{3}{\beta^2}\right)\right]\right\}. \quad (14)$$

The last, particularly simple, formula can be used for checking numerical computations. The exponent $\beta = 0$ gives us the shorter expressions:

$$\overset{\alpha\,0}{(dd\sigma)}_{\infty} = -8\,\frac{e^{-\alpha}}{\alpha}\left(\frac{1}{3} - \frac{1}{\alpha} - \frac{3}{\alpha^2} + \frac{2}{\alpha^3} + \frac{15}{\alpha^4} + \frac{15}{\alpha^5}\right), \quad (15)$$

$$\overset{\alpha\,0}{(dd\pi)}_{\infty} = 8\,\frac{e^{-\alpha}}{\alpha^2}\left(1 + \frac{2}{\alpha} - \frac{3}{\alpha^2} - \frac{15}{\alpha^3} - \frac{15}{\alpha^4}\right), \quad (16)$$

$$\overset{\alpha\,0}{(dd\delta)}_{\infty} = -8\,\frac{e^{-\alpha}}{\alpha^3}\left(1 + \frac{6}{\alpha} + \frac{15}{\alpha^2} + \frac{15}{\alpha^3}\right). \quad (17)$$

The evaluation of the integrals over the atomic sphere constitutes the bulk of the calculations. The limits of integration are

$$\int_s = \int_0^1 d\eta \int_1^{1+\eta} d\xi$$

and the integrals over ξ and η are not independent. We use here the abbreviation $\sigma = \alpha + \beta$.

$$
\begin{aligned}
(dd\sigma)_s^{\alpha\beta} = &-\frac{5}{2}\frac{e^{-\alpha}}{\alpha}\Bigg\{\frac{1}{\beta}\Bigg[1-\frac{1}{\beta}-\frac{4}{\beta^2}+\frac{12}{\beta^3}+\frac{24}{\beta^4}-\frac{120}{\beta^5}+24\frac{e^{-\beta}}{\beta^3}\left(1+\frac{4}{\beta}+\frac{5}{\beta^2}\right)+\\
&+\frac{1}{\alpha}\left(-1+\frac{2}{\beta}-\frac{12}{\beta^2}+\frac{24}{\beta^3}+\frac{168}{\beta^4}-\frac{720}{\beta^5}+24\frac{e^{-\beta}}{\beta^2}\left(1+\frac{7}{\beta}+\frac{23}{\beta^2}+\frac{30}{\beta^3}\right)\right)+\\
&+\frac{4}{\alpha^2}\left(-1-\frac{12}{\beta^2}+\frac{24}{\beta^3}+\frac{216}{\beta^4}-\frac{720}{\beta^5}-6\frac{e^{-\beta}}{\beta}\left(1-\frac{20}{\beta^2}-\frac{84}{\beta^3}-\frac{120}{\beta^4}\right)\right)+\\
&+\frac{6}{\alpha^3}\left(1-\frac{1}{\beta}-\frac{28}{\beta^2}+\frac{36}{\beta^3}+\frac{504}{\beta^4}-\frac{1080}{\beta^5}-4e^{-\beta}\left(1+\frac{7}{\beta}+\frac{20}{\beta^2}-\frac{144}{\beta^4}-\frac{270}{\beta^5}\right)\right)+\\
&+\frac{6}{\alpha^4}\left(5-\frac{1}{\beta}-\frac{60}{\beta^2}+\frac{36}{\beta^3}+\frac{1080}{\beta^4}-\frac{1080}{\beta^5}-4e^{-\beta}\left(4+\frac{23}{\beta}+\frac{84}{\beta^2}+\frac{144}{\beta^3}-\frac{270}{\beta^5}\right)\right)+\\
&+\frac{30}{\alpha^5}\left(1-\frac{12}{\beta^2}+\frac{216}{\beta^4}-4e^{-\beta}\left(1+\frac{6}{\beta}+\frac{24}{\beta^2}+\frac{54}{\beta^3}+\frac{54}{\beta^4}\right)\right)\Bigg]-\\
&-\frac{1}{\sigma}\Bigg[1-\frac{2}{\sigma}-\frac{4}{\sigma^2}-\frac{18}{\sigma^3}-\frac{162}{\sigma^4}+\frac{7560}{\sigma^6}+\frac{45360}{\sigma^7}+\frac{90720}{\sigma^8}-e^{-\sigma}\left(9+\frac{102}{\sigma}+\right.\\
&\left.+\frac{716}{\sigma^2}+\frac{3726}{\sigma^3}+\frac{14958}{\sigma^4}+\frac{45360}{\sigma^5}+\frac{98280}{\sigma^6}+\frac{136080}{\sigma^7}+\frac{90720}{\sigma^8}\right)+\\
&+\frac{1}{\alpha}\left(-1-\frac{2}{\sigma}-\frac{6}{\sigma^2}-\frac{108}{\sigma^3}-\frac{450}{\sigma^4}+\frac{2160}{\sigma^5}+\frac{27000}{\sigma^6}+\frac{90720}{\sigma^7}+\frac{90720}{\sigma^8}-\right.\\
&\left.-e^{-\sigma}\left(33+\frac{322}{\sigma}+\frac{2028}{\sigma^2}+\frac{9558}{\sigma^3}+\frac{34110}{\sigma^4}+\frac{89640}{\sigma^5}+\frac{163080}{\sigma^6}+\frac{181440}{\sigma^7}+\frac{90720}{\sigma^8}\right)\right)+\\
&+\frac{2}{\alpha^2}\left(-2+\frac{3}{\sigma}-\frac{15}{\sigma^2}-\frac{198}{\sigma^3}-\frac{216}{\sigma^4}+\frac{5400}{\sigma^5}+\frac{29160}{\sigma^6}+\frac{45360}{\sigma^7}-\right.\\
&\left.-2e^{-\sigma}\left(23+\frac{192}{\sigma}+\frac{1086}{\sigma^2}+\frac{4518}{\sigma^3}+\frac{13662}{\sigma^4}+\frac{28620}{\sigma^5}+\frac{37260}{\sigma^6}+\frac{22680}{\sigma^7}\right)\right)+\\
&+\frac{6}{\alpha^3}\left(1+\frac{4}{\sigma}-\frac{25}{\sigma^2}-\frac{144}{\sigma^3}+\frac{288}{\sigma^4}+\frac{4320}{\sigma^5}+\frac{9720}{\sigma^6}-2e^{-\sigma}\left(15+\frac{108}{\sigma}+\frac{550}{\sigma^2}+\right.\right.\\
&\left.\left.+\frac{1962}{\sigma^3}+\frac{4734}{\sigma^4}+\frac{7020}{\sigma^5}+\frac{4860}{\sigma^6}\right)\right)+\\
&+\frac{6}{\alpha^4}\left(5+\frac{4}{\sigma}-\frac{60}{\sigma^2}-\frac{144}{\sigma^3}+\frac{1080}{\sigma^4}+\frac{4320}{\sigma^5}-4e^{-\sigma}\left(9+\frac{58}{\sigma}+\frac{264}{\sigma^2}+\right.\right.
\end{aligned}
$$

$$+\frac{774}{\sigma^3}+\frac{1350}{\sigma^4}+\frac{1080}{\sigma^5}\Big)\Big)+$$

$$+\frac{30}{\alpha^5}\left(1-\frac{12}{\sigma^2}+\frac{216}{\sigma^4}-4e^{-\sigma}\left(1+\frac{6}{\sigma}+\frac{24}{\sigma^2}+\frac{54}{\sigma^3}+\frac{54}{\sigma^4}\right)\right)\Big]\Big\}. \tag{18}$$

$$\overset{\alpha\,\beta}{(dd\pi)_s}=\frac{15}{2}\frac{e^{-\alpha}}{\alpha}\left\{\frac{1}{\alpha\beta}\left[1-\frac{1}{\beta}-\frac{4}{\beta^2}+\frac{12}{\beta^3}+\frac{24}{\beta^4}-\frac{120}{\beta^5}+24\frac{e^{-\beta}}{\beta^3}\left(1+\frac{4}{\beta}+\frac{5}{\beta^2}\right)+\right.\right.$$

$$+\frac{1}{\alpha}\left(3-\frac{1}{\beta}-\frac{20}{\beta^2}+\frac{36}{\beta^3}+\frac{168}{\beta^4}-\frac{600}{\beta^5}+24\frac{e^{-\beta}}{\beta^3}\left(4+\frac{18}{\beta}+\frac{25}{\beta^2}\right)\right)+$$

$$+\frac{3}{\alpha^2}\left(1-\frac{20}{\beta^2}+\frac{24}{\beta^3}+\frac{216}{\beta^4}-\frac{480}{\beta^5}-8\frac{e^{-\beta}}{\beta}\left(1+\frac{4}{\beta}-\frac{33}{\beta^3}-\frac{60}{\beta^4}\right)\right)+$$

$$+\frac{24}{\alpha^3\beta}\left(-\frac{5}{\beta}+\frac{3}{\beta^2}+\frac{60}{\beta^3}-\frac{60}{\beta^4}-e^{-\beta}\left(4+\frac{18}{\beta}+\frac{33}{\beta^2}-\frac{60}{\beta^4}\right)\right)+$$

$$\left.+\frac{120}{\alpha^4\beta}\left(-\frac{1}{\beta}+\frac{12}{\beta^3}-e^{-\beta}\left(1+\frac{5}{\beta}+\frac{12}{\beta^2}+\frac{12}{\beta^3}\right)\right)\right]-$$

$$-\frac{1}{\sigma}\left[\frac{1}{\sigma}\left(1+\frac{1}{\sigma}-\frac{12}{\sigma^2}-\frac{72}{\sigma^3}-\frac{120}{\sigma^4}+\frac{1440}{\sigma^5}+\frac{10080}{\sigma^6}+\frac{20160}{\sigma^7}-\right.\right.$$

$$-3e^{-\sigma}\left(3+\frac{35}{\sigma}+\frac{228}{\sigma^2}+\frac{1016}{\sigma^3}+\frac{3240}{\sigma^4}+\frac{7200}{\sigma^5}+\frac{10080}{\sigma^6}+\frac{6720}{\sigma^7}\right)\Big)+$$

$$+\frac{1}{\alpha}\left(1+\frac{2}{\sigma}-\frac{3}{\sigma^2}-\frac{48}{\sigma^3}-\frac{192}{\sigma^4}+\frac{240}{\sigma^5}+\frac{5760}{\sigma^6}+\frac{20160}{\sigma^7}+\frac{20160}{\sigma^8}-\right.$$

$$-\frac{e^{-\sigma}}{\sigma}\left(33+\frac{329}{\sigma}+\frac{1848}{\sigma^2}+\frac{7128}{\sigma^3}+\frac{19440}{\sigma^4}+\frac{36000}{\sigma^5}+\frac{40320}{\sigma^6}+\frac{20160}{\sigma^7}\right)\Big)+$$

$$+\frac{1}{\alpha^2}\left(3+\frac{2}{\sigma}-\frac{20}{\sigma^2}-\frac{144}{\sigma^3}-\frac{264}{\sigma^4}+\frac{2160}{\sigma^5}+\frac{12960}{\sigma^6}+\frac{20160}{\sigma^7}-\right.$$

$$-\frac{4e^{-\sigma}}{\sigma}\left(23+\frac{193}{\sigma}+\frac{918}{\sigma^2}+\frac{2934}{\sigma^3}+\frac{6300}{\sigma^4}+\frac{8280}{\sigma^5}+\frac{5040}{\sigma^6}\right)\Big)+$$

$$+\frac{3}{\alpha^3}\left(1-\frac{20}{\sigma^2}-\frac{96}{\sigma^3}+\frac{72}{\sigma^4}+\frac{1920}{\sigma^5}+\frac{4320}{\sigma^6}-12\frac{e^{-\sigma}}{\sigma}\left(5+\frac{35}{\sigma}+\frac{138}{\sigma^2}+\right.\right.$$

$$\left.+\frac{346}{\sigma^3}+\frac{520}{\sigma^4}+\frac{360}{\sigma^5}\right)\Big)+$$

$$+\frac{24}{\alpha^4\sigma}\left(-\frac{5}{\sigma}-\frac{12}{\sigma^2}+\frac{60}{\sigma^3}+\frac{240}{\sigma^4}-e^{-\sigma}\left(9+\frac{53}{\sigma}+\frac{168}{\sigma^2}+\frac{300}{\sigma^3}+\frac{240}{\sigma^4}\right)\right)+$$

$$\left.+\frac{120}{\alpha^5\sigma}\left(-\frac{1}{\sigma}+\frac{12}{\sigma^3}-e^{-\sigma}\left(1+\frac{5}{\sigma}+\frac{12}{\sigma^2}+\frac{12}{\sigma^3}\right)\right)\right]\Big\}. \tag{19}$$

$$
\begin{aligned}
{}^{\alpha\beta}(dd\delta)_s = &-\frac{15}{2}\frac{e^{-\alpha}}{\alpha}\left\{\frac{1}{\alpha^2\beta}\left[1-\frac{1}{\beta}-\frac{4}{\beta^2}+\frac{12}{\beta^3}+\frac{24}{\beta^4}-\frac{120}{\beta^5}+24\frac{e^{-\beta}}{\beta^3}\left(1+\frac{4}{\beta}+\frac{5}{\beta^2}\right)+\right.\right.\\
&+\frac{3}{\alpha}\left(2-\frac{1}{\beta}-\frac{8}{\beta^2}+\frac{12}{\beta^3}+\frac{48}{\beta^4}-\frac{120}{\beta^5}-8\frac{e^{-\beta}}{\beta^2}\left(1-\frac{9}{\beta^2}-\frac{15}{\beta^3}\right)\right)+\\
&+\frac{3}{\alpha^2}\left(5-\frac{1}{\beta}-\frac{20}{\beta^2}+\frac{12}{\beta^3}+\frac{120}{\beta^4}-\frac{120}{\beta^5}-8\frac{e^{-\beta}}{\beta^2}\left(4+\frac{9}{\beta}-\frac{15}{\beta^3}\right)\right)+\\
&\left.+\frac{15}{\alpha^3}\left(1-\frac{4}{\beta^2}+\frac{24}{\beta^4}-8\frac{e^{-\beta}}{\beta^2}\left(1+\frac{3}{\beta}+\frac{3}{\beta^2}\right)\right)\right]-\\
&-\frac{1}{\sigma}\left[\frac{1}{\sigma^2}\left(1+\frac{3}{\sigma}-\frac{21}{\sigma^2}-\frac{120}{\sigma^3}+\frac{180}{\sigma^4}+\frac{2520}{\sigma^5}+\frac{5040}{\sigma^6}-\right.\right.\\
&\left.-3e^{-\sigma}\left(3+\frac{33}{\sigma}+\frac{193}{\sigma^2}+\frac{720}{\sigma^3}+\frac{1740}{\sigma^4}+\frac{2520}{\sigma^5}+\frac{1680}{\sigma^6}\right)\right)+\\
&+\frac{1}{\alpha\sigma}\left(1+\frac{4}{\sigma}-\frac{6}{\sigma^2}-\frac{93}{\sigma^3}-\frac{120}{\sigma^4}+\frac{1260}{\sigma^5}+\frac{5040}{\sigma^6}+\frac{5040}{\sigma^7}-\right.\\
&\left.-3\frac{e^{-\sigma}}{\sigma}\left(11+\frac{101}{\sigma}+\frac{489}{\sigma^2}+\frac{1500}{\sigma^3}+\frac{2940}{\sigma^4}+\frac{3360}{\sigma^5}+\frac{1680}{\sigma^6}\right)\right)+\\
&+\frac{1}{\alpha^2}\left(1+\frac{5}{\sigma}+\frac{5}{\sigma^2}-\frac{54}{\sigma^3}-\frac{192}{\sigma^4}+\frac{360}{\sigma^5}+\frac{3240}{\sigma^6}+\frac{5040}{\sigma^7}-\right.\\
&\left.-4\frac{e^{-\sigma}}{\sigma^2}\left(23+\frac{171}{\sigma}+\frac{657}{\sigma^2}+\frac{1530}{\sigma^3}+\frac{2070}{\sigma^4}+\frac{1260}{\sigma^5}\right)\right)+\\
&+\frac{3}{\alpha^3}\left(2+\frac{4}{\sigma}-\frac{5}{\sigma^2}-\frac{48}{\sigma^3}-\frac{24}{\sigma^4}+\frac{480}{\sigma^5}+\frac{1080}{\sigma^6}-\right.\\
&\left.-12\frac{e^{-\sigma}}{\sigma^2}\left(5+\frac{29}{\sigma}+\frac{83}{\sigma^2}+\frac{130}{\sigma^3}+\frac{90}{\sigma^4}\right)\right)+\\
&+\frac{3}{\alpha^4}\left(5+\frac{4}{\sigma}-\frac{20}{\sigma^2}-\frac{48}{\sigma^3}+\frac{120}{\sigma^4}+\frac{480}{\sigma^5}-24\frac{e^{-\sigma}}{\sigma^2}\left(3+\frac{13}{\sigma}+\frac{25}{\sigma^2}+\frac{20}{\sigma^3}\right)\right)+\\
&\left.\left.+\frac{15}{\alpha^5}\left(1-\frac{4}{\sigma^2}+\frac{24}{\sigma^4}-8\frac{e^{-\sigma}}{\sigma^2}\left(1+\frac{3}{\sigma}+\frac{3}{\sigma^2}\right)\right)\right]\right\}. \qquad (20)
\end{aligned}
$$

In particular, for $\beta = 0$ we have

$$
\begin{aligned}
{}^{\alpha 0}(dd\sigma)_s = &-\frac{1}{4}\frac{e^{-\alpha}}{\alpha}\left[\frac{11}{3}-\frac{16}{\alpha}-\frac{18}{\alpha^2}+\frac{102}{\alpha^3}+\frac{330}{\alpha^4}+\frac{270}{\alpha^5}+\frac{9420}{\alpha^6}-\right.\\
&-\frac{80640}{\alpha^7}-\frac{836640}{\alpha^8}-\frac{2721600}{\alpha^9}-\frac{2721600}{\alpha^{10}}+10\frac{e^{-\alpha}}{\alpha}\left(9+\frac{135}{\alpha}+\frac{1130}{\alpha^2}+\right.\\
&\left.\left.+\frac{6702}{\alpha^3}+\frac{30372}{\alpha^4}+\frac{105654}{\alpha^5}+\frac{273168}{\alpha^6}+\frac{491904}{\alpha^7}+\frac{544320}{\alpha^8}+\frac{272160}{\alpha^9}\right)\right], \qquad (21)
\end{aligned}
$$

$$(dd\pi)_s^{a\,0} = \frac{3}{4}\frac{e^{-a}}{a^2}\left[\frac{11}{3} - \frac{23}{3a} - \frac{66}{a^2} + \frac{30}{a^3} + \frac{1320}{a^4} + \right.$$

$$+ \frac{5160}{a^5} - \frac{10080}{a^6} - \frac{178080}{a^7} - \frac{604800}{a^8} - \frac{604800}{a^9} + 10\frac{e^{-a}}{a}\left(9 + \frac{138}{a} + \frac{1105}{a^2} + \right.$$

$$\left.\left. + \frac{5848}{a^3} + \frac{21996}{a^4} + \frac{59136}{a^5} + \frac{108528}{a^6} + \frac{120960}{a^7} + \frac{60480}{a^8}\right)\right], \qquad (22)$$

$$(dd\delta)_s^{a\,0} = -\frac{3}{4}\frac{e^{-a}}{a^3}\left[\frac{11}{3} - \frac{3}{a} - \frac{105}{a^2} + \frac{30}{a^3} + \frac{2550}{a^4} + \frac{3360}{a^5} - \frac{38640}{a^6} - \right.$$

$$- \frac{151200}{a^7} - \frac{151200}{a^8} + 10\frac{e^{-a}}{a}\left(9 + \frac{132}{a} + \frac{974}{\sigma^2} + \frac{4491}{a^3} + \frac{13608}{a^4} + \right.$$

$$\left.\left. + \frac{26544}{a^5} + \frac{30240}{a^6} + \frac{15120}{a^7}\right)\right]. \qquad (23)$$

In the actual numerical calculations of Fletcher (1951, 1952) and in my own (1955 a, b) as well, the whole sum (9) was not been evaluated. In the integration over all space, only terms with $\nu = 0, 1, 2, 3$ in the present notation have been retained, and in the integration over the atomic sphere, only terms with $\nu = 0$. It was argued that $a < c < b$. For instance, the 3 d electrons in transition metals have atomic functions which can be approximated by (3) taking $a = 2$, $b = 5$.

Therefore the formulas for the integrals over the atomic sphere with $\beta \neq 0$ which I have derived (1956) have not yet been used in numerical calculations.

I thank Dr. G. C. Fletcher for his kind correspondence concerning the two-center integrals in solids.

КРАТКОЕ СОДЕРЖАНИЕ

М. Суффчинский, *Бицентровые интегралы в кристаллах*

Описан метод Fletcher и Wohlfarth вычисления бицентровых интегралов энергии в кристаллах. Выписаны формулы для интегралов энергии, вычисленных по атомной сфере.

REFERENCES

Fletcher, G. C., Wohlfarth, E. P., *Phil. Mag.* **42**, 106 (1951).
Fletcher, G. C., *Proc. Phys. Soc.* **A 65**, 192 (1952).
Kotani & al., *Proc. Phys. Math. Soc.* Japan, **20** (1938); **22** (1940).
Rüdenberg, K., *J. chem. Phys.* **19**, 1459 (1951).
Slater, J. C., Koster, G. F., *Phys. Rev.* **94**, 1498 (1954).
Suffczyński, M., *Acta phys. Polon.* **14**, 493 (1955a); Nuovo Cimento **2**, 1320 (1955b); *Bull. Acad. Polon. Sci.* Cl. III, 4, 273 (1956).

SUPPLEMENTARY BOSON-FIELD METHOD AND COLLECTIVE OSCILLATIONS

By Zygmunt Galasiewicz

Institute of Theoretical Physics, Polish Academy of Sciences, Wrocław

(Received May 29, 1956)

In this paper, the method of second quantization is investigated for an ensemble of interacting fermions described by the quantized wave function ψ. The work here is based on the supplementary variables method (D. Zubarev, Candidate's Degree Dissertation, Moscow University, Moscow, 1953). Bohm and Pines, Phys. Rev., **92**, 609 (1953). A supplementary boson field has been introduced into the theory in such a way that the quanta of this field describe the collective motion of an ensemble of fermions (electrons). This is possible, after suitable transformations, since ooperatrs connected with the supplementary boson field appear in the Hamiltonian. It is further shown that the transformation of the Hamiltonian can be regarded as a transition to new fermion operators formed from the old fermion operators and from boson operators associated with the supplementary boson field. The method presented here is compared with the method given in the paper of Tomonaga (*Progr. theor. Phys.* **5**, 544 (1950).

Introduction

In this paper, the method of second quantization is investigated for an ensemble of N mteracting fermions described by the quantized wave function ψ.

The Hamiltonian of such an ensemble has the form

$$H = \frac{h^2}{2m} \int \nabla_{\boldsymbol{r}} \psi^+ (\boldsymbol{r}) \, \nabla_{\boldsymbol{r}} \psi (\boldsymbol{r}) \, d\boldsymbol{r} +$$

$$+ \frac{1}{2} \iint \psi^+ (\boldsymbol{r}_1) \, \psi^+ (\boldsymbol{r}_2) \, V (|\boldsymbol{r}_1 - \boldsymbol{r}_2|) \, \psi (\boldsymbol{r}_2) \, \psi (\boldsymbol{r}_1) \, d\boldsymbol{r}_2 \, d\boldsymbol{r}_1. \tag{1}$$

In this formula, m denotes the mass of the fermion, and $V(r)$, the potential energy of the interaction between the fermions.

Basing ourselves on the supplementary variables method (Zubarev 1953, Bohm and Pines 1953; see also Galasiewicz 1956), we introduce into the theory a supplementary boson field in such a way that the quanta of this field describe the collective motion of the group of fermions (electrons). This will be possible, after suitable transformations, since operators connected with the supplementary boson field appear in the Hamiltonian. There fore we assume that the wave function of the group depends not

only on the occupation numbers of the fermions, but also on the occupations numbers of the bosons associated with the supplementary field. We shall then compare this method with the method presented in the paper of Tomonaga (1950).

Transition to the momentum occupation representation

In order to put operator (1) in the momentum occupation representation, we expand ψ in terms of the eigenfunctions of the momentum operator:

$$\psi = \sum_f a_f e^{ifr} \tag{2}$$

Making the assumption that $V(r)$ is a Coulomb potential we then expand the interaction energy per unit volume in a Fourier series:

$$V(|r_1 - r_2|) = \sum_k{}' \frac{4\pi e^2}{k^2} e^{ik(r_1 - r_2)} \tag{3}$$

($-e$ is the charge of the electron). In summing over k, we have indicated that the term for $k = 0$ was excluded. This corresponds to regarding the electrons as being on the background of the neutralizing ionic charge (see e.g. Bohm and Pines 1952, 1953).

In the momentum occupation representation, the Hamiltonian of the second quantization has the form

$$H = \sum_f \frac{h^2 f^2}{2m} a_f^+ a_f + \frac{1}{2} \sum_k{}' \frac{4\pi e^2}{k^2} \sum_{f_1, f_2} a_{f_1}^+ a_{f_2}^+ a_{f_2+k} a_{f_1-k}. \tag{4}$$

Subsidiary condition

The wave function of the ensemble under consideration depends on the occupation numbers of the momentum configuration space and the occupation numbers of boson quanta of the supplementary field. Since the boson occupation numbers n_k form a set of additional dynamical variables, it is necessary to add certain equations. These equations will correspond to the subsidiary conditions imposed on the wave function in Zubarev's method (1953). In our case, the subsidiary conditions take the form

$$(b_k + b_{-k}^+)\, \varphi = 0, \tag{5}$$

where b_k, b_k^+ are the Fourier amplitudes of the supplementary boson field.

We shall now investigate more closely the restrictions placed on φ by imposition of subsidiary conditions (5). For this purpose, we expand the wave function φ in terms of $|\ldots n_{k'}, \ldots n_{k''} >$:

$$\varphi = \sum_{n_k/0}^{\infty} \sum_{n_{-k}/0}^{\infty} | n_k, n_{-k} > < n_k, n_{-k} | \varphi >. \tag{6}$$

Because of the equality

$$b_k \mid n_k, n_{-k} > = \sqrt{n_k + 1} \mid n_k + 1, n_{-k} >,$$
$$b^+_{-k} \mid n_k, n_{-k} > = \sqrt{n_{-k}} \mid n_k, n_{-k} - 1 >, \tag{7}$$

we may write the subsidiary conditions in the form

$$\sum_{n_k/0}^{\infty} \sum_{n_{-k}/0}^{\infty} \{\sqrt{n_k + 1} < n_k, n_{-k} \mid \varphi > + \sqrt{n_{-k} + 1} < n_k + 1, n_{-k} + 1 \mid \varphi >\} \mid n_k + 1, n_{-k} > +$$
$$+ \sum_{n_{-k}/0}^{\infty} \sqrt{n_{-k} + 1} \mid 0, n_{-k} > < 0, n_{-k} + 1 \mid \varphi > = 0 \tag{8}$$

Therefore

$$< 0, n_{-k} + 1 \mid \varphi > = 0$$

and

$$\sqrt{n_k + 1} < n_k, n_{-k} \mid \varphi > + \sqrt{n_{-k} + 1} < n_k + 1, n_{-k} + 1 \mid \varphi > = 0 \tag{9}$$

for $n_k, n_{-k} \varepsilon [0, \infty]$.

If we introduce the notation

$$< n_k, n_{-k} \mid \varphi > = C\,(n.\ m), \tag{10}$$

then equations (9) can be written

$$C\,(0, m + 1) = 0,$$
$$C\,(n, m) = - \sqrt{\frac{m + 1}{n + 1}}\, C\,(n + 1, m + 1). \tag{11}$$

Because of the symmetry with respect to n and m, we obtain, after brief calculation,

$$C(n, m) = 0 \qquad \text{for } n \neq m$$

and

$$C\,(n.\ n) = - C\,(n + 1, n + 1) = C\,(0,0)\,(-1)^n. \tag{12}$$

Hence

$$\mid C\,(n, n) \mid^2 = \mid C\,(0,0) \mid^2 \tag{13}$$

for $n = 0,1, \ldots \infty$.

Thus the only states in expansion (6) permitted by the subsidiary conditions are those for which the number of bosons with a momentum $\boldsymbol{k}$ is equal to the number of bosons with a momentum $-\boldsymbol{k}$. All these states are equally probable.

Transformation of the subsidiary conditions

Our purpose here is to show that by means of the subsidiary condition (5), we can, with the help of the unitary transformation

$$U = e^{s} = \exp\left\{-\left(\frac{2\pi}{h\omega}\right)^{1/2} e \sum_{f} \sum_{|k|\leqslant k_0} \frac{1}{k} (b_{-k} - b_{k}^{+})\, a_{f-k}^{+}\, a_{f}\right\}, \tag{14}$$

reduce Hamiltonian (4) to a form in which appear terms containing the operators b_k and b_k^+ describing the collective oscillations. The frequency ω appearing in equation (14) will be determined later when we shall transform the Hamiltonian (4). The quantity k_0 is the quantum mechanical equivalent to the quantity $k_D \cong 1/\lambda_D$ appearing in classical plasma theory, where λ_D is the so-called Debye length (see e.g. Bohm and Pines 1952, 1953).

In this connection we shall now consider the transformation of subsidiary conditions (5) with the aid of unitary transformation (14).

The subsidiary conditions can be written

$$U(b_k + b_{-k}^{+})\, U^{+} U\varphi = e^{s}(b_k + b_{-k}^{+})\, e^{-s}\, \Phi = 0 \tag{15}$$

where $\Phi = U\varphi$.

We shall make use of the following relation which holds for any arbitrary operator A:

$$UAU^{+} = e^{s} A\, e^{-s} = A + \frac{1}{1!}[S, A] + \frac{1}{2!}[S, [S, A]] + =$$

$$= A + \sum_{n/1}^{\infty} \frac{1}{n!} \overset{(n)}{[S, A]}. \tag{16}$$

As can be seen from (14), S has the form

$$S = -\left(\frac{2\pi}{h\omega}\right)^{1/2} e \sum_{f} \sum_{|k|\leqslant k_0} \frac{1}{k} (b_{-k} - b_{k}^{+})\, a_{f-k}^{+}\, a_{f}. \tag{17}$$

Operators b_k, b_k^+ satisfy the following commutation relations:

$$\begin{aligned} &b_{k_1} b_{k_2}^{+} - b_{k_2}^{+} b_{k_1} = \delta_{k_1 k_2}, \\ &b_{k_1} b_{k_2} - b_{k_2} b_{k_1} = 0, \\ &b_{k_1}^{+} b_{k_2}^{+} - b_{k_2}^{+} b_{k_1}^{+} = 0. \end{aligned} \tag{18}$$

Employing (16) and taking into account (18), the transformed subsidiary conditions have the form

$$\left[\frac{hk}{2}\left(\frac{\omega}{2\pi h}\right)^{1/2} (b_k + b_{-k}^{+}) - e \sum_{f} a_{f-k}^{+}\, a_{f}\right] \Phi = 0 \tag{19}$$

for $|k| \leqslant k_0$.

We shall make use of these relations when investigating the term in the Hamiltonian corresponding to the Coulomb interaction.

Transformation of the Hamiltonian

We shall now transform the Hamiltonian (4) using the transformation (14). We shall first deal with the part corresponding to kinetic energy. According to (16),

$$U \sum_f f^2 a_f^+ a_f U^+ = \sum_f f^2 a_f^+ a_f + \sum_{n/1}^{\infty} \frac{1}{n!} \left[\overset{(n)}{S}, \sum_f f^2 a_f^+ a_f \right]. \tag{20}$$

If we introduce the notation

$$\left(\frac{2\pi}{h\omega} \right)^{1/2} e \frac{1}{k} (b_{-k} - b_k^+) = a_k \tag{21}$$

(a_k commutes with the operators a_k), then

$$S = - \sum_{|k| \leqslant k_0} a_k \sum_f a_{f-k}^+ a_f. \tag{22}$$

Operators a_k satisfy the following commutation relations:

$$\begin{aligned} a_{k_1} a_{k_2}^+ + a_{k_2}^+ a_{k_1} &= \delta_{k_1 k_2}, \\ a_{k_1} a_{k_2} + a_{k_2} a_{k_1} &= 0, \\ a_{k_1}^+ a_{k_2}^+ + a_{k_2}^+ a_{k_1}^+ &= 0. \end{aligned} \tag{23}$$

Making use of the above, we obtain

$$\left[\overset{(1)}{S}, \sum_f f^2 a_f^+ a_f \right] = 2 \sum_f \sum_{|k| \leqslant k_0} a_k k \left(\frac{k}{2} - f \right) a_{f-k}^+ a_f,$$

$$\left[\overset{(2)}{S}, \sum_f f^2 a_f^+ a_f \right] = 2 \sum_f \sum_{\substack{|k_1| \leqslant k_0 \\ |k_2| \leqslant k_0}} a_{k_1} a_{k_2} (k_1 k_2) a_{f-k_1-k_2}^+ a_f,$$

$$\left[\overset{(3)}{S}, \sum_f f^2 a_f^+ a_f \right] = 0. \tag{24}$$

Therefore

$$\left[\overset{(n)}{S}, \sum_f f^2 a_f^+ a_f \right] = 0 \qquad \text{for } n \geqslant 3 \tag{25}$$

Thus the series of terms in the sum in equation (2) terminates after the second term.

We shall now take up the Coulomb interaction. This can be split into short-range and long-range parts ($k \leqslant k_0, k > k_0$):

$$\begin{aligned} &\frac{1}{2} \sum_k \frac{4\pi e^2}{k^2} \sum_{f_1, f_2} a_{f_1}^+ a_{f_2}^+ a_{f_2+k} a_{f_1-k} \\ &= \left\{ \frac{1}{2} \sum_{|k| \leqslant k_0} + \frac{1}{2} \sum_{|k| > k_0} \right\} \frac{4\pi e^2}{k^2} \sum_{f_1, f_2} a_{f_1}^+ a_{f_2}^+ a_{f_2+k} a_{f_1-k}. \end{aligned} \tag{26}$$

We shall represent the Coulomb interaction in another form. This will be done for two reasons: firstly, in order to utilize subsidiary condition (19) in a simple manner, and secondly, in order to show that the term corresponding to the Coulomb interaction does not undergo any change in consequence of the application of transformation U to the Hamiltonian (4).

If we make use of the relations

$$a_{f_1}^+ a_{f_2}^+ a_{f_2+k} a_{f_1-k} = a_{f_1}^+ a_{f_1-k} a_{f_2}^+ a_{f_2+k} - a_{f_1}^+ a_{f_2+k} \delta_{f_1-k,\, f_2}, \tag{27}$$

and

$$\sum_f a_f^+ a_f = N,$$

then the long-range interaction can be represented in the form

$$\frac{1}{2} \sum_{|k| \leqslant k_0}{}' \frac{4\pi e^2}{k^2} \sum_{f_1} a_{f_1+k}^+ a_{f_1} \sum_{f_2} a_{f_2-k}^+ a_{f_2} - \frac{1}{2} \sum_{k \leqslant k_0}{}' \frac{4\pi e^2}{k^2} N \tag{28}$$

to which subsidiary condition (19) is easily applied. Since we have the following equality holding for the operators (operating on wave function Φ):

$$\sum_f a_{f-k}^+ a_f = \frac{hk}{2e} \left(\frac{\omega}{2\pi h} \right)^{1/2} (b_k + b_{-k}^+) \qquad \text{for } |k| \leqslant k_0 \tag{29}$$

we can then replace the sums $\sum_{f_1} a_{f_1+k}^+ a_{f_1}$ and $\sum_{f_2} a_{f_2-k}^+ a_{f_2}$ in the first term of equation (28) by the corresponding expressions containing the boson amplitudes b_k and b_k^+. This term then becomes

$$\sum_{|k| \leqslant k_0} \frac{h\omega}{4} (b_{-k} + b_k^+) \, (b_k + b_{-k}^+) \tag{30}$$

From the right-side of equation (24.2), we now separate out the terms of which $k_1 + k_2 = 0$:

$$- \frac{4\pi e^2 N}{m} \frac{1}{\omega} \frac{h}{4} \sum_{|k| \leqslant k_0} (b_{-k} - b_k^+) \, (b_k - b_{-k}^+). \tag{31}$$

If we assume that $\omega = \sqrt{\dfrac{4\pi e^2 N}{m}}$ (frequency of the Langmuir oscillations of the plasma), then (31) reduces to the form

$$- \sum_{|k| \leqslant k_0} \frac{h\omega}{4} (b_{-k} - b_k^+) \, (b_k - b_{-k}^+) \tag{32}$$

and can be joined to (30). As a result, we obtain part of the transformed Hamiltonian, which we denote by H_{osc}:

$$H_{osc} = \sum_{|k| \leqslant k_0} h\omega \, (b_k^+ b_k + 1/2) \tag{33}$$

This is the Hamiltonian of the second quantization of oscillators vibrating with the Langmuir frequency. It describes the collective oscillations of an ensemble of fermions. (It can be shown that assuming a Coulomb interaction between fermions, the separation of H_{osc} is possible only if ω is the frequency of the Langmuir oscillations.)

The part of the Hamiltonian corresponding to the Coulomb energy commutes with transformation U. This can be most easily shown by bringing both terms of (26) to the form given in equation (28). Thus, after employing the subsidiary conditions, Hamiltonian (4) transformed with the help of (14) takes the form

$$H' = UHU^+ = \sum_f \frac{h^2 f^2}{2m} a_f^+ a_f + \sum_{|k| \leqslant k_0} \hbar\omega \, (b_k^+ b_k + 1/2) - 1/2 \sum_{k \leqslant k_0} \frac{4\pi e^2}{k^2} N +$$

$$+ \frac{e}{m} \sum_{|k| \leqslant k_0} \sum_f \left(\frac{2\pi h}{\omega}\right)^{1/2} \varepsilon_k \left(\frac{h\boldsymbol{k}}{2} - h\boldsymbol{f}\right) (b_{-k} - b_k^+) \, a_{f-k}^+ a_f + \tag{34}$$

$$+ \frac{e^2}{2m} \sum_{\substack{|k_1| \leqslant k_0 \\ |k_2| \leqslant k_0 \\ k_1 + k_2 \neq 0}} \sum_f \left(\frac{2\pi h}{\omega}\right) (\varepsilon_{k_1} \varepsilon_{k_2}) \, (b_{-k_1} - b_{k_1}^+) \, (b_{-k_2} - b_{k_2}^+) \, a_{f-k_1-k_2}^+ a_f +$$

$$+ \frac{1}{2} \sum_{|k| > k_0} \frac{4\pi e^2}{k^2} \sum_{f_1, f_2} a_{f_1}^+ a_{f_2}^+ a_{f_2+k} a_{f_1-k}$$

where ε_k is a unit vector parallel to vector $\boldsymbol{k}$. This Hamiltonian describes interacting fermions by means of a short range (screened — see Bohm and Pines 1953) Coulomb potential, bosons with an energy $h\omega \left(\omega = \sqrt{\frac{4\pi e^2 N}{m}}\right)$ and an interaction between the bosons and fermions. (In Zubarev's paper (1953), Hamiltonian (34) was obtained by a method different from that given here.)

Transition to new fermion operators

The transformation of Hamiltonian (4) with the help of (14) can be regarded as a transition from operators a_k to new operators A_k. Thus $H' = UHU^+$ can also be written in the form

$$H' = \sum_f \frac{h^2 f^2}{2m} A_f^+ A_f + \frac{1}{2} \sum_k{}' \frac{4\pi e^2}{k^2} \sum_{f_1, f_2} A_{f_1}^+ A_{f_2}^+ A_{f_2+k} A_{f_1-k} \tag{35}$$

where $A_f = U a_f U^+$.
Using equation (16), we obtain

$$A_f = U a_f U^+ = a_f + \sum_{n/1}^{\infty} \frac{1}{n!} [S, a_f]^{(n)}. \tag{36}$$

Taking into account (22) and (23), we calculate the respective commutator brackets

$$\overset{(1)}{[S, a_f]} = \sum_{|k|\leqslant k_0} a_k a_{f+k}, \tag{37}$$

$$\overset{(2)}{[S, a_f]} = \sum_{\substack{|k_1|\leqslant k_0 \\ |k_2|\leqslant k_0}} a_{k_1} a_{k_2} a_{f+k_1+k_2} \tag{38}$$

By induction, it can be shown that

$$\overset{(n)}{[S, a_f]} = \sum_{\substack{|k_1|\leqslant k_0 \\ |k_n|\leqslant k_0}} a_{k_1} a_{k_2} \cdots a_{k_n} a_{f+k_1+k_2++k_n}. \tag{39}$$

Hence, after replacing a_k from (21) we obtain

$$A_f = a_f + \sum_{n/1}^{\infty} \frac{\beta^n}{n!} \sum_{|k_1|\leqslant k_0} \cdots \sum_{|k_n|\leqslant k_0} \frac{(b_{-k_1} - b_{k_1}^+)}{k_1} \cdots \frac{(b_{-k_n} - b_{k_n}^+)}{k_n} a_{f+\sum_{j/1}^{n} k_j},$$

$$A_f^+ = a_f^+ + \sum_{n/1}^{\infty} \frac{(-\beta)^n}{n!} \sum_{|k_1|\leqslant k_0} \cdots \sum_{|k_n|\leqslant k_0} \frac{(b_{-k_1} - b_{k_1}^+)}{k_1} \cdots \frac{(b_{-k_n} - b_{k_n}^+)}{k_n} a^+_{f-\sum_{j/1}^{n} k_j} \tag{40}$$

where $\beta = \left(\frac{2\pi}{h\omega}\right)^{1/2} e$ is a small parameter.

U is a unitary transformation, and therefore, operators A_f, like operators a_f, describe a fermion field. From the point of view of the operator (35) acting on the wave function $\Phi = U\psi$ operators A_k, A_k^+ are „old" and operators a_k, a_k^+ „new")

Comparison with Tomonaga's method

The use of Zubarev's and Bohm and Pines idea of supplementary variables (1953) for investigating a group of interacting fermions on the basis of a second quantization gives us a new possibility for comparing the elementary perturbation method of the plasma oscillation type with the method proposed by Tomonaga (1950).

Since the operators A_f describe a fermion field, the "fermion branch" in the energy spectrum is conserved. The new operators are constructed from fermion operators a_k and from boson operators b_k associated with the boson field. As a result, there appears in the Hamiltonian a quanta energy corresponding to the collective oscillations. This problem was solved for the three-dimensional case.

In the method proposed by Tomonaga, a transition is made from operators a_k which describe a fermion field, to operators ϱ_k, which describe a boson field. Here the "fermion branch" does not appear in the energy spectrum. The boson operators ϱ_k are constructed from the fermion operators a_k. The problem was solved for the one--dimensional case.

I would like to thank Professor M. Günther for helpful discussion.

КРАТКОЕ СОДЕРЖАНИЕ

З. Галясевич, *Метод „добавочного" бозонового поля, а коллективное колебание*

В работе изучается посредством метода вторичного квантоваыия система воздействующих фермионов, описанный сквантованной волновой функцией ψ. По примеру метода пере- „добавочных" менных (Зубарев Д. Кандидатская дисеертация, Московский Университет, Москва 1953 Бохм и Пинес, Phys. Rev., **92**, 609 (1653), введено в теорию „добавочное" бозоновое поле так, чтобы кванты этого поля описывали коллективное движение системы фермионов (электронов). Это возможно после соответствующих преобразований, когда в гамильтониане появятся операторы, связанные с „добавочным" бозоновым полем. Дальше доказано, что преобразование гамильтониана можно считать переходом к новым фермионовым операторам, построенным из старых фермионовых операторов и операторов бозоновых, связанных с „добавочным" бозоновым полем. Представленный метод сравнен с методом в труде Томонаго [Progr. Theor. Phys. **5**, 544 1950)].

REFERENCES

Bohm, D. and Pines, D., *Phys. Rev.* **85**, 338 (1952); **92**, 609 (1953).

Galasiewicz, Z., *Acta phys. Polon.* **15**, 49 (1956).

Tomonaga, S., *Progr. theor. Phys.* **5**, 544 (1950).

Zubarev, D., Candidate's Degree Dissertation, Moscow University, Moscow, 1953.

A POSSIBLE EXPLANATION OF THE DIURNAL VARIATION IN THE INTENSITY OF THE NIGHT GLOW LINE (0 I) 5577 Å

By Ludwik Liszka

Institute of Experimental Physics, Jagiellonian University, Cracow

(Received June 2, 1956)

This paper discusses a possible explanation for the diurnal changes in the intensity of the green line of the night glow. These changes may be evoked by periodic changes of pressure in the upper layers of the atmosphere arising from the tidal activity of the sun and the moon.The correctness of the above hypothesis can be confirmed by investigating the relation between the position of the moment of maximum green line intensity and the lunar phase. It can be seen from the curve drawn on the basis of published curves of green line intensity changes available to the author that such a relationship actually exists.

Photometry of the night glow spectrum provides very interesting results. Among those facts which have been established is the occurrence of diurnal variations in the intensity of the green line 5577 Å arising from the forbidden transition $^1S_0 \rightarrow {}^1D_2$ of neutral oxygen. The character of these changes is rather curious and so far has not been fully explained. The intensity of the green line increases during the night, generally achieving a sharp maximum in the interval between 23 *h.* and 03 *h.* local time, and then decreases. Up to the present, there has been no explanation in the literature on this question of the changes of the position of the maximum green line intensity during the night. Some possibility of explaining this phenomenon is provided by considering the general conditions under which the forbidden transitions occur. The green line arises, as mentioned above, as a result of the transition of the atom from the $^1S_0$ state to the $^1D_2$ state. They are both metastable states of the oxygen atom. The oxygen atom, excited to the state $^1S_0$ can remain in this state a relatively long time (mean life is 0.5 sec) and make the transition to one of the lower levels. The atom may leave the metastable state by:

1) dropping to a lower energy level with the radiation of a quanta,

2) absorption of radiation — the atom makes a transition to a higher energy level,

3) a collision of the second kind with another atom or molecule,

4) a collision with an electron — the excitation energy of the atom is entirely converted into the kinetic energy of the electron.

The probability of the transition from a metastable state by means of a collision of the second kind with atoms and particles is, in general, very great when the gas density is high. This explains the fact that it is very difficult to obtain the forbidden radiation in pure gases under laboratory conditions. The excitation energy of the atoms or molecules causing the transition from the metastable states must be less than the energy for exciting the atom to the metastable state. If the excitation energy of the lowest excited level of the atoms causing the transition from the metastable state is greater than the energy of the metastable state, an elastic collision occurs without the loss of energy. For example, the oxygen atom can remain in the metastable state in an atmosphere of inert gases, since their lowest excitation energy is several times greater than the energy of the metastable state. Use is made of this in obtaining forbidden radiation under laboratory conditions. If there are present atoms which can cause transitions in atoms in a metastable state, radiation of the forbidden lines can occur only when

$$\tau\varepsilon \leqslant \vartheta \tag{1}$$

where τ is the mean time between two such collisions, ϑ is the mean lifetime of the metastable state, and ε is the efficiency coefficient for the collision. The mean number of collisions which suffices to cause the transition from the metastable state is given by the value of $\frac{1}{\varepsilon}$. This is a first approximation of the problem; it assumes that all atoms have the same lifetime. In reality, many atoms have a shorter lifetime in the metastable state.

Transitions from metastable states of atmospheric oxygen are probably caused by molecular nitrogen and oxygen. These molecules have densely distributed energy levels very near the metastable energy levels of oxygen. In this case can be taken roughly as equal to unity.

It is well-known from molecular physics that

$$\tau = \varkappa \frac{\sqrt{T}}{p} \tag{2}$$

where p is the gas pressure, T is the temperature, and $\varkappa$ is a constant for the given gas. At constant temperature, τ depends only on p. As a result of condition (1) the forbidden radiation can occur only from a certain value:

$$p_d \leqslant \varkappa \frac{\sqrt{T}}{\vartheta} \tag{3}$$

If we consider the possibility of forbidden radiation arising in the earth's atmosphere, we see that this can occur in those layers beginning at a height h_d corresponding to a pressure p_d.

For the sake of simplicity, we assume here that the temperature of these layers is constant and equal to 240°K.

We shall calculate the intensity of forbidden radiation falling within a unit solid angle. Small zenith distances will be taken for simplicity. It can be seen from Fig. 1 that the intensity dI arising from an element of volume at a height h is proportional to the number of excited atoms in unit volume $n\,(h)$, to the size of the element and inver-

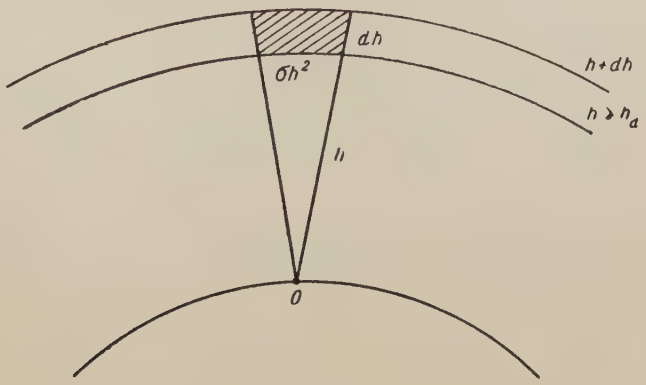

Fig. 1

sely proportional to the square of the distance from the observer O. The element of volume is cut out from a layer of thickness dh by a unit solid angle and has a base proportional to h^2 and height dh. We can write

$$dI = \alpha \frac{n\,(h)\,h^2\,dh}{h^2} = \alpha\, n(h)\,dh \tag{4}$$

where α is a proportionality factor.

The complete intensity will be

$$I = \alpha \int_{h_d}^{\infty} n(h)\,dh \tag{5}$$

For heights greater than h_d, the number of excited atoms in a unit volume will be proportional to the total number of oxygen atoms under consideration. It can be assumed that the number of excited atoms changes in accordance with the function

$$n\,(h) = n_0\, e^{-\beta h} \tag{6}$$

Substituting this into the expression for I

$$I\,(h_d) = \alpha n_0 \int_{h_d}^{\infty} e^{-\beta h}\,dh = \frac{\alpha\, n_0}{\beta}\, e^{-\beta h_d} \tag{7}$$

We thus see that changes in intensity of the forbidden lines will take place when changes of pressure, and therefore of height h_d, occur in the upper layers of the atmosphere.

It so happens that such changes of pressure in the earth's atmosphere actually occur. From the theory of atmospheric tides it is known that as a result of the gravitational effects of the sun and moon, tides arise in the atmosphere. Maximum rarefaction occurs at the time of the lower culmination of the sun and moon. During the new moon the effect is additive. On the surface of the earth this tide phenomenon is very weak and therefore it is difficult to establish. The amplitude of the solar tidal wave is 0.26% of the barometric pressure. The activity due to the moon is still weaker. The amplitude of the lunar wave is barely 1/16 of the solar wave amplitude. The phenomenon is quite distinct in upper layers of the atmosphere. It is known from Appleton and Weekes' investigation of the behaviour of radio waves in the E region of the ionosphere that at this height (above 100 km), the amplitude of the lunar wave is about 10% of the static pressure. If we denote the change of pressure resulting from the tide (caused by the moon) by Δp and the static pressure by p_0, then the relative change of pressure will be

$$\left(\frac{\Delta p}{p_0}\right)_{h=100\text{ km}} = 10^4 \left(\frac{\Delta p}{p_0}\right)_{h=0} \tag{8}$$

There the solar amplitude is greater by nearly one order of magnitude.

Let us return to the calculation of the effect of a change in pressure on the intensity of the forbidden line. For the increase in intensity we obtain the equation

$$\Delta I(h_d) = \frac{dI}{dh_d}\,\Delta h_d = -\alpha n_0 e^{-\beta h_d}\,\Delta h_d \tag{9}$$

The relative change in intensity will be

$$\frac{\Delta I}{I} = -\beta \Delta h_d \tag{10}$$

The quantity Δh_d can be calculated if we know the change of pressure Δp at height h_d, since

$$p(h) = p_0 e^{-\gamma h} \tag{11}$$

(for the earth's atmosphere $\gamma = 1.5 \times 10^{-4}$ cm^{-1}) then

$$\Delta h_d = \frac{1}{\gamma p(h_d)}\,\Delta p(h_d) \tag{12}$$

These formulae connect the relative increase in intensity of the forbidden line with changes of pressure in the upper atmosphere.

We see that in considering the conditions giving rise to forbidden radiation from oxygen in the atmosphere, the density changes resulting from the tides cannot be ignored. Around the time of the new moon the tidal waves add to each other; maximum rarefaction, and therefore, maximum green line intensity, does not however occur at midnight, local time, but about one hour afterwards (analogous to the port time in marine tides) as a result of the inertia of the atmosphere. After the new moon, the maxi-

mum of the lunar wave occurs later, and before the new moon, it occurs earlier. The resultant maximum rarefactions and the maximum green line intensities which accompany them should be similarly distributed in time. The photometry of the night sky spectrum can be made only around the time of the new moon, since, in this period, the light of the moon will cause no interference. The correctness of the above explanation can be checked by investigating the correlation between the position of the maximum green line intensity and the lunar phase. With this aim in mind, the times of

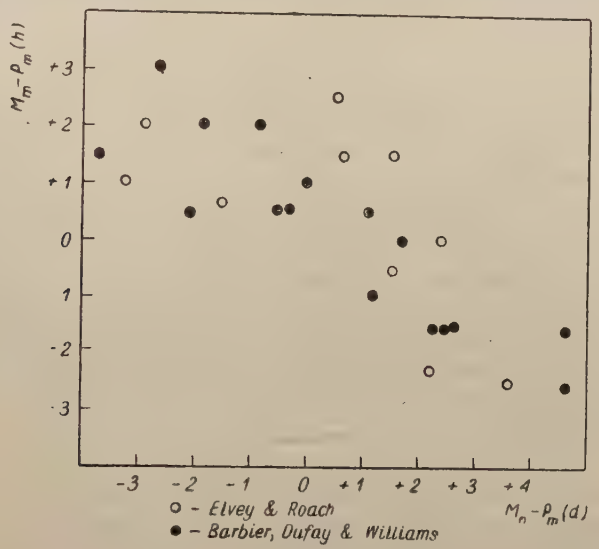

Fig. 2

maximum green line intensity for different nights were taken from curves published by Elvey and Roach, and Barbier, Dufay and Williams; the corresponding times of the new moon were taken from issues of the „Nautical Almanac". Denoting the time of the maximum by M_m, the time of the new moon by M_n, local midnight by P_m, the time interval $M_m - P_m$ in hours and $M_n - P_m$ in days, were calculated for the 26 curves that were used. I used all the curves published by Elvey. Of those published by Barbier (where the accuracy of the measurements and of the reading of the maximum point was considerably less) only the curves with a distinct maximum were used. Some curves (especially Elvey's) had a secondary maximum weaker than the main one. In these cases also, the times corresponding to the main maximum were taken. The data gathered cover the period running from the fourth night immediately preceding the new moon to the fifth night immediately following .The times of the maxima, and therefore the intervals $M_m - P_m$ are determined to an error of $\pm$ 0.5 h. The curve shown represents the time interval $M_m - P_m$ as the function of the lunar phase, and therefore of the time interval $M_n - P_m$. The appearance of a distinct dependence between the moment when maximum green line intensity occurs and the lunar phase

seems to support the correctness of the suggested explanation. The discrepancies which appear can be explained not only by errors of measurement, but also by the dependency of the magnitude of the tides on the distance between the earth and the moon at the time of the new moon; this distance is known to be variable. For a final confirmation of the hypothesis presented, and of the curves obtained (Fig. 2), it is necessary to make a considerably greater number of observations.

In conclusion, I would like to thank Professor H. Niewodniczański for his valuable remarks on the problem of forbidden radiation and for his helpful discussion on the above problem.

КРАТКОЕ СОДЕРЖАНИЕ

Л. Лишка, *О некоторой возможности объяснения суточных изменений напряжения зелёной линии свечения ночного неба* OI *5577* Å.

Настоящая работа занимается некоторой возможностью объяснения суточных изменений напряжения зелёной линии свечения ночного неба. Они могут быть вызваны периодическими изчененіями в высоких слоях атмосферы. Происходят они от приливного действия солнца и луны. Справедливость вышеупомянутой гипотезы можно удостоверить, изучая зависимость между положением момента максимальной интенсивности зелёной линии и фазой луны. Из диаграммы, совершенной на основании доступных автору опубликованных кривых изменений интенсивности зелёной линии, видно, что такая зависимость существует в самом деле.

REFERENCES

Appleton, E. V., Weekes, K., *Proc. Roy. Soc.* Ser A. 71 (1939).
Barbier, D., Dufay, T., Williams, D., *Observ. Haute-Provence* Vol. 2, No. 26 (1951).
Elvey, C. T., Roach, F. E., *Journ. Geophys. Res.* (1952).
Wilkes, H., *Oscillations of the Earth's Atmosphere*, Cambr. Univ. Press. (1949).

HALBKLASSISCHES BILD DER SPINWELLE IM FERRIMAGNETIKUM

Von H. Cofta

Laboratorium für Ferromagnetika des Physikalischen Instituts der Polnischen Akademie der Wissenschaft, Poznań

(Eingegangen am 4 Juni 1956)

Im ersten Teil ist eine kurze Begründung des halbklassischen Spinwellenbildes angegeben. Dabei wird eine Differenzengleichung für die lineare Atomkette gebraucht, anstatt der oft benutzten Differentialgleichung für die kontinuierliche Spinverteilung.

Im Hauptteil sind die durch Keffer, Kaplan und Yafet auf Grund des halbklassischen Spinwellenbildes für Ferromagnetika und Antiferromagnetika hergeleiteten Dispersionformeln $\omega(k)$, auf den Fall des Ferrimagnetismus und Antiferrimagnetismus im Sinne von Smart verallgemeinert. In der Smartschen Nomenklatur bedeutet der Ferrimagnetismus gleichgerichtete Nachbarspins, und der Antiferrimagnetismus — entgegengesetzt gerichtete. In beiden Fällen ergibt sich eine gleichartige Abhängigkeit $\omega(k) \sim k^2$, die mit dem makroskopischen Verhalten beider Magnetikumstypen übereinstimmt. Die Formel $\omega(k) \sim k$ für Antiferromagnetismus lässt sich nicht durch gewöhnlichen Grenzübergang $S_2 \to S_1$, d. h. durch Betrachtung des Antiferromagnetismus als speziellen Fall des Antiferrimagnetismus, erhalten.

I. Die Spin-Präzessionswelle

Spinwellen treten bekanntlich schon in der Theorie auf, die auf dem Heisenbergschen Modell gestützt ist. Die physikalische Deutung der Lösungen des Bloch-Slaterschen Gleichungssystems führt nämlich zu einer Spinumkehrungs-Welle. Ein genaueres Bild dieser Erscheinung erhält man, wenn man aus der quantenmechanischen Bewegungsgleichung für den m-ten Spin ausgeht (die sogenannte phänomenologische Auffassung, s. Heller u. Kramers 1934)

$$ih \frac{d\hat{\vec{S}}_m}{dt} = [\hat{\vec{S}}_m, \hat{\mathcal{H}}], \tag{1}$$

wobei $\hat{\mathcal{H}}$ der Energie-Operator des Systems und $\hat{\vec{S}}_m$ der Spindrehimpulsoperator für das m-te Atom ist (hier hat er die Dimension des Drehimpulses). Wird die Austauschenergie durch die Diracsche Formel (Dirac 1947) ausgedrückt, dann ist die Gesamt-

energie $\hat{\mathcal{H}}$ in einem konstanten magnetischen Feld $\vec{H}_0$ gleich

$$\hat{\mathcal{H}} = -\mu_0 \gamma \sum_j \hat{\vec{S}}_j \vec{H}_0 - \frac{1}{\hbar^2} \sum_{i \neq j} \sum A_{ij} \hat{\vec{S}}_i \cdot \hat{\vec{S}}_j, \tag{2}$$

wobei $\gamma = e/m$ der giromagnetische Faktor für Spinmomente und A_{ij} das Austauschintegral zwischen dem i-ten und j-ten Spin bedeutet. Setzen wir $\hat{\mathcal{H}}$ in die Gl. (1) ein, so lässt sich der Kommutator zur rechten Seite auf Grund der Vertauschungsrelationen umformen (siehe Herring u. Kittel 1951, Appendix A) und dann ergibt sich

$$\frac{d\hat{\vec{S}}_m}{dt} = \hat{\vec{S}}_m \times \left\{ \mu_0 \gamma \vec{H}_0 + \frac{2}{\hbar^2} \sum_j A_{mj} \hat{\vec{S}}_j \right\} \tag{3}$$

Der Übergang von den Operatoren zu den Erwartungswerten ist mit dem Übergang zum halbklassischen Bild gleichbedeutend. Dieses Bild ist selbstverständlich vom streng quantentheoretischen verschieden. Z. B. im Falle der linearen Atomkette haben wir in halbklassischer Näherung die Gleichung (wenn wir nur Austauschwirkungen zwischen den Nachbaratomen berücksichtigen)

$$\frac{d\vec{S}_m}{dt} = \vec{S}_m \times \left\{ \mu_0 \gamma \vec{H}_0 + \frac{2A}{\hbar^2} (\vec{S}_{m+1} + \vec{S}_{m-1}) \right\} \tag{4}$$

Ihre physikalische Deutung ist leicht ersichtlich, wenn wir zur rechten Seite ein Nullglied

$$-\vec{S}_m \times \frac{4A}{\hbar^2} \vec{S}_m \tag{5}$$

hinzufügen und erhalten so

$$\frac{d\vec{S}_m}{dt} = \vec{S}_m \times \left\{ \mu_0 \gamma \vec{H}_0 + \frac{2A}{\hbar^2} [(\vec{S}_{m+1} - \vec{S}_m) - (\vec{S}_m - \vec{S}_{m-1})] \right\}. \tag{6}$$

Diese Gleichung ist vom Typus einer Präzessionswellengleichung, weil das Glied

$$(\vec{S}_{m+1} - \vec{S}_m) - (\vec{S}_m - \vec{S}_{m-1})$$

eine zweite Differenz darstellt und damit der zweiten Ableitung entspricht. Die strenge quantenmechanische Gleichung ist nicht von demselben Charakter, da für die Operatoren der Ausdruck (5) infolge der Unvertauschbarkeit von Spinkomponenten nicht verschwindet.

Die exakte Lösung von Gl. (4) bzw. der äquivalenten Gl. (6) ergibt eine Spin-Präzessionwelle

$$\vec{S}_m = \vec{S}_{mz} + \vec{B} \cos \varphi_m(t) + \vec{C} \sin \varphi_m(t) \tag{7}$$

mit $\varphi_m(t) = akm - \omega t$

Dabei muss $\vec{S}_{mz} \perp \vec{B} \perp \vec{C}$ und $|\vec{B}| = |\vec{C}|$ gelten. Die Konstante a bedeutet hier den Abstand zwischen Nachbaratomen. Die Wellenzahl k ist mit ω mittels der Beziehung

$$\omega = \mu_0 \gamma H_0 + \frac{4A}{\hbar^2} (1 - \cos ak) S_{mz} \tag{8}$$

gebunden. Der Ausdruck (7) ist eine Lösung der Gl.(6) nur dann, wenn $\vec{S}_{mz}$ die vektorielle Komponente von $\vec{S}_m$ um die durch $\vec{H}_0$ festgelegte z-Achse ist. Dieser Vektor $\vec{H}_0$ setzt also die Richtung der Präzessionsachse fest und die Winkelgeschwindigkeit der Präzession können wir wie folgt schreiben

$$\vec{\omega} = \pm \left\{ \mu_0 \gamma \vec{H}_0 + \frac{4A}{\hbar^2} (1 - \cos ak) \vec{S}_{mz} \right\} . \tag{9}$$

Die Richtung der Präzessionsachse ist für sämtliche Atome dieselbe. Die Rolle des konstanten Vektors $\vec{H}_0$ wird von der Resultante des äusseren Magnetfeldes und des Anisotropiefeldes gespielt. Auch ein drittes Glied kann mit inbegriffen werden, nämlich ein Ersatzfeld $\vec{H}_c$ für den Einfluss von Leitungselektronen. Nach Heber (1952a, 1952b, 1953) lässt sich dieser Einfluss näherungsweise dadurch beschreiben, dass in den Klammern auf der rechten Seite von (3) noch ein weiteres Glied $\varkappa \vec{S}_0$ erscheint, das zum Gesamtspin $\vec{S}_0$ aller n Atome proportional ist. Der Zustand mit einer Spinwelle ist der absoluten Sättigung so nahe, das der Vektor $\vec{S}_0$ als konstant betrachtet werden kann, und somit

$$\vec{H}_c = \frac{\varkappa}{\mu_0 \gamma} \vec{S}_0$$

Da $\vec{H}_c$ als Summand des Vektors $\vec{H}_0$ auftreten kann, dürfte sich die Beteiligung von Leitungselektronen in dem Betrag des Larmorschen Gliedes der Winkelgeschwindigkeit äussern, natürlich in sehr tiefen Temperaturen. Die Präzessionswelle schreitet also nach (7) in solcher Weise fort, dass die Phasendifferenz Θ zwischen Nachbaratomen gleich

$$\Theta = \varphi_{m+1} - \varphi_m = ak \tag{10}$$

ist. Für kleine Wellenzahlen $k \ll (1/a)$ wird $1 - \cos ak \approx \frac{1}{2} a^2 k^2$ und (8) geht in die bekannte Formel

$$\omega = \mu_0 \gamma H_0 + \frac{2A}{\hbar^2} a^2 k^2 S_{mz} \tag{11}$$

über, die sich aus der Präzessionswellengleichung für das kontinuierliche Spinvektorfeld ergibt (siehe z. B. Döring 1948).

II. Spinwellen in einem ferromagnetischen und antiferromagnetischen Medium nach Auffassung von Keffer, Kaplan und Yafet

Zusammenfassend können wir sagen, dass das halbklassische Bild der Spinwelle sich auf dem Vektormodell eines um eine feste Achse präzessierenden Spins stützt. Im Grundzustand ist für jeden Gitterpunkt $|S_{mz}| = S_{max}$, worin S_{max} den maximalen Betrag der Spinvektorkomponente bezeichnet. Für den ersten angeregten Zustand gilt $|S_{mz}| = S_{max} - (1/n)$ (siehe Heller u. Kramers 1934). In den höheren Zuständen wird S_{mz} noch weiter vermindert, weil jede weitere Spinwelle die $|S_{mz}|$ um $1/n$ verkleinert; der Präzessionsradius

$$R = \sqrt{S_x^2 + S_y^2}$$

nimmt dadurch mit der Temperatur zu[1].

Unter Anwendung dieses einfachen geometrischen Modells, haben Keffer, Kaplan und Yafet (1953) auf elementarem Wege die angenäherte Abhängigkeit ω (k) für Ferromagnetika abgeleitet[2], nämlich

$$\omega = \mu_0 \gamma H_0 - \frac{2A}{\hbar^2} a^2 k^2 S \tag{11a}$$

Der Unterschied mit (11) besteht nur darin, dass anstatt der Komponente S_z der absolute Betrag S des Spinvektors auftritt. (Das Vorzeichen des Austauschgliedes stimmt mit (11) überein, weil $\vec{S}$ gegenüber $\vec{H}_0$ die entgegengesetzte Richtung hat.) Auf ähnliche Weise haben die obengenannten Verfasser auch die analoge Formel für Antiferromagnetika erhalten, nämlich

$$\omega \approx \mu_0 \gamma H_0 \pm \frac{2A}{\hbar^2} S \cdot ak \tag{12}$$

die schon früher auf anderem Wege abgeleitet worden ist (s. Hulthén 1936 und Anderson 1952). Dabei hat es sich erwiesen, dass bei abwechselnd gerichteten Nachbarspins eine Präzessionswelle im strengerem Sinne (d. h. ω wird für alle Atome gleich) nur dann durchlaufen kann, wenn der Präzessionsradius R_p für Rechtsspins von dem Präzessionsradius R_l für Linksspins verschieden wird. Infolgedessen werden auch die Komponenten S_z für die beiden Spinrichtungen verschieden und damit wird eine resultierende Komponente $\sum_m^n S_{mz} \neq 0$ des ganzen Gitters auftreten. Das Zeichen dieser Resultante, wie das Keffer (1952) erwiesen hat, hängt noch vom Wellentypus ab (es kann nämlich entweder $R_p < R_L$ oder $R_p > R_L$ sein), und ihr Betrag nimmt für jede erregte Spin-

[1] R hat die Dimension eines Drehimpulses.

[2] Dazu genügt eine Betrachtung der linearen Kette. Im Folgenden werden wir uns nur auf diesen Fall beschränken.

welle desselben Typus um $\hbar$ zu. Die Gleichberechtigung beider Wellentypen führt zu Antiferromagnetismus. Bei Überlegenheit nur eines Wellentypus haben wir dagegen Ferrimagnetismus, obwohl alle Spinvektoren gleichen absoluten Betrag haben.

III. Spinwellen in einem beliebigen Ferrimagnetikum

Die Betrachtungen von Keffer, Kaplan u. Yafet können für den Fall verschiedener Beträge $S_1 \neq S_2$ benachbarter Spinvektoren verallgemeinert werden. Es wird bequem sein hier die Nomenklatur, die Smart (1955, S. 369) vorgeschlagen hat, zu übernehmen. Mit dem Namen „Ferrimagnetismus" werden wir nämlich den Fall bezeichnen, wo die benachbarten Spinvektoren gleichgerichtet sind, mit „Antiferrimagnetismus" dagegen einen solchen mit entgegengesetzten Nachbarspinvektoren. Noch allgemeiner: wir werden über „Ferrimagnetismus" reden, wenn die Spinvektoren in verschiedenen Gitter-Überstrukturen gleichgerichtet sind, über „Antiferrimagnetismus" dagegen, wenn diese entgegengesetzt sind. Mithin werden wir den Ferrimagnetismus im Néelschen Sinne als Antiferrimagnetismus bezeichnen. Bei einer solchen Nomenklatur erweist sich der Ferromagnetismus als spezieller Fall des Ferrimagnetismus für $S_1 = S_2$ und der Antiferromagnetismus als spezieller Fall von Antiferrimagnetismus für $S_1 = S_2$.

a) Der ferrimagnetische Fall

Auf ähnliche Weise wie bei Keffer, Kaplan und Yafet und mit denselben Näherungen werden wir die Beziehung $\omega(k)$ für das ferrimagnetische Medium im Sinne von Smart herleiten. Einfachheitshalber setzen wir $H_0 = 0$, da das Larmorsche Glied in allen behandelten Fällen identisch bleibt.

Bezeichnen wir die Summe benachbarter Spinvektoren $\vec{S}_{m-1} + \vec{S}_{m+1}$ durch $\vec{\Sigma}_1$, wenn beide Vektoren zur Überstruktur I gehören, und durch $\vec{\Sigma}_2$, wenn sie zur Überstruktur II gehören, dann ist nach Gl. (4) das auf den m-ten Spinvektor wirkende Drehmoment für die Überstruktur I

$$G_1 = \frac{2A}{\hbar^2} S_1 \Sigma_2 \sin \Phi_1 \tag{13a}$$

und für die Überstruktur II

$$G_2 = -\frac{2A}{\hbar^2} S_2 \Sigma_1 \sin \Phi_2 \tag{13b}$$

gleich (S. Abb. 1.). Wegen der Kleinheit von θ, Φ_1 und Φ_2 können wir

$$\Sigma_1 \approx 2S_1 \qquad \Sigma_2 \approx 2S_2$$

$$\sin \Phi_1 \approx \frac{x}{S_1} \qquad \sin \Phi_2 \approx \frac{y}{S_2} \approx \frac{y}{S_1} \tag{14}$$

setzen. Für die Präzessionsbewegung gilt

$$\omega = \frac{G}{R} \tag{15}$$

daher führt die Forderung

$$\omega_1 = \omega_2 = \omega \tag{16}$$

zu der Bedingung

$$\frac{x}{R_1} = -\frac{y}{R_2} \tag{17}$$

Mit Hilfe von elementaren geometrischen Überlegungen berechnet man (siehe Keffer, Kaplan u. Yafet 1953, Fig. 1)

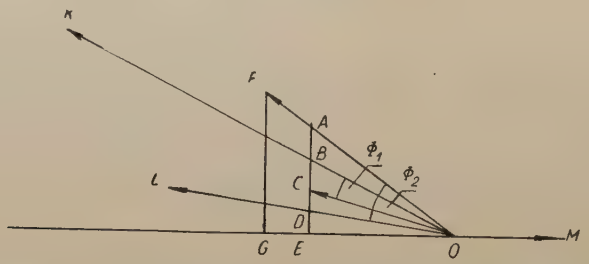

Abb. 1 Achsenschnitt durch die betrachtete Prazessionskegeln im Falle des Ferrimagnetismus

$S_1 = OC$ $\quad R_1 = EC$ $\quad H_0 = OM$
$S_2 = OF$ $\quad R_2 = GF$
$S_1' = OA$ $\quad R_1' = EA$
$\Sigma_1 = OL$ $\quad x = CB$
$\Sigma_2 = OK$ $\quad y = DA$

$$x = R_2' - R_1 - \frac{1}{2} a^2 k^2 R_2'$$

$$y = R_2' - R_1 + \frac{1}{2} a^2 k^2 R_1 \tag{18}$$

also

$$\frac{x}{R_1} = \frac{-y}{R_2} = \frac{x - y}{R_1 + R_2} \tag{19}$$

Da in diesem Ausdruck nur noch Summen auftreten, können wir annähernd schreiben (s. Abb. 1)

$$R_1 \approx R_2' = \frac{S_2'}{S_2} R_2 \approx \frac{S_1}{S_2} R_2. \tag{20}$$

Damit wird

$$\frac{x}{R_1} = -a^2 k^2 \frac{S_1}{S_1 + S_2} \tag{21}$$

und schliesslich

$$\omega = -\frac{4A}{\hbar^2}\frac{S_1 \cdot S_2}{S_1 + S_2} a^2 k^2 \tag{22}$$

Für $S_1 = S_2 = S$ geht die abgeleitete Formel in die Abhängigkeit (11a) mit $H_0 = 0$ über

b) Der antiferrimagnetische Fall

Die analoge Beziehung für das antiferrimagnetische Medium wird im Folgenden an Hand von Abbildung 2 hergeleitet. Mit den oben angeführten Bezeichnungen ergibt sich

$$G_1 = -\frac{2A}{\hbar^2} S_1 \Sigma_2 \sin(\pi - \Phi_1) \text{ für Überstruktur I,}$$

$$G_2 = \frac{2A}{\hbar^2} S_2 \Sigma_1 \sin(\pi - \Phi_2) \text{ für Überstruktur II} \tag{23}$$

und mit den Näherungen (14)

$$G_1 = -\frac{4A}{\hbar^2} S_2 x,$$

$$G_2 = \frac{4A}{\hbar^2} S_2 y. \tag{24}$$

Es gilt nun

$$\omega_1 = \frac{G_1}{R_1}, \quad \omega_2 = -\frac{G_2}{R_2} \tag{25}$$

mithin ergibt die Bedingung (16)

$$\frac{x}{R_1} = \frac{y}{R_2}. \tag{26}$$

Ähnlich wie im vorhergehenden Falle kann man

$$x = R_2' - R_1 - \frac{a^2 k^2}{8} R_2'$$

$$y = R_2' - R_1 + \frac{a^2 k^2}{8} R_1 \tag{27}$$

erhalten (siehe Keffer, Kaplan u. Yafet 1953, Fig. 2) und daher

$$R_2' - R_1 = \frac{a^2 k^2}{8} \frac{R_2 R_2' + R_1^2}{R_2 - R_1} \tag{28}$$

Für kleine k wird also

$$\frac{x}{R_1} = \frac{y}{R_2} = \frac{x+y}{R_1 + R_2} = \left(2 - \frac{a^2 k^2}{8}\right) \frac{R_2' - R_1}{R_2 + R_1} \approx 2 \frac{R_2' - R_1}{R_2 + R_1}$$

$$= \frac{a^2 k^2}{4} \frac{R_2 R_2' + R_1^2}{R_2^2 - R_1^2} \tag{29}$$

Mit den Näherungen (20) erhält man

$$\frac{x}{R_1} \approx \frac{a^2 k^2}{4} \frac{\frac{S_2}{S_1} R_1^2 + R_1^2}{\left(\frac{S_2}{S_1}\right)^2 R_1^2 - R_1^2} = \frac{a^2 k^2}{4} \cdot \frac{S_1}{S_2 - S_1} \tag{30}$$

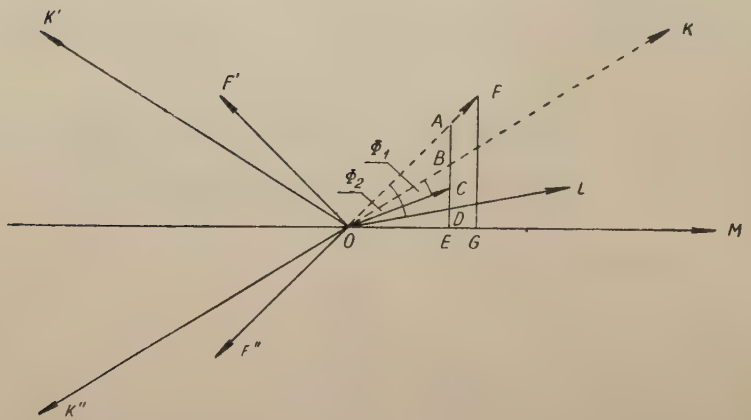

Abb. 2 Achsenschnitt durch die betrachtete Prazessionskegeln im Falle des Antiferrimagnetismus

$S_1 = OC$ $\quad R_1 = EC$ $\quad H_0 = MO$
$S_2 = OF' = OF'' = FO$ $\quad R_2 = GF$
$S_2' = \mathrm{OA}$ $\quad R_2' = EA$
$\Sigma_1 = \mathrm{OL}'$ $\quad x = CB$
$\Sigma_2 = OK' = OK'' = OK$ $\quad y = DA$

und schliesslich

$$\omega = \frac{A}{\hbar^2} \frac{S_1 S_2}{S_1 - S_2} a^2 k^2 \tag{31}$$

Um die Formel (12) zu erhalten, muss man schon in (27) $R'_2 = R_2$ setzen und dann Keffer, Kaplan u. Yafet folgen.

Herrn Prof. Dr. Szczepan Szczeniowski fühle ich mich verpflichtet, für die mit mir durchgeführte Besprechung der obigen Arbeit und die genaue Durchsicht des Manuskriptes, meinen besten Dank auszusprechen.

КРАТКОЕ СОДЕРЖАНИЕ

Г. Цофта, *Полуклассическая картина спиновой волны в ферримагнетизме*

В первой части настоящей работы дана в сокращённом виде мотивировка полуклассического изображения спиновой волны. Использовано при этом дифференционные уравнедля для линейной цепи спинов вместо применяемого часто дифференционьного уравнения непреривного размещения спинов.

В коренной же части работы дисперсионные формулы ω (k), полученные, на основании полуклассического изображения спиновых волн, Кефером, Капланом и Яфетом для ферромагнетиков и для антиферромагнетиков, обобщены на случай ферримагнетизма и антиферримагнетизма в толковании Смарта. Ферримагнетизм в номенклатуре Смарта обозначает согласованно направленные соседние спины, а антиферримагнетизм — спины, направленные противоположно. В обоих случаях получена зависимость того же самого типа: ω (k)$\sim$k^2, что согласуется с макроскопическим поведением обоих родов магнетиков. Формулу ω (k)$\sim$k для антиферромагнетиков нельзя получить из выведенной зависимости ω (k) для антиферримагнетиков посредством обыкновенного перехода к пределу $S_2 \to S_1$, т. е. рассматривая антиферромагнетизм, как особый случей антиферримагнетизма.

LITERATURHINWEISE

Anderson, P.W., Phys. Rev., **86**, 694 (1952).
Dirac, P. A. M., *The Principles of Quantum Mechanics*, 3-th Ed.
Döring, W., Z. Phys., **124**, 501 (1948).
Heber, G., Wiss. Z. Univ. Jena, **1**, 79 (1952a); **1**, 95 (1952b); Ann. Phys. (Leipzig), **13**, 44 (1953).
Heller, G. and Kramers, H. A., Proc. K. Ned. Akad. Wetensch., **37**, 378 (1934).
Herring, C. and Kittel, C., Phys. Rev., **81**, 869 (1951).
Hulthén, Proc. K. Ned. Akad. Wetensch., **39**, 190 (1936).
Keffer, F., thesis, Berkeley, January 1952.
Smart, J. S., Amer. J. Phys. **23**, 356 (1955).
Keffer, F., Kaplan, H. and Yafet, Y., Amer. J. Phys. **21**, 250 (1953).

RELATIVISTIC TWO-BODY PROBLEM IN ONE-TIME FORMULATION SEPARATION OF ANGULAR VARIABLES IN THE CASE OF ONE-QUANTUM INTERACTION IN ELECTRODYNAMICS

By W. Królikowski

Institute of Physics of the Polish Academy of Sciences, Warsaw

J. Rzewuski

Institute of Physics of the Polish Academy of Sciences, Wrocław

(Received June 18, 1956)

The separation of angular variables in the relativistic one-time equation for the two-fermion problem in quantum electrodynamics is carried out for the case of one--quantum interaction. The momentum representation is used. A system of integral equations in one variable is obtained. This system reduces to four equations in the case of $j = 0$, and to eight equations for $j \neq 0$.

1. Introduction

In a previous paper (Królikowski and Rzewuski 1955, referred to hereafter as I) the relativistic many-time equation of the two-fermion problem in quantum field theory was transformed into the one-time equation possessing the form of a Schrödinger equation. The operator playing the role of the potential in this equation is, in general, a complex quantity. The imaginary part of this "potential" is due to the instability of the two-fermion states and determines the life-time of these states. Using in the kernels of the original many-time equations the functonis S^{ret} (as in Günther's paper (1952, 1954)), we obtain the single-particle theory of fermions; using instead the functions $\frac{i}{2} S_F$ (as in the Bethe-Salpeter paper (Salpeter and Bethe 1951, cf. also Schwinger 1951)), we get the symmetrical hole theory.

The one-time equations of the many-body problem in quantum field theory were further discussed (Królikowski and Rzewuski 1956) from a more general point of view. The resulting equations describe bare particles; if, however, the renormalization procedure may be carried out (Matthews and Salam 1954, Johnson 1956), they become the equations of physical particles. In these considerations (Królikowski and Rzewuski

1956) we have used the initial condition corresponding to the single-particle version of the theory of fermions. Using the initial condition of Feynman's type, one gets the symmetrical hole version.

The next step should be the solution of the equations and comparison with experiment. In the present paper we solve the angular part of the two-fermion problem and use the solution for the separation of angular variables. The resulting set of integral equations in one variable is then investigated further.

In virtue of I (cf., in particular, Section 4. of paper I), we have the following equation for the two-fermion problem in quantum electrodynamics if we consider the one-quantum interaction only:

$$[W - H_1(-i\hbar\vec{\partial}_1) - H_2(-i\hbar\vec{\partial}_2)]\,\Phi(\vec{x}_1, \vec{x}_2) = \int d_3 x_1' \, d_3 x_2' \, V(\vec{x}_1, \vec{x}_2; \vec{x}_1', \vec{x}_2')\,\Phi(\vec{x}_1', \vec{x}_2'), \tag{1,1}$$

where

$$H_i(\vec{p}) = \gamma_4^{(i)}(ic\vec{\gamma}_i\vec{p} + m_i c^2) = c\vec{\alpha}_i\vec{p} + \beta_i m_i c^2, \quad (\gamma_\mu) = (-i\beta\vec{\alpha}, \beta), \tag{1,2}$$

$$V(\vec{x}_1, \vec{x}_2; \vec{x}_1', \vec{x}_2') = \lambda\hbar c\,[\gamma_4^{(1)} A_0^{(1)}(\vec{x}_1, \vec{x}_2; \vec{x}_1', \vec{x}_2') + \gamma_4^{(2)} A_0^{(2)}(\vec{x}_1, \vec{x}_2; \vec{x}_1', \vec{x}_2')]\,\gamma_4^{(1)}\gamma_4^{(2)} \tag{1,3}$$

and $W = \overline{E} - i\Gamma$.

Using the kernels of the many-time equations in Günther's form, we get

$$V(\vec{x}_1, \vec{x}_2; \vec{x}_1', \vec{x}_2') = \pm e^2\Big[\int dx_1''\,\gamma_4^{(2)} S_1^{ret}(x_1 - x_1'')\,\gamma_\mu^{(1)}\gamma_\mu^{(2)} D_+(x_1'' - x_2)\,S_1(x_1'' - x_1')\,S_2(x_2 - x_2') + \int dx_2''\,\gamma_4^{(1)} S_2^{ret}(x_2 - x_2'')\,\gamma_\mu^{(1)}\gamma_\mu^{(2)} D_+(x_1 - x_2'')\,S_1(x_1 - x_1')\,S_2(x_2'' - x_2')\Big]\gamma_\mu^{(1)}\gamma_\mu^{(2)}, \tag{1,4}$$

where the upper sign corresponds to charges with opposite signs and the lower, to equal signs. Taking these kernels in the Bethe-Salpeter form, we obtain formula (1,4) in which S_i^{ret} are replaced by iS_{+i}. The functions $D_+ = (1/2)\,D_F$ and $S_{+i} = (1/2)\,S_{F_i}$ are the Feynman solutions of the equations

$$\Box D_+(x) = i\,\delta(x) \quad \text{and} \quad (\underline{\partial} + \varkappa_i)\,S_{+i}(x) = -i\,\delta(x),$$

and

$$S_i^{ret}(x) = \theta^+(t)\,S_i(x), \quad \text{where } \theta^+(t) = \begin{cases} 0 & t < 0 \\ 1 & t > 0 \end{cases}$$

is the retarded solution of the equation

$$(\underline{\partial} + \varkappa_i)\,S_i^{ret}(x)\,\delta(x).$$

Making use of the formula

$$S_i(x) = e^{-\frac{i}{\hbar}H_i(-i\hbar\vec{\partial})t}\, i\,\delta(\vec{x})\,\gamma_4^{(i)} \tag{1,5}$$

we may rewrite (1.4) in the form

$$V(\vec{x}_1, \vec{x}_2; \vec{x}_1', \vec{x}_2')$$

$$= \mp ie^2 c \int_{-\infty}^{0} dt \left[e^{\frac{i}{\hbar}H_1(-i\hbar\vec{\partial}_1)t}\, \Gamma D_+(\vec{x}_1 - \vec{x}_2, ct)\, e^{-\frac{i}{\hbar}H_1(-i\hbar\vec{\partial}_1)t} + \right.$$

$$\left. + e^{\frac{i}{\hbar}H_2(-i\hbar\vec{\partial}_2)t}\, \Gamma D_+(\vec{x}_1 - \vec{x}_2, ct)\, e^{-\frac{i}{\hbar}H_2(-i\hbar\vec{\partial}_2)t} \right] \delta(\vec{x}_1 - \vec{x}_1')\,\delta(\vec{x}_2 - \vec{x}_2')$$

$$= V(\vec{x}_1, \vec{x}_2)\,\delta(\vec{x}_1 - \vec{x}_1')\,\delta(\vec{x}_2 - \vec{x}_2'), \tag{1,6}$$

where

$$\Gamma = \gamma_4^{(1)}\gamma_4^{(2)}\gamma_\mu^{(1)}\gamma_\mu^{(2)} = 1 - \vec{\alpha}_1\vec{\alpha}_2. \tag{1,7}$$

Taking the kernels in Bethe-Salpeter's form and using the formula

$$S_{+i}(x) = \Lambda_+(-i\hbar\vec{\partial})\,\varepsilon(t)\,\frac{1}{i}\,S(x) \quad \text{where } \varepsilon(t) = \begin{cases} 1 & t > 0 \\ -1 & t < 0 \end{cases},$$

$$\Lambda_\pm(-i\hbar\vec{\partial}) = \frac{|H_i(-i\hbar\vec{\partial})| \pm H_i(-i\hbar\vec{\partial})}{2|H_i(-i\hbar\vec{\partial})|} \begin{cases} + & t>0 \\ - & t<0 \end{cases}$$

we get instead of (1,6):

$$V(\vec{x}_1, \vec{x}_2; \vec{x}_1', \vec{x}_2') =$$

$$= \mp ie^2 c \left[\Lambda_+^{(1)}(-i\hbar\vec{\partial}_1) \int_{-\infty}^{0} dt\, e^{\frac{i}{\hbar}H_1(-i\hbar\vec{\partial}_1)t}\, \Gamma D_+(\vec{x}_1 - \vec{x}_2, ct)\, e^{-\frac{i}{\hbar}H_1(-i\hbar\vec{\partial}_1)t} - \right.$$

$$- \Lambda_-^{(1)}(-i\hbar\vec{\partial}_1) \int_{0}^{\infty} dt\, e^{\frac{i}{\hbar}H_1(-i\hbar\vec{\partial}_1)t}\, \Gamma D_+(\vec{x}_1 - \vec{x}_2, ct)\, e^{-\frac{i}{\hbar}H_1(-i\hbar\vec{\partial}_1)t} +$$

$$+ \Lambda_+^{(2)}(-i\hbar\vec{\partial}_2) \int_{-\infty}^{0} dt\, e^{\frac{i}{\hbar}H_2(-i\hbar\vec{\partial}_2)t}\, \Gamma D_+(\vec{x}_1 - \vec{x}_2, ct)\, e^{-\frac{i}{\hbar}H_2(-i\hbar\vec{\partial}_2)t} -$$

$$\left. - \Lambda_-^{(2)}(-i\hbar\vec{\partial}_2) \int_{0}^{\infty} dt\, e^{\frac{i}{\hbar}H_2(-i\hbar\vec{\partial}_2)t}\, \Gamma D_+(\vec{x}_1 - \vec{x}_2, ct)\, e^{-\frac{i}{\hbar}H_2(-i\hbar\vec{\partial}_2)t} \right] \times$$

$$\times\, \delta(\vec{x} - \vec{x}_1')\,\delta(\vec{x} - \vec{x}_2') = V(\vec{x}_1, \vec{x}_2)\,\delta(\vec{x}_1 - \vec{x}_1')\,\delta(\vec{x}_2 - \vec{x}_2') \tag{1,6'}$$

2. Transition to the momentum representation

First, we perform the calculation for Günther's case.

Equation (1,1), in the momentum representation, takes the form

$$[W - H_1(\vec{p}_1) - H_2(\vec{p}_2)]\,\Phi(\vec{p}_1, \vec{p}_2) = \int d_3 p_1'\, d_3 p_2'\, V(\vec{p}_1, \vec{p}_2; \vec{p}_1', \vec{p}_2')\,\Phi(\vec{p}_1', \vec{p}_2') \tag{2,1}$$

where

$$\Phi(\vec{p}_1, \vec{p}_2) = \int d_3 x_1\, d_3 x_2 < \vec{p}_1 \vec{p}_2 \mid \vec{x}_1 \vec{x}_2 > \Phi(\vec{x}_1, \vec{x}_2),$$

$$V(\vec{p}_1, \vec{p}_2; \vec{p}_1', \vec{p}_2') = \int d_3 x_1\, d_3 x_2 < \vec{p}_1 \vec{p}_2 \mid \vec{x}_1 \vec{x}_2 > V(\vec{x}_1, \vec{x}_2) < (\vec{x}_1 \vec{x}_2 \mid \vec{p}_1' \vec{p}_2' >; \tag{2,2}$$

here we have

$$< \vec{x}_1 \vec{x}_2 \mid \vec{p}_1 \vec{p}_2 > = (2\pi\hbar)^{-3}\, u_1(\vec{p}_1)\, u_2(\vec{p}_2)\, e^{\frac{i}{\hbar} \vec{p}_1 \vec{x}_1}\, e^{\frac{i}{\hbar} \vec{p}_2 \vec{x}_2} \tag{2,3}$$

$$\left(H_i(\vec{p})\, u_i(\vec{p}) = E_i(\vec{p})\, u_i(\vec{p}),\ E_i(\vec{p}) = \pm c\sqrt{\vec{p}^2 + (m_i c)^2},\ u_i^*(\vec{p})\, u_i(\vec{p}) = 1\right)$$

Thus, because of (1,6) and (2,3), and using the formulae

$$D_+(x) = \frac{1}{2}\,\frac{1}{(2\pi)^3} \int dk\, \delta_+(k^2)\, e^{ikx},$$

$$\delta_\pm(\omega) = \frac{1}{\pi} \int_0^\infty dt\, e^{\mp i\omega t} = \delta(\omega) \pm P\frac{(\pi i)^{-1}}{\omega}$$

we get

$$V(\vec{p}_1, \vec{p}_2; \vec{p}_1', \vec{p}_2')$$

$$= \mp \frac{i e^2}{4\pi}\, u_1^*(\vec{p}_1)\, u_2^*(\vec{p}_2)\, \Gamma\, u_1'(\vec{p}_1')\, u_2'(\vec{p}_2')\, \delta(\vec{p}_1 + \vec{p}_2 - \vec{p}_1' - \vec{p}_2') \times$$

$$\times \frac{1}{4\pi\hbar} \int_{-\infty}^{+\infty} d\omega \left\{ \delta_+ \left[(\vec{p}_1 - \vec{p}_1') - \frac{\hbar^2}{c^2}\,\omega^2 \right] \delta_+ [\omega_1(\vec{p}_1) - \omega_1(\vec{p}_1') - \omega] + \right.$$

$$\left. + \delta_+ \left[(\vec{p}_2 - \vec{p}_2')^2 - \frac{\hbar^2}{c^2}\,\omega^2 \right] \delta_+ [\omega_2(\vec{p}_2) - \omega_2(\vec{p}_2') - \omega] \right\}, \tag{2,4}$$

where $E_i(\vec{p}) = \hbar\omega_i(\vec{p}) = \pm c\sqrt{\vec{p}^2 + (m_i c)^2}$.

Going over to the centre-of-mass system (where we have $\vec{p}_1 = -\vec{p}_2 = \vec{p}$) and neglecting the imaginary part of V, we obtain

$$[E - H_1(\vec{p}) - H_2(-\vec{p})]\,\Phi(\vec{p}) = \int d_3 p'\, V(\vec{p}, \vec{p}')\,\Phi(\vec{p}'), \tag{2,5}$$

where

$$V(\vec{p},\vec{p}') = \mp \frac{e^2}{4\pi} u_1^*(\vec{p})\, u_2^*(-\vec{p})\, \Gamma\, u_1'(\vec{p}')\, u_2'(-\vec{p}') \times$$

$$\times \frac{1}{(2\pi)^2\hbar}\frac{1}{|\vec{p}-\vec{p}'|}\left[\frac{1}{|\vec{p}-\vec{p}'|+\frac{1}{c}(E_1-E_1')} + \frac{1}{|\vec{p}-\vec{p}'|+\frac{1}{c}(E_2-E_2')}\right]; \quad (2,6)$$

here we have used the notation $E_i = E_i(\vec{p})$ and $E_i' = E_i(\vec{p}')$.

We note that equation (2,5) in the position representation take the form

$$[E - H_1(-i\hbar\vec{\partial}) - H_2(i\hbar\vec{\partial})]\,\Phi(\vec{x}) = \int d_3x'\, V(\vec{x},\vec{x}')\,\Phi(\vec{x}'), \quad (2,7)$$

where

$$\Phi(\vec{x}) = \int d_3p < \vec{x}\,|\,\vec{p} > \Phi(\vec{p}),$$

$$V(\vec{x},\vec{x}') = \int d_3p\, d_3p' < \vec{x}\,|\,\vec{p} > V(\vec{p},\vec{p}') < \vec{p}'\,|\,\vec{x}' >; \quad (2,8)$$

here we have

$$< \vec{x}\,|\,\vec{p} > = (2\pi\hbar)^{-3/2} u_1(\vec{p})\, u_2(-\vec{p})\, e^{\frac{i}{\hbar}\vec{p}\vec{x}} \quad (2,9)$$

In the static approximation the kernel (2,8) has the wellknown form (in (2,6) we put $E_i - E_i' = 0$):

$$V(\vec{x},\vec{x}') = \mp \frac{e^2}{4\pi}\frac{\Gamma}{|\vec{x}|}\,\delta(\vec{x}-\vec{x}') = V(\vec{x})\,\delta(\vec{x}-\vec{x}') \quad (2,10)$$

Equation (2.7) is then the Breit equation with instantaneous electromagnetic interaction.

The wave function $\Phi(\vec{p})$ in equation (2,5) is labelled by the unit spinors u_1 and u_2: $\Phi(\vec{p}) = (\Phi_{u_1 u_2}(\vec{p}))$. We now go over to the new wave function, $\Phi(\vec{p}) = (\Phi_{\alpha_1\alpha_2}(\vec{p}))$ labelled by the spinor indices α_1 and α_2, similar to $\Phi(\vec{x}) = (\Phi_{\alpha_1\alpha_2}(\vec{x}))$. Performing the transformation

$$\Phi_{\alpha_1\alpha_2}(\vec{p}) = \sum_{u_1u_2} u_{\alpha_1}^{(1)}(\vec{p})\, u_{\alpha_2}^{(2)}(-\vec{p})\, \Phi_{u_1u_2}(\vec{p})$$

and using the formula

$$\sum_{spin} u_\alpha^{(i)}(\vec{p})\, u_\beta^{(i)}(\vec{p}) = \Lambda_{\pm\alpha\beta}^{(i)}(\vec{p}), \text{ where } \Lambda_\pm^{(i)}(\vec{p}) = \frac{|E_i(\vec{p})| \pm H_i(\vec{p})}{2\,|E_i(\vec{p})|}, \quad (2,11)$$

we obtain from (2,5), an equation of the same form as (2.5), where now

$$V(\vec{p},\vec{p}') = \mp \frac{e^2}{4\pi}\frac{1}{(2\pi)^2\hbar}\frac{1}{|\vec{p}-\vec{p}'|}\cdot\frac{1}{4}\sum_{sign}\left[\frac{(H_1+E_1)\,\Gamma\,(H_1'+E_1')}{E_1E_1'\left(|\vec{p}-\vec{p}'|+\frac{1}{c}(E_1-E_1')\right)} + \right.$$

$$\left. + \frac{(H_2-E_2)\,\Gamma\,(H_2'+E_2')}{E_2E_2'\left(|\vec{p}-\vec{p}'|+\frac{1}{c}(E_2-E_2')\right)}\right]; \quad (2,12)$$

here we use the notation

$$H_1 = H_1(\vec{p}), \quad H_2 = H_2(-\vec{p}), \quad H_1' = H_1(\vec{p}'), \quad H_2' = H_2(-\vec{p}')$$

and

$$\sum_{sign} f(E_i, E_i') = f(E_i, E_i') + f(-E_i, E_i') + f(E_i, -E_i') + f(-E_i, -E_i').$$

Introducing the notation

$$\varepsilon = E/c, \quad \varepsilon_i = E_i/c \quad (i = 1, 2), h_1 = \frac{1}{c} H_1(\vec{p}),$$

$$h_2 = \frac{1}{c} H_2(-\vec{p}), \quad h_1' = \frac{1}{c} H_2(\vec{p}'), \quad h_2' = \frac{1}{c} H_2(-p')$$

we may rewrite the two-fermion equation with one-quantum interaction in the form

$$(\varepsilon - h_1 - h_2)\,\Phi(\vec{p}) = \mp \frac{a}{4(2\pi)^2} \int \frac{d_3 p'}{|\vec{p} - \vec{p}'|} \times$$

$$\times \sum_{sign} \left[\frac{(h_1 + \varepsilon_1)\,\Gamma(h_1' + \varepsilon_1')}{\varepsilon_1 \varepsilon_1' (|\vec{p} - \vec{p}'| + \varepsilon_1 - \varepsilon_1')} + \frac{(h_2 + \varepsilon_2)\,\Gamma(h_2' + \varepsilon_2')}{\varepsilon_2 \varepsilon_2' (|\vec{p} - \vec{p}'| + \varepsilon_2 - \varepsilon_2')} \right] \Phi(\vec{p}'), \qquad (2{,}13)$$

where $a = e^2/4\pi\hbar c =$ „1/137".

In the Bethe-Salpeter case we may use a calculation similar to Günther's case. Then, instead of (2,4) and (2,6), we get, respectively

$$V(\vec{p}_1, \vec{p}_2; \vec{p}_1', \vec{p}_2') = \mp \frac{i e^2}{4\pi} u_1^*(\vec{p}_1)\, u_2^*(\vec{p}_2)\, \Gamma u_1'(\vec{p}_1')\, u_2'(\vec{p}_2')\, \delta(\vec{p}_1 + \vec{p}_2 - \vec{p}_1' - \vec{p}_2') \times$$

$$\times \frac{1}{4\pi\hbar} \int_{-\infty}^{+\infty} d\omega \left\{ \frac{\omega_1(\vec{p}_1)}{|\omega_1(\vec{p}_1)|}\, \delta_+ \left[(\vec{p}_1 - \vec{p}_1')^2 - \frac{\hbar^2}{c^2}\omega^2 \right] \delta_+ \right.$$

$$\left[\frac{\omega_1(\vec{p}_1)}{|\omega_1(\vec{p}_1)|} (\omega_1(\vec{p}_1) - \omega_1(\vec{p}_1')) - \omega \right] + \frac{\omega_2(\vec{p}_2)}{|\omega_2(\vec{p}_2)|}\, \delta_+ \left[(\vec{p}_2 - \vec{p}_2')^2 - \frac{\hbar^2}{c^2}\omega^2 \right] \delta_+ \times$$

$$\left. \times \left[\frac{\omega_2(\vec{p}_2)}{|\omega_2(\vec{p}_2)|} (\omega_2(\vec{p}_2) - \omega_2(\vec{p}_2)) - \omega \right] \right\} \qquad (2{,}4')$$

and

$$V(\vec{p}, p') = \mp \frac{e^2}{4\pi} u_1^*(\vec{p})\, u_2^*(-\vec{p})\, \Gamma u_1'(\vec{p}')\, u_2'(-\vec{p}') \times$$

$$\times \frac{1}{(2\pi)^2 \hbar} \frac{1}{|\vec{p} - \vec{p}'|} \left[\frac{\frac{E_1}{|E_1|}}{|\vec{p} - \vec{p}'| + \frac{1}{c}\frac{E_1}{|E_1|}(E_1 - E_1')} + \right.$$

$$\left. + \frac{\frac{E_2}{|E_2|}}{|\vec{p} - \vec{p}'| + \frac{1}{c}\frac{E_2}{|E_2|}(E_2 - E_2')} \right] \qquad (2{,}6')$$

Formula (2,6′) takes, in the static approximation in the position representation, the well-known form

$$V(\vec{x}, \vec{x}') = \mp \frac{e^2}{4\pi} [\Lambda_+^{(1)}(-i\hbar\vec{\partial})\Lambda_+^{(2)}(i\hbar\vec{\partial}) - \Lambda_-^{(1)}(-i\hbar\vec{\partial})\Lambda_-^{(2)}(i\hbar\vec{\partial})] \frac{\Gamma}{|\vec{x}|} \delta(\vec{x} - \vec{x}')$$
$$= V(\vec{x})\,\delta(\vec{x} - \vec{x}'). \qquad (2,10')$$

Instead of (2,13), we now have the following two-fermion equation with one-quantum interaction:

$$(\varepsilon - h_1 - h_2)\,\Phi(\vec{p}) = \mp \frac{a}{4(2\pi)^2} \int \frac{d_3 p'}{|\vec{p} - \vec{p}'|} \times$$
$$\times \sum_{sign} \left[\frac{\varepsilon_1}{|\varepsilon_1|} \frac{(h_1 + \varepsilon_1)\,\Gamma(h_1' + \varepsilon_1')}{\varepsilon_1 \varepsilon_1' \left(|\vec{p} - \vec{p}'| + \frac{\varepsilon_1}{|\varepsilon_1|}(\varepsilon_1 - \varepsilon_1') \right)} + \right.$$
$$\left. + \frac{\varepsilon_2}{|\varepsilon_2|} \frac{(h_2 + \varepsilon_2)\,\Gamma(h_2' + \varepsilon_2')}{\varepsilon_2 \varepsilon_2' \left(|\vec{p} - \vec{p}'| + \frac{\varepsilon_2}{|\varepsilon_2|}(\varepsilon_2 - \varepsilon_2') \right)} \right] \Phi(\vec{p}') \qquad (2,13')$$

Both equations (2,13′) and (2,13) may be written in the common form

$$(\varepsilon - h_1 - h_2)\,\Phi(\vec{p})$$
$$= \mp \frac{a}{2\pi^2} \int d_3 p' \frac{1}{8} \sum_{sign} [(h_1 + \varepsilon_1)\,\Gamma(h_1' + \varepsilon_1')\,M(\varepsilon_1, \varepsilon_1') +$$
$$+ (h_2 + \varepsilon_2)\,\Gamma(h_2' + \varepsilon_2')\,M(\varepsilon_2, \varepsilon_2')]\,\Phi(\vec{p}'), \qquad (2,14)$$

where

$$M(\varepsilon, \varepsilon') = \begin{cases} \{|\vec{p} - \vec{p}'|\,\varepsilon\varepsilon'\,[|\vec{p} - \vec{p}'| + \varepsilon - \varepsilon']\}^{-1} & \text{in Günther's case} \\ \frac{\varepsilon}{|\varepsilon|} \left\{ |\vec{p} - \vec{p}'|\,\varepsilon\varepsilon' \left[|\vec{p} - \vec{p}'| + \frac{\varepsilon}{|\varepsilon|}(\varepsilon - \varepsilon') \right] \right\}^{-1} & \text{in the Bethe-Salpeter case} \end{cases} \qquad (2,15)$$

3. Solution of the angular problem

As a first step towards the solution of equation (2.14), we shall try to separate the angular variables. This is certainly possible due to the invariance of our dynamical system with respect to rotations in three-dimensional space. This invariance secures the conservation of the total angular momentum of the system,

$$J_i = -i\hbar M_i, \qquad M_i = m_i + s_i,$$
$$m_i = p_j \frac{\partial}{\partial p_k} - p_k \frac{\partial}{\partial p_j}, \qquad S_i = \frac{1}{2}(\gamma_j^{(1)} \gamma_k^{(1)} + \gamma_j^{(2)} \gamma_k^{(2)})$$
$$(i = 1, 2, 3; \qquad i, j, k = \text{cyclic permutation of } 1, 2, 3) \qquad (3,1)$$

and, consequently, its commutability with the integral operator of equation (2,14). We may therefore consider a system of three commuting observables (there are three degrees of freedom left after separation of the centre of mass variables) consisting of the integral operator of equation (2,14) and of the differential operators

$$J_3 \text{ and } J_i^2 = J_1^2 + J_2^2 + J_3^2. \tag{3,2}$$

The full system of equations now consists of (2,14) and of the two equations

$$J_3 \Phi(\vec{p}) = \hbar m \Phi(\vec{p}), \tag{3,3}$$

$$J_i^2 \Phi(\vec{p}) = \hbar^2 j(j+1) \Phi(\vec{p}). \tag{3,4}$$

We easily verify the commutability of the operators (3.2)

$$[J_i^2, J_3] = 0, \tag{3,5}$$

which is a simple consequence of the well-known relations

$$[M_i, M_j] = -M_k \tag{3,6}$$

It may be interesting to verify also explicitly the commutability of J_i (and therefore, also of J_i^2) with the integral operator of equation (2,14). For this purpose, we first calculate the commutators of M_i with h_1 and h_2. From (1,2) and (3,1) we easily get

$$[M_i, h_1] = [M_i, h_2] = 0 \quad (i = 1, 2, 3) \tag{3,7}$$

Commutability of M_i with an integral operator of the form $\int d_3 p' F(\vec{p}, \vec{p}')$ means that

$$M_i \int d_3 p' F(\vec{p}, \vec{p}') \Phi(\vec{p}') = \int d_3 p' F(\vec{p}, \vec{p}') M_i' \Phi(\vec{p}'), \tag{3,8}$$

where M_i' may be obtained from M_i by replacing p_i by p_i' and $\frac{\partial}{\partial p_i}$ by $\frac{\partial}{\partial p_i'}$. To show that relation (3.8) is, in fact, true for the integral operator of equation (2.14), we first note that

$$[M_i, \Gamma] = 0 \qquad (i=1,2,3) \tag{3,9}$$

and, due to (2.15),

$$p_j \frac{\partial M(\varepsilon, \varepsilon')}{\partial p_k} - p_k \frac{\partial M(\varepsilon, \varepsilon')}{\partial p_j} = -p_j' \frac{\partial M(\varepsilon, \varepsilon')}{\partial p_k'} + p_k' \frac{\partial M(\varepsilon, \varepsilon')}{\partial p_j'} \tag{3,10}$$

Because of (3,1), (3,7), (3,9) and (3,10), we may now write for the first part of the integral operator occuring in (2.14)

$$\begin{aligned} & M_i \int d_3 p' (h_1 + \varepsilon_1) \Gamma(h_1' + \varepsilon_1') M(\varepsilon_1, \varepsilon_1') \\ &= \int d_3 p' (h_1 + \varepsilon_1) \Gamma(m_i + s_i) (h_1' + \varepsilon_1') M(\varepsilon_1, \varepsilon_1') \\ &= \int d_3 p' (h_1 + \varepsilon_1) \Gamma \Big[s_i (h_1' + \varepsilon_1') M(\varepsilon_1, \varepsilon_1') - \\ &- (h_1' + \varepsilon_1') \left(p_j' \frac{\partial M(\varepsilon_1, \varepsilon_1')}{\partial p_k'} - p_k' \frac{\partial M(\varepsilon_1, \varepsilon_1')}{\partial p_j'} \right) \Big]. \end{aligned} \tag{3,11}$$

The vector space under consideration consists of functions $\Phi(\vec{p})$, which are quadratically integrable and therefore vanish for $|\vec{p}| \to \infty$ (the integration domain is the entire three-dimensional space of the momentum variables). Thus we may carry out in (3,11) an integration by parts, the contributions from the infinite boundary being dropped.

$$\begin{aligned} & M_i \int d_3 p' \, (h_1 + \varepsilon_1) \, \Gamma \, (h_1' + \varepsilon_1') \, M(\varepsilon_1, \varepsilon_1') \, \Phi(\vec{p}') \\ &= \int d_3 p' \, (h_1 + \varepsilon_1) \, \Gamma \, M(\varepsilon_1, \varepsilon_1') \, M_i' \, (h_1' + \varepsilon_1') \, \Phi(\vec{p}') \\ &= \int d_3 p' \, (h_1 + \varepsilon_1) \, \Gamma \, (h_1' + \varepsilon_1') \, M(\varepsilon_1, \varepsilon_1') \, M_i' \, \Phi(\vec{p}'). \end{aligned} \tag{3,12}$$

An analogous relation holds for the second part of the integral operator in (2.14); this completes the proof of the commutability (cf. (3,8)) of this operator with M_i and, therefore, with any function of M_i as well, e.g with M_i^2.

Equation (2,14) is inconvenient for direct treatment insofar as it contains angular variables both under the integral sign and outside the integral by the intermediary of the operators h_1 and h_2. We shall remove this dependence on h_1 and h_2 by means of a unitary transformation

$$\bar{\Phi} = U\Phi, \qquad \bar{F} = UFu^{-1}, \tag{3,13}$$

where F is an arbitrary operator and U is the unitary operator

$$U = e^{s_3 \vartheta} \, e^{s_2 \varphi}, \qquad *) \tag{3,14}$$

ϑ and φ being the angular coordinates of the vector $\vec{p}$ in an arbitrary polar coordinate system

$$\begin{aligned} p_1 &= p \sin\vartheta \cos\varphi, \\ p_2 &= p \sin\vartheta \sin\varphi, \\ p_3 &= p \cos\vartheta. \end{aligned} \tag{3,15}$$

The set of equations (2,14) and (3,3−4) is transformed by (3,13−14) into

$$\begin{aligned} & (\varepsilon - \bar{h}_1 - \bar{h}_2) \, \bar{\Phi}(\vec{p}) \\ &= \frac{\alpha}{2\pi^2} \int d_3 p' \, \frac{1}{8} \sum_{sign} [(\bar{h}_1 + \varepsilon_1) \, U\Gamma U^{-1'} \, (\bar{h}_1' + \varepsilon_1') \, M(\varepsilon_1, \varepsilon_1') + \\ &\quad + (\bar{h}_2 + \varepsilon_2) \, U\Gamma U^{-1'} \, (\bar{h}_2' + \varepsilon_2') \, M(\varepsilon_2, \varepsilon_2')] \, \Phi(\vec{p}'), \end{aligned} \tag{3,16}$$

$$\bar{J}_3 \bar{\Phi}(\vec{p}) = \hbar m \, \bar{\Phi}(\vec{p}), \tag{3,17}$$

$$\bar{J}_i^2 \bar{\Phi}(\vec{p}) = \hbar^2 j \, (j+1) \, \bar{\Phi}(\vec{p}). \tag{3,18}$$

*) Transformations of this type were used e.g. by Sommerfeld in the case of the hydrogen atom (A. Sommerfeld, Atombau und Spektrallinien, II. Band, 4. Kapitel and Zusatz 15) and by M. Günther (unpublished) in his treatment of the relativistic two-body problem. We are very much indebted to Dr. Günther for showing us his manuscript prior to publication and for valuable discussions.

In (3,16) $\bar{h}_1$ and $\bar{h}_2$ as well as $\bar{h}'_1$ and $\bar{h}'_2$ do not depend any longer on the variables ϑ and φ. Let us verify this in the case of $\bar{h}_1$. The dependence on φ and ϑ occurs here by the intermediary of the factor

$$\begin{aligned}\gamma_i^{(1)} p_i &= p\,[\sin\vartheta\,(\gamma_1^{(1)}\cos\varphi + \gamma_2^{(1)}\sin\varphi) + \gamma_3^{(1)}\cos\vartheta] \\ &= e^{-\frac{1}{2}\gamma_1^{(1)}\gamma_2^{(1)}\varphi}\, p\,(\gamma_1^{(1)}\sin\vartheta + \gamma_3^{(1)}\cos\vartheta)\, e^{\frac{1}{2}\gamma_1^{(1)}\gamma_2^{(1)}\varphi} \\ &= e^{-\frac{1}{2}\gamma_1^{(1)}\gamma_2^{(1)}\varphi}\, e^{-\frac{1}{2}\gamma_3^{(1)}\gamma_1^{(1)}\vartheta}\, p\,\gamma_3^{(1)}\, e^{\frac{1}{2}\gamma_3^{(1)}\gamma_1^{(1)}\vartheta}\, e^{\frac{1}{2}\gamma_1^{(1)}\gamma_2^{(1)}\varphi}\end{aligned} \tag{3,19}$$

The spinors $\gamma_\mu^{(2)}$ occuring in (3,14) commute with $\gamma_\mu^{(1)}$. The products $\gamma_i^{(1)}\gamma_j^{(1)}$ as well as $\gamma_i^{(2)}\gamma_j^{(2)}$ $(i, j = 1, 2, 3)$ commute with $\gamma_4^{(1)}$ and $\gamma_4^{(2)}$. We have therefore

$$\bar{h}_1 = U\gamma_4^{(1)}(ip_i\gamma_i^{(1)} + m_i c)\,U^{-1}$$

$$= \gamma_4^{(1)} i\, e^{\frac{1}{2}\gamma_3^{(1)}\gamma_1^{(1)}\vartheta}\, e^{\frac{1}{2}\gamma_1^{(1)}\gamma_2^{(1)}\varphi}\, p_i\gamma_i^{(1)}\, e^{-\frac{1}{2}\gamma_1^{(1)}\gamma_2^{(1)}\varphi}\, e^{-\frac{1}{2}\gamma_3^{(1)}\gamma_1^{(1)}\vartheta} + \gamma_4^{(1)} m_1 c, \tag{3,20}$$

and finally

$$\bar{h}_1 = \gamma_4^{(1)}(ip\gamma_3^{(1)} + m_1 c). \tag{3,21}$$

Similary

$$\bar{h}_2 = \gamma_4^{(2)}(-ip\gamma_3^{(2)} + m_2 c). \tag{3,22}$$

The commutation relations (3,7), (3,8) and (3,12) are, of course, not affected by the transformation (3,13).

To find the dependence of the eigensolutions of (3,16) on the angular variables ϑ and φ, we first have to solve equations (3,17 – 18). For this purpose we have to find the transformed operators $\bar{J}_3$ and $\bar{J}_i^2$. This is very easy in the case of $\bar{J}_3$. Indeed, we have in polar variables

$$M_3 = \frac{\partial}{\partial\varphi} + s_3 \tag{3,23}$$

and

$$\bar{M}_3 = \frac{\partial}{\partial\varphi}. \tag{3,24}$$

In the case of $\bar{J}_i^2$, the calculation is more involved. We have

$$\begin{aligned}M_1 &= -\cos\varphi\,\mathrm{ctg}\,\vartheta\,\frac{\partial}{\partial\varphi} - \sin\varphi\,\frac{\partial}{\partial\vartheta} + s_1, \\ M_2 &= -\sin\varphi\,\mathrm{ctg}\,\vartheta\,\frac{\partial}{\partial\varphi} + \cos\varphi\,\frac{\partial}{\partial\vartheta} + s_2.\end{aligned} \tag{3,25}$$

With help of the relation

$$e^{\gamma_i \gamma_k \chi} = \cos \chi + \gamma_i \gamma_k \sin \chi$$

we find first

$$U \frac{\partial}{\partial \varphi} U^{-1} = \frac{\partial}{\partial \varphi} - s_3 \cos \vartheta + s_1 \sin \vartheta,$$

$$U \frac{\partial}{\partial \vartheta} U^{-1} = \frac{\partial}{\partial \vartheta} - s_2,$$

$$U s_1 U^{-1} = s_1 \cos \vartheta \cos \varphi - s_2 \sin \varphi + s_3 \sin \vartheta \cos \varphi,$$

$$U s_2 U^{-1} = s_1 \cos \vartheta \sin \varphi + s_2 \cos \varphi + s_3 \sin \vartheta \sin \varphi. \qquad (3.27)$$

Transforming now the formulae (3,25) we get, on account of (3,27),

$$\overline{M}_1 = - \cos \varphi \operatorname{ctg} \vartheta \frac{\partial}{\partial \varphi} - \sin \varphi \frac{\partial}{\partial \vartheta} + \frac{\cos \varphi}{\sin \vartheta} s_3,$$

$$\overline{M}_2 = - \sin \varphi \operatorname{ctg} \vartheta \frac{\partial}{\partial \varphi} + \cos \varphi \frac{\partial}{\partial \vartheta} + \frac{\sin \varphi}{\sin \vartheta} s_3 \qquad (3,28)$$

and, with help of (3,24),

$$\overline{M}_i^2 = \frac{1}{\sin \vartheta} \frac{\partial}{\partial \vartheta} \left(\sin \vartheta \frac{\partial}{\partial \vartheta} \right) + \frac{1}{\sin^2 \vartheta} \left(\frac{\partial^2}{\partial \varphi^2} - 2 s_3 \cos \vartheta \frac{\partial}{\partial \varphi} + s_3^2 \right). \qquad (3,29)$$

Having thus obtained the transformed operators $\overline{M}_3$ and $\overline{M}_i^2$, we may proceed to the solution of equations (3,17 – 18). The first of these equations (3,17) takes, on account of (3,24) and (3,1), the form

$$\frac{\partial \overline{\Phi}}{\partial \varphi} = im \overline{\Phi} \qquad (3,30)$$

and possesses solutions of the form

$$\overline{\Phi} (\varphi, \vartheta, p) = e^{im} \chi (\vartheta, p). \qquad (3,31)$$

The boundary conditions $\overline{\Phi} (\varphi, \vartheta, p) = \overline{\Phi} (\varphi + 2\pi, \vartheta, p)$ are satisfied if m is an integer

$$m = 0, \pm 1, \pm 2, \ldots \qquad (3,32)$$

Introducing (3,31) into (3,18) we get, on account of (3,29),

$$\left[\frac{1}{\sin \vartheta} \frac{\partial}{\partial \vartheta} \left(\sin \vartheta \frac{\partial}{\partial \vartheta} \right) + \frac{1}{\sin^2 \vartheta} (- m^2 - 2 im s_2 \cos \vartheta + s_3^2) \right] \chi (\vartheta, p)$$
$$= - j (j + 1) \chi (\vartheta, p). \qquad (3,33)$$

Let us first solve equation (3,33) for $m = 0$. In this case if we write out s_3^2 explicitly, it takes the form

$$\left\{ \frac{1}{\sin \vartheta} \frac{\partial}{\partial \vartheta} \left(\sin \vartheta \frac{\partial}{\partial \vartheta} \right) - \frac{\left[\frac{1}{2} (1 - \gamma_1^{(1)} \gamma_2^{(1)} \gamma_1^{(2)} \gamma_2^{(2)}) \right]^2}{\sin^2 \vartheta} \right\} \chi (\vartheta, p)$$
$$= - j (j + 1) \chi (\vartheta, p). \qquad (3,34)$$

Here use has been made of the fact that

$$-s_3^2 = \frac{1}{2}\left(1 - \gamma_1^{(1)}\gamma_2^{(1)}\gamma_1^{(2)}\gamma_2^{(2)}\right) \tag{3,35}$$

is an idempotent operator

$$\left[\frac{1}{2}\left(1 - \gamma_1^{(1)}\gamma_2^{(1)}\gamma_1^{(2)}\gamma_2^{(2)}\right)\right]^2 = \frac{1}{2}\left(1 - \gamma_1^{(1)}\gamma_2^{(1)}\gamma_1^{(2)}\gamma_2^{(2)}\right). \tag{3,36}$$

Equation (3,34) possesses the form of the differential equation of spherical harmonics with the upper index $-s_3^2 = \frac{1}{2}\left(1 - \gamma_1^{(1)}\gamma_2^{(1)}\gamma_1^{(2)}\gamma_2^{(2)}\right)$ and with the lower index j

$$Z_j^0(\cos\vartheta) = P_j^{-s_3^2}(\cos\vartheta). \tag{3,37}$$

The meaning of (3.37) becomes immediately clear if one considers that the two mutually orthogonal operators $\frac{1}{2}\left(1 - \gamma_1^{(1)}\gamma_2^{(1)}\gamma_1^{(2)}\gamma_2^{(2)}\right)$ and $\frac{1}{2}\left(1 + \gamma_1^{(1)}\gamma_2^{(1)}\gamma_1^{(2)}\gamma_2^{(2)}\right)$ are idempotent and possess, therefore, the eigenvalues 0 and 1. We may thus write instead of (3,37)

$$P_j^{-s_3^2}(\cos\vartheta) = \frac{1}{2}\left(1 + \gamma_1^{(1)}\gamma_2^{(1)}\gamma_1^{(2)}\gamma_2^{(2)}\right) P_j^0(\cos\vartheta) +$$

$$+ \frac{1}{2}\left(1 - \gamma_1^{(1)}\gamma_2^{(1)}\gamma_1^{(2)}\gamma_2^{(2)}\right) P_j^1(\cos\vartheta) \tag{3,38}$$

Due to the relation

$$P_j^1 = \frac{1}{\sqrt{j(j+1)}}\frac{\partial P_j^0}{\partial\vartheta}, \tag{3,39}$$

we may write (3.38) also in the form

$$Z_j^0 = P_j^{-s_3^2} = \left[\frac{1}{2}\left(1 + \gamma_1^{(1)}\gamma_2^{(1)}\gamma_1^{(2)}\gamma_2^{(2)}\right) +\right.$$

$$\left. + \frac{1}{\sqrt{j(j+1)}}\frac{1}{2}\left(1 - \gamma_1^{(1)}\gamma_2^{(1)}\gamma_1^{(2)}\gamma_2^{(2)}\right)\frac{\partial}{\partial\vartheta}\right] P_j^0 \tag{3,40}$$

We use throughout this paper spherical harmonics normalized to unity

$$\int_0^\pi P_j^m P_k^m \sin\vartheta\, d\vartheta = \delta_{jk}. \tag{3,41}$$

They are defined in the following way:

$$P_j^m(x) = (-1)^m \sqrt{j + \frac{1}{2}}\sqrt{\frac{(j-m)!}{(j+m)!}}(1-x^2)^{\frac{m}{2}}\frac{1}{2^j j!}\frac{d^{j+m}(x^2-1)^j}{dx^{j+m}} \tag{3,42}$$

Due to the rotational invariance of our equations in three-dimensional momentum space, the equations for the radial component cannot depend on the value of the quantum number m and therefore we may already use the eigenfunctions Z_j^0 of equation (3,34) for the separation of the variable ϑ. Nevertheless, it may be of some interest to know also the eigensolutions of the general equation (3,33) with m an arbitrary integer. These eigensolutions were derived by M. Günther (cf. footnote on page 329) from Z_j^0 as a generating function by changing the pole of the polar coordinate system. The result is

$$Z_j^m(\cos\vartheta) = \left[\frac{1}{2}(1+\gamma_1^{(1)}\gamma_2^{(1)}\gamma_1^{(2)}\gamma_2^{(2)}) + \frac{1}{\sqrt{j(j+1)}}\frac{1}{2}(1-\gamma_1^{(1)}\gamma_2^{(1)}\gamma_1^{(2)}\gamma_2^{(2)}) \times \right.$$
$$\left. \times\left(\frac{\partial}{\partial\vartheta} - i\gamma_1^{(1)}\gamma_2^{(1)}\frac{m}{\sin\vartheta}\right)\right] p_j^m(\cos\vartheta) \tag{3,43}$$

Thus for $m = 0$, we obtain the functions (3,40).

It may be verified directly that the Z_j^m are eigensolutions of equation (3,33). For this purpose it is convenient to write the second order differential operator occurring in (3,33) as the square of a first order differential operator

$$\frac{1}{\sin\vartheta}\frac{\partial}{\partial\vartheta}\left(\sin\vartheta\frac{\partial}{\partial\vartheta}\right) + \frac{1}{\sin^2\vartheta}(-m^2 - 2im\,s_3\cos\vartheta + s_3^2) = k^2 \tag{3,44}$$

where

$$k = \gamma_2^{(1)}\left(\frac{\partial}{\partial\vartheta} + i\gamma_1^{(1)}\gamma_2^{(1)}\frac{m}{\sin\vartheta} - s_3^2\operatorname{ctg}\vartheta\right). \tag{3,45}$$

It is now easy for us to verify that Z_j^m is an eigenfunction of K. Due to the orthogonality of $\frac{1}{2}(1+\gamma_1^{(1)}\gamma_2^{(1)}\gamma_1^{(2)}\gamma_2^{(2)})$ and $-s_3^2 = \frac{1}{2}(1-\gamma_1^{(1)}\gamma_2^{(1)}\gamma_1^{(2)}\gamma_2^{(2)})$, we get

$$K Z_j^m = \gamma_2^{(1)}\left[\frac{1}{2}(1+\gamma_1^{(1)}\gamma_2^{(1)}\gamma_1^{(2)}\gamma_2^{(2)})\left(\frac{\partial}{\partial\vartheta} + i\gamma_1^{(1)}\gamma_2^{(2)}\frac{m}{\sin\vartheta}\right) + \right.$$
$$\left. + \frac{1}{\sqrt{j(j+1)}}\frac{1}{2}(1-\gamma_1^{(1)}\gamma_2^{(1)}\gamma_1^{(2)}\gamma_2^{(2)})\left(\frac{\partial^2}{\partial\vartheta^2} + \operatorname{ctg}\vartheta\frac{\partial}{\partial\vartheta} - \frac{m^2}{\sin^2\vartheta}\right)\right] P_j^m$$
$$= \sqrt{j(j+1)}\, Z_j^m \gamma_2^{(1)}\gamma_1^{(2)}\gamma_2^{(2)} \tag{3,46}$$

and therefore

$$K^2 Z_j^m = -j(j+1) Z_j^m. \tag{3,47}$$

4. *Separation of the angular variables*

Having thus obtained the eigensolutions of the angular problem (3,17 – 18) we may now proceed to the separation of the angular variables from the integral equation (3,16). As already stated above the result of the separation cannot depend on m, and therefore we may use for our purposes the functions $Z_j^0(\cos\vartheta)$.

We write the solution in the form

$$\bar{\Phi}(\vec{p}) = Z_j^0(\cos\vartheta) f(p); \tag{4,1}$$

we introduce this into the integral equation (3.16), multiply on the left with $Z_j^0(\cos\vartheta)$ and integrate over the solid angle ($d\omega = \sin\vartheta\, d\vartheta\, d\varphi$). Due to the commutability of Z_j^0 with $\bar{h}_1$ and $\bar{h}_2$, we may write the result in the form

$$\int d\omega\, Z_j^0\, Z_j^0\, (\varepsilon - \bar{h}_1 - \bar{h}_2)\, f(p)$$

$$= \mp \frac{a}{2\pi^2} \int_0^\infty dp' p'^2 \frac{1}{8} \sum_{sign} [(\bar{h}_1 + \varepsilon_1)\, \Gamma K_j(\varepsilon_1, \varepsilon_1')\, (\bar{h}_1' + \varepsilon_1') +$$

$$+ (\bar{h}_2 + \varepsilon_2)\, \Gamma K_j(\varepsilon_2, \varepsilon_2')\, (\bar{h}_2' + \varepsilon_2')]\, f(p') \tag{4,2}$$

with

$$K_j(\varepsilon, \varepsilon') = \int d\omega\, d\omega'\, Z_j^0\, UM(\varepsilon, \varepsilon')\, U'^{-1}\, Z_j^{0\prime}\,. \tag{4,3}$$

The functions Z_j^0 form, according to their definition (3,38) and according to (3,41), an orthogonal set

$$\int_0^\pi d\vartheta \sin\vartheta\, Z_j^0\, Z_k^0 = 0 \quad \text{for } j \neq k \tag{4,4}$$

For $j \geqslant 1$ they are normalized to unity

$$\int_0^\pi d\vartheta \sin\vartheta\, Z_j^0\, Z_j^0 = 1 \tag{4,5}$$

and for $j = 0$

$$\int_0^\pi d\vartheta \sin\vartheta\, Z_0^0\, Z_0^0 = \frac{1}{2}\,(1 + \gamma_1^{(1)}\, \gamma_2^{(1)}\, \gamma_1^{(2)}\, \gamma_2^{(2)}). \tag{4,6}$$

We may therefore replace, for $j \neq 0$, the integral on the lefthand side of equation (4,2) by 2π. For $j = 0$ we get 2π times the factor (4,6). This factor, however, occurs on both sides of the equation in connexion with the appearance of $Z_0^0 = \frac{1}{2}(1 + \gamma_1^{(1)}\, \gamma_2^{(1)}\, \gamma_1^{(2)}\, \gamma_2^{(2)})\, P_0^0$. It commutes with $\bar{h}_1$ and $\bar{h}_2$ and is idempotent. It may therefore be joined with $f(p)$. Thus, for $j = 0$ as well as for $j \neq 0$, we may write equation (4,2) in the final form

$$(\varepsilon - \bar{h}_1 - \bar{h}_2) f(p)$$

$$= \mp \frac{a}{4\pi^3} \int_0^\infty dp' p'^2 \frac{1}{8} \sum_{sign} [(\bar{h}_1 + \varepsilon_1)\, \Gamma K_j(\varepsilon_1, \varepsilon_1')\, (\bar{h}_1' + \varepsilon_1') +$$

$$+ (\bar{h}_2 + \varepsilon_2)\, \Gamma K_j(\varepsilon_2, \varepsilon_2')\, (h_2' + \varepsilon_2')]\, f(p'). \tag{4,7}$$

The angular variables no longer occur in this set of equations. It determines the energy eigenvalues of the relativistic two-body problem in the desired approximation (one-quantum interaction).

The fact that for $j = 0$ the projection operator $\frac{1}{2}(1 + \gamma_1^{(1)}\gamma_2^{(1)}\gamma_1^{(2)}\gamma_2^{(2)})$ occurs as a factor in the solution $f(p)$ shows that the lowest state of the total angular momentum may be realized only in such a way that the orbital momentum as well as the total spin is zero $\left(\frac{1}{2}(\gamma_1^{(1)}\gamma_{2+}^{(1)}\gamma_1^{(2)}\gamma_2^{(2)})\, f(p) = 0\right)$, i.e. the particles possess opposite spins.

For further treatment of equation (4.7), we need, first of all, the explicit form of $K_j(\varepsilon, \varepsilon')$. Instead of $K_j(\varepsilon, \varepsilon')$ we shall calculate the expressions

$$K_{jl}(\varepsilon, \varepsilon') = \int d\omega d\omega'\, Z_j^0\, UM(\varepsilon, \varepsilon')\, U'^{-1} Z_l^{0\prime} \tag{4,8}$$

and we shall show that

$$K_{jl} = \delta_{jl} K_j. \tag{4,9}$$

This result will at once confirm our statement that the functions Z_j^0 bring equation (3,16) into the form (4,7). In fact if we introduce (4,1) into (3,16), multiply on the left with Z_l^0 $(l \neq j)$ instead of Z_j^0 and integrate over the solid angle, we get zero on the left due to (4,4), and zero on the right due to (4,9).

To calculate (4.8) we first note that $M(\varepsilon, \varepsilon')$ depends implicitly on the angular variables through the intermediary of

$$|\vec{p} - \vec{p}'| = \sqrt{p^2 + p'^2 - 2pp'\cos\theta} \tag{4,10}$$

(cf. (2.15)), where $\cos\theta = \cos\vartheta\cos\vartheta' + \sin\vartheta\sin\vartheta'\cos(\varphi - \varphi')$ is the angle between $\vec{p}$ and $\vec{p}'$. We may therefore expand $M(\varepsilon, \varepsilon')$ in a series of Legendre's polynomials

$$M(\varepsilon, \varepsilon') = \sum_{k=0}^{\infty} M_k(\varepsilon, \varepsilon')\, P_k(\cos\theta),$$

$$M_k(\varepsilon, \varepsilon') = \int_0^{\pi} M(\varepsilon, \varepsilon')\, P_k(\cos\theta)\sin\theta\, d\theta. \tag{4,11}$$

Inserting (4.11) into (4.8) we obtain

$$K_{jl} = \sum_{k=0}^{\infty} M_k(\varepsilon, \varepsilon')\, A_{k,jl}\,, \tag{4,12}$$

where

$$A_{k,jl} = \int d\omega\, d\omega'\, Z^0\, U\, P_k(\cos\theta)\, U'^{-1} Z_l^{0\prime}. \tag{4,13}$$

Using finally the summation theorem of spherical harmonics

$$P_k(\cos\theta) = \frac{1}{\sqrt{k + \frac{1}{2}}} \sum_{m=-k}^{m=+k} P_k^m(\cos\vartheta)\, P_k^m(\cos\vartheta')\, e^{im(\varphi - \varphi')} \tag{4,14}$$

$(P_k^{-m} = (-1)^m P_k^m)$, we may write (4,13) in the form

$$A_{k,jl} = \frac{1}{\sqrt{k+\frac{1}{2}}} \sum_{m=-k}^{m=+k} \int d\omega\, d\omega'\, Z_j^0\, UP_k^m\, e^{im(\varphi-\varphi')}\, P_k^{m'}\, U'^{-1}\, Z_l^{0'}. \tag{4,15}$$

We first carry out the integration over the angles φ and φ'. On account of (3,14) we have to evaluate the following integral

$$\int_0^{2\pi} d\varphi \int_0^{2\pi} d\varphi'\, e^{im(\varphi-\varphi')}\, e^{s_3(\varphi-\varphi')} = 2\pi \int_0^{2\pi} d\varphi\, e^{im\varphi}\, e^{s_3\varphi} \tag{4,16}$$

With help of formula (3,26), or expanding the exponential and using the fact that $-s_3^2$ is an idempotent operator (cf. (3,35 – 36)), one easily verifies the relation

$$e^{s_3\varphi} = e^{\frac{1}{2}(\gamma_1^{(1)}\gamma_2^{(1)} + \gamma_1^{(2)}\gamma_2^{(2)})\varphi}$$

$$= \frac{1}{2}(1 + \gamma_1^{(1)}\gamma_2^{(1)}\gamma_1^{(2)}\gamma_2^{(2)}) + \frac{1}{2}(1 - \gamma_1^{(1)}\gamma_2^{(1)}\gamma_1^{(2)}\gamma_2^{(2)})\cos\varphi +$$

$$+ \frac{1}{2}(\gamma_1^{(1)}\gamma_2^{(1)} + \gamma_1^{(2)}\gamma_2^{(2)})\sin\varphi. \tag{4,17}$$

Introducing (4,17) into (4,16) and carrying out the integrations, one gets

$$\int_0^{2\pi} d\varphi \int_0^{2\pi} d\varphi'\, e^{im(\varphi-\varphi')}\, e^{s_3(\varphi-\varphi')} = (2\pi)^2 \left[\frac{1}{2}(1 + \gamma_1^{(1)}\gamma_2^{(1)}\gamma_1^{(2)}\gamma_2^{(2)})\,\delta_{m,o} + \right.$$

$$+ \frac{1}{2}(1 - \gamma_1^{(1)}\gamma_2^{(1)}\gamma_1^{(2)}\gamma_2^{(2)})\,\frac{1}{2}(\delta_{m,-1} + \delta_{m,+1}) +$$

$$\left. + \frac{1}{2}(\gamma_1^{(1)}\gamma_2^{(1)} + \gamma_1^{(2)}\gamma_2^{(2)})\,\frac{1}{2i}(\delta_{m,-1} - \delta_{m,+1})\right]. \tag{4,18}$$

By virtue of (4,18) and (3,38), we may now write (4,15) in the form $(P_k^{-m} = (-1)^m P_k^m)$

$$A_{k,jl} = \frac{(2\pi)^2}{\sqrt{k+\frac{1}{2}}} \int_0^{\pi} d\vartheta \sin\vartheta \int_0^{\pi} d\vartheta' \sin\vartheta'\, Z_j^0\, e^{s_3\vartheta} \times \cdot$$

$$\times \left[\frac{1}{2}(1 + \gamma_1^{(1)}\gamma_2^{(1)}\gamma_1^{(2)}\gamma_2^{(2)})\, P_k^0\, P_k^{0'} + \frac{1}{2}(1 - \gamma_1^{(1)}\gamma_2^{(1)}\gamma_1^{(2)}\gamma_2^{(2)})\, P_k^1\, P_k^{1'}\right] e^{-s_2\vartheta'}\, Z_l^{0'}$$

$$= \frac{(2\pi)^2}{\sqrt{k+\frac{1}{2}}} \int_0^{\pi} d\vartheta \sin\vartheta \int_0^{\pi} d\vartheta' \sin\vartheta'\, Z_j^0\, e^{s_2\vartheta}\, Z_k^0\, Z_k^{0'}\, e^{-s_2\vartheta'}\, Z_l^{0'}. \tag{4,19}$$

We are thus left with integrals of the type

$$I_{jk}^{\pm} = \int_0^{\pi} d\vartheta \sin\vartheta \, Z_j^0 \, e^{\pm i\varepsilon\vartheta} \, Z_k^0. \tag{4,20}$$

Using (3,1), (3,35 – 36) and the mutual orthogonality of the operators $\frac{1}{2}(1 \pm \gamma_1^{(1)} \gamma_2^{(1)} \gamma_1^{(2)} \gamma_2^{(2)})$, we obtain

$$I_{jk}^{\pm} = \int_0^{\pi} d\vartheta \sin\vartheta \left[\frac{1}{2}(1 + \gamma_1^{(1)}\gamma_2^{(1)}\gamma_1^{(2)}\gamma_2^{(2)}) P_j^0 P_k^0 + \frac{1}{2}(1 - \gamma_1^{(1)}\gamma_2^{(1)}\gamma_1^{(2)}\gamma_2^{(2)}) P_j^1 P_k^1\right] \times$$

$$\times \left[\frac{1}{2}(1 + \gamma_3^{(1)}\gamma_1^{(1)}\gamma_3^{(2)}\gamma_1^{(2)}) + \frac{1}{2}(1 - \gamma_3^{(1)}\gamma_1^{(1)}\gamma_3^{(2)}\gamma_1^{(2)}) \cos\vartheta\right] \pm$$

$$\pm \int_0^{\pi} d\vartheta \sin\vartheta \left[\frac{1}{2}(1 + \gamma_1^{(1)}\gamma_2^{(1)}\gamma_1^{(2)}\gamma_2^{(2)}) P_j^0 P_k^1 + \frac{1}{2}(1 - \gamma_1^{(1)}\gamma_2^{(1)}\gamma_1^{(2)}\gamma_2^{(2)}) P_j^1 P_k^0\right] \times$$

$$\times \frac{1}{2}(\gamma_3^{(1)}\gamma_1^{(1)} + \gamma_3^{(2)}\gamma_1^{(2)}) \sin\vartheta. \tag{4,21}$$

The integrals may be evaluated with help of the well-known recurrence relations for spherical harmonics. In our normalization these relations take the form

$$\cos\vartheta \, P_j^0 = \frac{j+1}{\sqrt{(2j+1)(2j+3)}} P_{j+1}^0 + \frac{j}{\sqrt{(2j-1)(2j+1)}} P_{j-1}^0,$$

$$\cos\vartheta \, P_j^1 = \sqrt{\frac{j(j+2)}{(2j+1)(2j+3)}} P_{j+1}^1 + \sqrt{\frac{(j-1)(j+1)}{(2j-1)(2j+1)}} P_{j-1}^1,$$

$$\sin\vartheta \, P_j^0 = -\sqrt{\frac{(j+1)(j+2)}{(2j+1)(2j+3)}} P_{j+1}^1 + \sqrt{\frac{(j-1)j}{(2j-1)(2j+1)}} P_{j-1}^1. \tag{4,22}$$

Putting (4,22) into (4,21) and employing the orthonormality relations (3,41), one gets after some calculations

$$I_{jk}^{\pm} = \frac{1}{2}(1 + \gamma_3^{(1)}\gamma_1^{(1)}\gamma_3^{(2)}\gamma_1^{(2)}) \delta_{jk} +$$

$$+ \frac{1}{2}(1 - \gamma_3^{(1)}\gamma_1^{(1)}\gamma_3^{(2)}\gamma_1^{(2)}) \left\{\frac{1}{2}(1 + \gamma_1^{(1)}\gamma_2^{(1)}\gamma_1^{(2)}\gamma_2^{(2)}) [j+1 \mp \gamma_3^{(1)}\gamma_1^{(1)} \sqrt{(j+1)(j+2)}] + \right.$$

$$\left. + \frac{1}{2}(1 - \gamma_1^{(1)}\gamma_2^{(1)}\gamma_1^{(2)}\gamma_2^{(2)}) [\sqrt{j(j+2)} \pm \gamma_3^{(1)}\gamma_1^{(1)} \sqrt{j(j+1)}]\right\} \frac{\delta_{j+1,k}}{\sqrt{(2j+1)(2j+3)}} +$$

$$+ \frac{1}{2}(1 - \gamma_3^{(1)}\gamma_1^{(1)}\gamma_3^{(2)}\gamma_1^{(2)}) \left\{\frac{1}{2}(1 + \gamma_1^{(1)}\gamma_2^{(1)}\gamma_1^{(2)}\gamma_2^{(2)}) [j \pm \gamma_3^{(1)}\gamma_1^{(1)} \sqrt{(j-1)j}] + \right.$$

$$\left. + \frac{1}{2}(1 - \gamma_1^{(1)}\gamma_2^{(1)}\gamma_1^{(2)}\gamma_2^{(2)}) [\sqrt{(j-1)(j+1)} \mp \right.$$

$$\left. \mp \gamma_3^{(1)}\gamma_1^{(1)} \sqrt{j(j+1)}]\right\} \frac{\delta_{j-1,k}}{\sqrt{(2j-1)(2j+1)}}. \tag{4,23}$$

From the above one obtains after a rather lengthy, but straightforward calculation

$$I_{jk}^{+} I_{kl}^{-} = \frac{1}{2}(1 + \gamma_3^{(1)} \gamma_1^{(1)} \gamma_3^{(2)} \gamma_1^{(2)})\, \delta_{jl}\, \delta_{kl} +$$

$$+ \frac{1}{2}(1 - \gamma_3^{(1)} \gamma_1^{(1)} \gamma_3^{(2)} \gamma_1^{(2)}) \left\{ \frac{1}{2} \left[1 + \frac{\gamma_1^{(1)} \gamma_2^{(1)} \gamma_1^{(2)} \gamma_2^{(2)}}{2j+1} (1 - \gamma_3^{(1)} \gamma_1^{(1)} 2\sqrt{j(j+1)}) \right] \delta_{k,j+1} + \right.$$

$$\left. + \frac{1}{2} \left[1 - \frac{\gamma_1^{(1)} \gamma_2^{(1)} \gamma_1^{(2)} \gamma_2^{(2)}}{2j+1} (1 - \gamma_3^{(1)} \gamma_1^{(1)} 2\sqrt{j(j+1)}) \right] \delta_{k,l-1} \right\} \delta_{jl}. \quad (4,24)$$

With help of (4,24) we may easily calculate $A_{k,jl}$ (cf. (4,19)) and introduce the result into (4,12). Due to the occurrence of the Kronecker symbols, we obtain, finally, relation (4,9) with

$$\frac{K_j}{(2\pi)^2} = \frac{1}{2}(1 + \gamma_3^{(1)} \gamma_1^{(1)} \gamma_3^{(2)} \gamma_1^{(2)}) \frac{M_j(\varepsilon, \varepsilon')}{\sqrt{j + \frac{1}{2}}} +$$

$$+ \frac{1}{2}(1 - \gamma_3^{(1)} \gamma_1^{(1)} \gamma_3^{(2)} \gamma_1^{(2)}) \left\{ \frac{1}{2} \left[1 + \frac{\gamma_1^{(1)} \gamma_2^{(1)} \gamma_1^{(2)} \gamma_2^{(2)}}{2j+1} (1 - \gamma_3^{(1)} \gamma_1^{(1)} 2\sqrt{j(j+1)}) \right] \frac{M_{j+1}(\varepsilon, \varepsilon')}{\sqrt{j - \frac{3}{2}}} + \right.$$

$$\left. + \frac{1}{2} \left[1 - \frac{\gamma_1^{(1)} \gamma_2^{(1)} \gamma_1^{(2)} \gamma_2^{(2)}}{2j+1} (1 - \gamma_3^{(1)} \gamma_1^{(1)} 2\sqrt{j(j+1)}) \right] \frac{M_{j-1}(\varepsilon, \varepsilon')}{\sqrt{j - \frac{1}{2}}} \right\}. \quad (4,25)$$

The functions $M_j(\varepsilon, \varepsilon')$ occurring in (4,25) are given by the formulae (4,11) and (2,15). The integrals may, in principle, be evaluated by elementary integrations, but we did not succeed in finding the general formula for arbitrary j. We shall write out these integrals explicitly using Günther's form of interaction (cf. (2,15)) and evaluate them for the two simplest cases: $j = 0$ and $j = 1$.

$$M_k(\varepsilon, \varepsilon') = \frac{1}{\varepsilon\varepsilon'} \int_0^{\pi} \frac{P_k(\cos\theta) \sin\theta\, d\theta}{p^2 + p'^2 - 2pp' \cos\theta + (\varepsilon - \varepsilon')\sqrt{p^2 + p'^2 - 2pp' \cos\theta}}, \quad (4,26)$$

$$M_0(\varepsilon, \varepsilon') = \sqrt{\frac{1}{2}} \frac{1}{\varepsilon\varepsilon'} \frac{1}{pp'} \ln \left| \frac{p + p' + \varepsilon - \varepsilon'}{p - p' + \varepsilon - \varepsilon'} \right|,$$

$$M_1(\varepsilon, \varepsilon') = \sqrt{\frac{3}{2}} \frac{1}{\varepsilon\varepsilon'} \frac{1}{pp'} \left[-1 + \frac{\varepsilon - \varepsilon'}{p} + \right.$$

$$\left. + \frac{p^2 + p'^2 - (\varepsilon - \varepsilon')^2}{2pp'} \ln \left| \frac{p + p' + \varepsilon - \varepsilon'}{p - p' + \varepsilon - \varepsilon'} \right| \right]. \quad (4,27)$$

5. *Reduction of the system*

The integral equation (4,7) represents a system of sixteen equations for the sixteen components of the spinor $f(p)$ (cf. the definition of $\Phi_{\alpha_1 \alpha_2}(\vec{p})$ on page 325). This system may be reduced, for $j \geqslant 1$, to eight equations for eight unknown functions, and for

$j = 0$, to four equations with four unknown functions. This is due to the fact that for $j \geqslant 1$ the spinors $\gamma_2^{(1)}$ and $\gamma_2^{(2)}$ occur only through the intermediary of their product $\gamma_2^{(1)}\gamma_2^{(2)}$ (cf. (4,7) and (4,25)). For $j = 0$ the terms in (4,25) containing $\gamma_3^{(1)}\gamma_1^{(1)}$ vanish and the resulting equations contain another pair of spinors occurring only in the form of their product, namely, $\gamma_1^{(1)}$ and $\gamma_2^{(2)}$.

Thus, in the general case $j \geqslant 1$, there occur in our equations (4.7) the spinors

$$\gamma_1^{(1)}, \gamma_3^{(1)}, \gamma_4^{(1)}, \gamma_1^{(2)}, \gamma_3^{(2)}, \gamma_4^{(2)}, \gamma_2^{(1)}\gamma_2^{(2)}, \tag{5,1}$$

satisfying the following commutation relations

$$\begin{aligned}
&[\gamma_\mu^{(1)}, \gamma_\nu^{(1)}]_+ = 2\delta_{\mu\nu} \\
&[\gamma_\mu^{(2)}, \gamma_\nu^{(2)}]_+ = 2\delta_{\mu\nu} \quad (\text{for } \mu, \nu = 1, 3, 4) \qquad (5,2)\\
&[\gamma_2^{(1)}\gamma_2^{(2)}, \gamma_\nu^{(1)}]_+ = 0 \\
&[\gamma_2^{(1)}\gamma_2^{(2)}, \gamma_\nu^{(2)}]_+ = 0 \quad (\text{for } \nu = 1, 3, 4)
\end{aligned}$$

$$([a, b]_\pm = ab \pm ba). \tag{5,3}$$

These relations are satisfied if we represent the spinors (5,1) as products of the second rank Pauli matrices

$$1,\ \sigma_1^p, \sigma_2^p, \sigma_3^p;\ [\sigma_i^p, \sigma_j^p]_+ = 2\delta_{ij}\sigma_i^p\,\sigma_j^p = i\sigma_k^p \tag{5,4}$$

corresponding to three different two-dimensional spinor spaces. To distinguish between these spaces we denote the corresponding Pauli matrices (5,4) by σ_i, ϱ_i and Σ_i, respectively.

We now put

$$\begin{aligned}
\gamma_1^{(1)} &= \sigma_3\varrho_1 = \sigma_3^p \times \sigma_1^p \times 1 = (\sigma_{3\alpha\beta}^p\,\sigma_{1\gamma\delta}^p\,\delta_{\varepsilon\eta}),\\
\gamma_3^{(1)} &= \sigma_2\varrho_1 = \sigma_2^p \times \sigma_1^p \times 1 = (\sigma_{2\alpha\beta}^p\,\sigma_{1\gamma\delta}^p\,\delta_{\varepsilon\eta}),\\
\gamma_4^{(1)} &= \sigma_1\varrho_1 = \sigma_1^p \times \sigma_1^p \times 1 = (\sigma_{1\alpha\beta}^p\,\sigma_{1\gamma\delta}^p\,\delta_{\varepsilon\eta}),\\
\gamma_1^{(2)} &= \varrho_1\Sigma_3 = 1 \times \sigma_1^p \times \sigma_3^p = (\delta_{\alpha\beta}\,\sigma_{1\gamma\delta}^p\,\sigma_{3\varepsilon\eta}^p),\\
\gamma_3^{(2)} &= \varrho_1\Sigma_2 = 1 \times \sigma_1^p \times \sigma_2^p = (\delta_{\alpha\beta}\,\sigma_{1\gamma\delta}^p\,\sigma_{2\varepsilon\eta}^p),\\
\gamma_4^{(2)} &= \varrho_1\Sigma_1 = 1 \times \sigma_1^p \times \sigma_1^p = (\delta_{\alpha\beta}\,\sigma_{1\gamma\delta}^p\,\sigma_{1\varepsilon\eta}^p),\\
\gamma_2^{(1)}\gamma_2^{(2)} &= \varrho_2 = 1 \times \sigma_2^p \times 1 = (\delta_{\alpha\beta}\,\sigma_{2\gamma\delta}^p\,\sigma_{\varepsilon\eta}).
\end{aligned} \tag{5,5}$$

One easily verifies, with help of (5.4), that the spinors defined by (5,5) satisfy relations (5,3).

We may now express all spinors occurring in our equations by means of the products of the second rank matrices σ_1, ϱ_1 and Σ_i. The function $f(p)$ appears now as a spinor possessing three indices β, δ, η corresponding to the three two-dimensional spinor spaces. Each of the indices takes on the values 1 and 2. Equations (4,7) represent, therefore, a set of eight equations for the eight components $f_{\beta\delta\eta}(p)$ $(\beta, \delta, \eta = 1, 2)$ of the spinor $f(p)$.

In the case $j = 0$ there occur only the spinors

$$\gamma_3^{(1)}, \gamma_4^{(1)}, \gamma_3^{(2)}, \gamma_4^{(2)}, \gamma_1^{(1)}\gamma_1^{(2)}, \gamma_2^{(1)}\gamma_2^{(2)} \tag{5,6}$$

satisfying the commutation relations

$$[\gamma_\mu^{(1)}, \gamma_\nu^{(1)}]_+ = 2\delta_{\mu\nu}$$

$$[\gamma_\mu^{(2)}, \gamma_\nu^{(2)}]_+ = 2\delta_{\mu\nu} \quad (\mu, \nu = 3, 4), \tag{5,7}$$

$$[\gamma_\mu^{(1)}\gamma_\mu^{(2)}, \gamma_\nu^{(1)}\gamma_\nu^{(2)}]_- = 0 \quad (\mu, \nu = 3, 4), \tag{5,8}$$

$$[\gamma_\mu^{(1)}\gamma_\mu^{(2)}, \gamma_\nu^{(1)}]_+ = 0$$

$$[\gamma_\mu^{(1)}\gamma_\mu^{(2)}, \gamma_\nu^{(2)}]_+ = 0 \quad (\mu = 1,2\ \nu = 3, 4) \tag{5,9}$$

To reduce the system of equations we need now only two two-dimensional spinor spaces with the Pauli matrices σ_i and Σ_i. Putting

$$\gamma_3^{(1)} = \sigma_2 = \sigma_2^p \times 1 = (\sigma_{2\alpha\beta}^p \delta_{\gamma\delta}),$$

$$\gamma_4^{(1)} = \sigma_1 = \sigma_1^p \times 1 = (\sigma_{1\alpha\beta}^p \delta_{\gamma\delta}),$$

$$\gamma_3^{(2)} = \sum_2 = 1 \times \sigma_2^p = (\delta_{\alpha\beta}\, \sigma_{2\gamma\delta}^p),$$

$$\gamma_4^{(2)} = \sum_1 = 1 \times \sigma_1^p = (\delta_{\alpha\beta}\, \sigma_{1\gamma\delta}^p),$$

$$\gamma_1^{(1)}\gamma_1^{(2)} = \gamma_2^{(1)}\gamma_2^{(2)} = \sigma_3 \sum_3 = \sigma_3^p \times \sigma_3^p = (\sigma_{3\alpha\beta}^p\, \sigma_{3\gamma\delta}^p) \tag{5,10}$$

we satisfy relations (5,7 – 9) and express at once all spinors in our equations in terms of the second rank matrices σ_i and Σ_i. We thus obtain a system of four equations for the four components $f_{\beta\delta}(p)$ $(\beta, \delta = 1,2)$ of the spinor $f(p)$.

6. *Discussion*

We did not succeed, so far, in solving equation (4,7) exactly. This seems to be very difficult, if at all possible. However, equation (4,7) offers already certain advantages as compared with the original equation (1,1) or (2,14). Due to the fact that it is an integral equation with one independent variable only, one has better possibilities of applying variational numerical methods here than with the original equations in three independent variables. In general, the fact that one obtains equations with one independent variable seems to be the main advantage of the one-time formulation over the many-time formulation of Bethe-Salpeter and Günther, which even after separation of the angular variables (cf. Günther's paper, footnote, page 329) remain equations with two independent variables.

Another advantage seems to be the possibility of applying stationary perturbation methods. E. g. in equation (4,7) we may use as the unperturbed equation the static approximation of (4,7) in Günther's case (cf. (2,10)). Putting in K_j $\varepsilon - \varepsilon' = 0$ we get

$$(\varepsilon - \bar{h}_1 - \bar{h}_2) f(p) = \mp \frac{a\Gamma}{4\pi^3} \int_0^\infty dp' p'^2\, K_j^{static}\ (p, p') f(p') \tag{6,1}$$

with $K_j^{static}(p, p')$ given by the formula (4,25), where for M_j one has to take expression (4,26) multiplied by $\varepsilon\varepsilon'$ and with $\varepsilon - \varepsilon' = 0$

$$M_k^{static}(p, p') = \int_0^\infty \frac{P_k(\cos\theta)\,\sin\theta\,d\theta}{p^2 + p'^2 - 2pp'\cos\theta} \tag{6,2}$$

If it is possible to find exact eigensolutions and eigenvalues of (6.1), one may perform the conventional perturbation calculation to find the corrections to the eigenvalues and eigenfunctions caused by retardation and, in this way, estimate the applicability of the static approximation (6.1). We hope to return to this question elsewhere.

КРАТКОЕ СОДЕРЖАНИЕ

В. Круликовский, Г. Ржевуский, *Релятивитская проблема двух тел в одновременном определении. — Разделение угловых переменных в случае одноквантового взаимодействия в электродинамике.*

Осуществлена сепарация угловых переменных в условном одновременном уравнении для проблемы двух фермионов в квантовой электродинамике. Рассчёт произведен в двигательном представлении. Получена схема шестнадцати интегральных уравнений с одной независимой переменной. Схема эта сокращается до схемы восьми уравнений для j=0 j—квантовое число полного момента быстроты), и до схемы четырёх уравнений для j=0.

REFERENCES

Günther, M., *Phys. Rev.* **88**, 1411 (1952); **94**, 1347 (1954).

Johnson, K. A., *Phys. Rev.* **101**, 448 (1956).

Królikowski, W. and Rzewuski, J., *Nouvo Cimento* **2**, 203 (1955); *Bull. Acad. Polon. Sci.* Cl. III, **3**, 353 (1955).

Królikowski, W., and Rzewuski, J. *Nuovo Cimento* **3**, 260 (1956); *Bull. Acad. Polon. Sci.* Cl. III, **4**, 19 (1956).

Matthews, P. T. and Salam, A., *Phys. Rev.* **94**, 185 (1954).

Salpeter, E. E. and Bethe, H. A., *Phys. Rev.* **84**, 1232 (1951).

Schwinger, J., *Proc. Nat. Acad. Sci. U. S.* **37**, 452 (1951).

LABORATORY EQUIPMENT AND TECHNIQUES

TWO SIDED SPARK COUNTER WITH LARGE COUNTING AREA FOR REGISTERING SLOW NEUTRONS

By. J. A. Janik and A. Szkatuła

Institute of Nuclear Research, Polish Academy of Sciences, Cracow

(Received April 20, 1956)

This paper describes a two-sided spark counter for detecting thermal neutrons. The counter has cathode area of 7.5×11 cm^2 and is covered on both sides by a coating of boron. The total length of the 0.08 mm diam. nickeline wires which form the anode of the counter is about 3 mm. From the accompanying characteristics drawn for different concentrations of CO_2 in the air forming the atmosphere of the counter, it can be seen that as the CO_2 concentration increases, the counter efficiency increases, the plateau length decreases and the slope of the characteristic increases. The conditions necessary for the stable operation of the counter are given.

1. Introduction

In recent years a new type of counter, the spark counter has been developed. This counter is particularly suitable for recording strongly ionizing particles. Since the first prototype of this counter was built by Chang and Rosenblum (1945), some constructional changes have been introduced. From these changes, three basic types of spark counters have evolved.

1) A counter consisting of a cathode in the form of a plate and an anode in the form of one or more thin wires running parallel to the cathode at exactly the same distance from it.

2) A counter consisting of two parallel plates, one of which forms the anode and the other, the cathode.

3) A counter consisting of a cylindrical cathode and a wire running along the axis of the cylinder. This type of spark counter has a design similar to G—M counters, but works at a considerably higher voltage and is characterized by a different type of discharge (Bella et al. 1948, 1949; Connor 1949, 1951, 1952; Eichholz 1952; Madansky et al. 1948, 1949; Müller at al. 1953).

Hereafter we will restrict ourselves to a description of the properties of the first of the above three types of spark counters.

As already mentioned, this counter consists of a cathode in the form of a highly polished plate and an anode in the form of one or more wires of about 0.1 mm diameter stretched parallel to the cathode at a distance of 1 to 2 mm from it. Due to the applied high voltage (of the order of several kV) a corona discharge takes place. If an alpha particle passes through the area of this corona discharge between a given wire and the cathode (in a direction more or less perpendicular to the cathode), a spark occurs.

The counter thus described is completely stable in dry air at atmospheric pressure. It was established (Payne 1949) that the addition of a small amount of carbon dioxide increases the efficiency of the alpha particle counting and even the ability to record protons and beta particles.

This type of spark counter was employed by Savel (1952a, 1952b, 1954) to record slow neutrons. This application is based on the coating of the counter cathode with a layer of amorphous boron. Czownicka and Janik (1955) designed a counter similar to Savel's. All these counters had a relatively small cathode area (about 20 cm^2) and had a number of wires, whose total length did not exceed 80 cm, stretched above one of the surfaces of the cathode and running parallel to it.

In this paper, a two-sided spark counter for recording slow neutrons will be described. This counter is distinguished by its relatively large cathode surface (about 100 cm^2) and total length of wire of about 330 cm.

2. Spark Counter Design

The design of the spark counter for recording slow neutrons is shown in Figs. 1 and 2. The basic features of its design are as follows: The cathode is a well polished aluminium plate having an area of 7.5×11 cm^2 and thickness of 5 mm and coated on both sides by a layer of amorphous boron 3 mg/cm^2 thick. For coating the cathode, a proper amount of boron was weighed out and a suspension of the boron in alcohol was prepared. A small amount (1 to 2 drops) of Canadian balsam was added to this. Then the suspension was smeared over the entire surface of the cathode with the help of a brush, an effort being made to obtain as even a coating of boron as possible. After drying, a relatively strongly adhering boron layer resulted. However, because of the dielectric properties of Canadian balsam, the preparation of the layer in this manner made it difficult to obtain a corona which was evenly distributed along the wires, and therefore, the boron surface was then coated (by spraying) with a 0.1 μ layer of metallic aluminium.

The anode of the counter was constructed from resistance wire of 0.08 mm dia. wound between two brass posts fixed in such a manner that the cathode was located in the counter between the two rows of wires. Thus a set of 22 wires faced both sides of the cathode surface; a two-sided counter was therefore obtained.

Plexiglass was used as the insulating material.

The counter was placed in a metal box fitted with two glass plates whose surface was parallel to the surface of the counter cathode. The glass plates were set on rubber

seals and high-voltage terminals were mounted on one of them. The counter was fastened to the high-voltage terminals by suitably chosen screws. The box in which the counter was placed was supplied with two metal cocks through which the box could be filled with different gases.

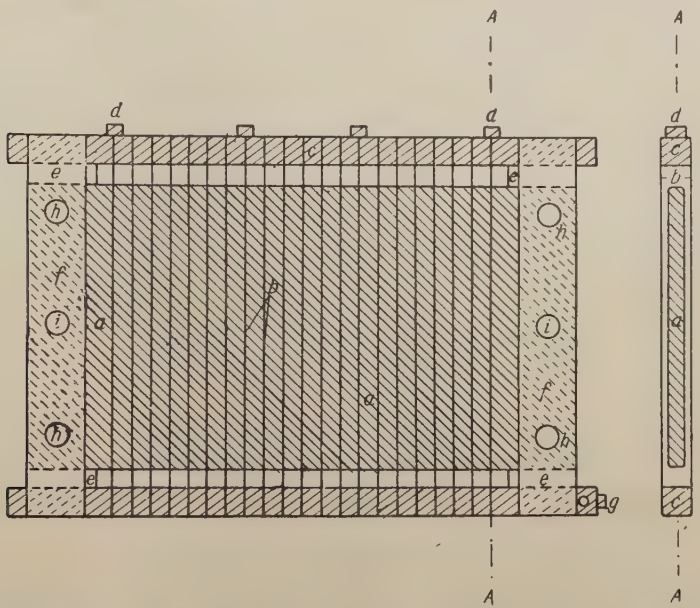

Fig. 1. Diagram of the spark counter: *a*) cathode, *b*) anode, *c*) brass frame on which the anode wires are wound, *d*) screws for holding the wires in place, *e*) plexiglass washers *f*) plexiglass slats for increasing the rigidity of the counters *g*) high-voltage input to anode *h*) screws for holding place the plexiglass slats *i*) screws for fastening the counter inside the gas-tight box described in the paper.

Fig. 2. View of the spark counter.

The following features of the counter should be noted, since they are decisive in determining the stability of operation:

a) The wires must be closely maintained parallel to the cathode surface; the wire tension must be chosen so as to prevent deflection of the wire under the influence of the electric field. *b*) The counter must be kept dust-free, and the boron grains

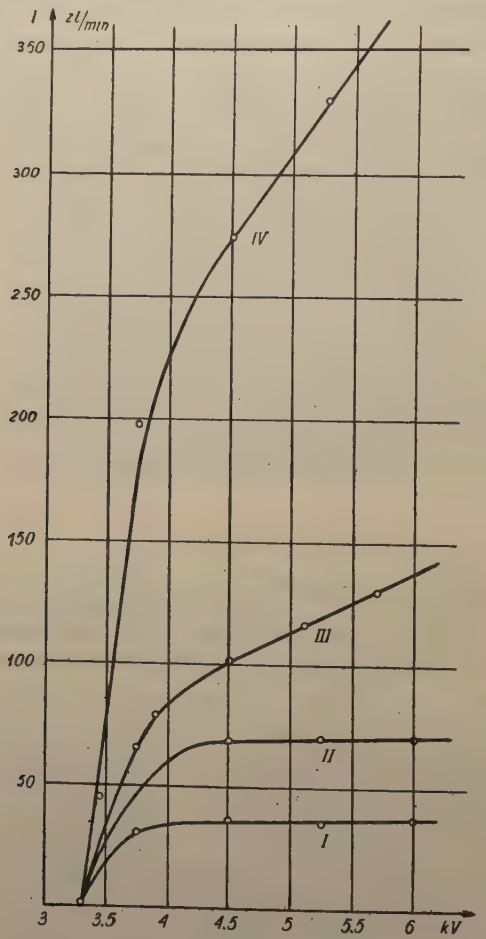

Fig. 3. Characteristics of the spark counter for various concentrations of CO_2 in air: Curve I — air under a pressure of 1 atm. with 0% CO_2; Curve II — air under a pressure of 1 atm. with 2% CO_2; Curve III — air under a pressure of 1 atm. with 3% CO_2; Curve IV — air under a pressure of 1 atm with 5% CO_2.

cleaned before spraying, etc. *c*) It is recommended that the counter be filled with air (or air mixed with CO_2) from which the moisture has been carefully removed. Traces of water vapour can prevent the operation of the counter. A well-prepared counter has a background of about 1 discharge per 6 minutes. Any inhomogeneity of the corona glow (strong glows appearing at points along one of the wires, or different

intensity of glow for individual wires) can lead to a considerable increase of background or even make the functioning of the counter impossible. If the above conditions are fulfilled, the corona will have a uniform intensity of glow on all wires. This appears to be an indispensable condition for the stable operation of the counter. Other constructional features of the counter shown in Fig. 1, but not discussed above, are designed to prevent surface discharges, facilitate the winding of the wires, and so on.

Fig. 3 shows the characteristics of the counter for different concentrations of CO_2 in the air filling the box of the counter. As can be seen, an increase in the concentration of CO_2 causes an increase in the efficiency of counting slow neutrons and, at the same time, shortens the plateau of the characteristic and increases its slope.

The counter registers 0.025% of the neutrons falling on the surface of the cathode.

This counter was used by the authors for determining the moisture of walls by using neutrons (Janik, Szkatuła 1955).

3. Electronic Equipment used with the Counter

In Fig. 4 is shown the schematic diagram of the electronic equipment used with the counter.

Fig. 5 is a photograph of the arrangement.

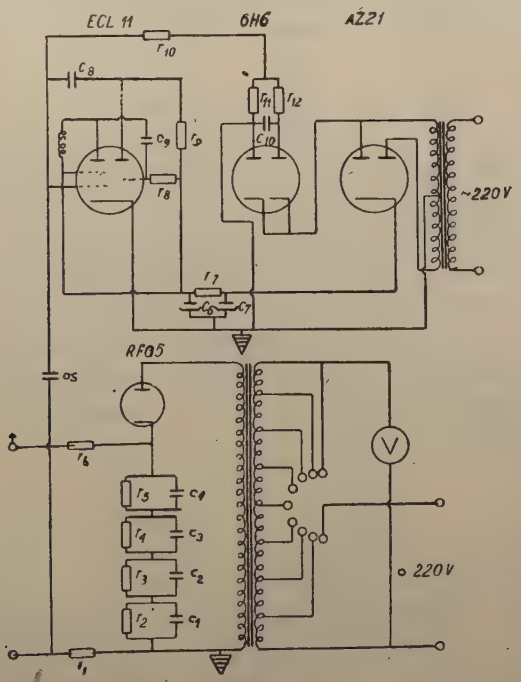

Fig. 4. Schematic diagram of electronic equipment: $r_1 = 1M$, $r_2 = r_3 = r_4 = r_5 = 2.5M$, $r_6 = 10M$, $r_7 = 600\,\Omega$, $r_8 = 1M$, $r_9 = 0.2\,M$, $r_{10} = 2M$, $r_{11} = 240K$, $r_{12} = 500K$, $C_1 = C_2 = C_3 = C_4 = 0.1\mu\,F$, $C_5 = 100\,\mu\,F$, $C_6 = C_7 = 16\,\mu F$, $C_8 = 50000\,pF$, $C_9 = 60\,pF$, $C_{10} = 1\mu F$.

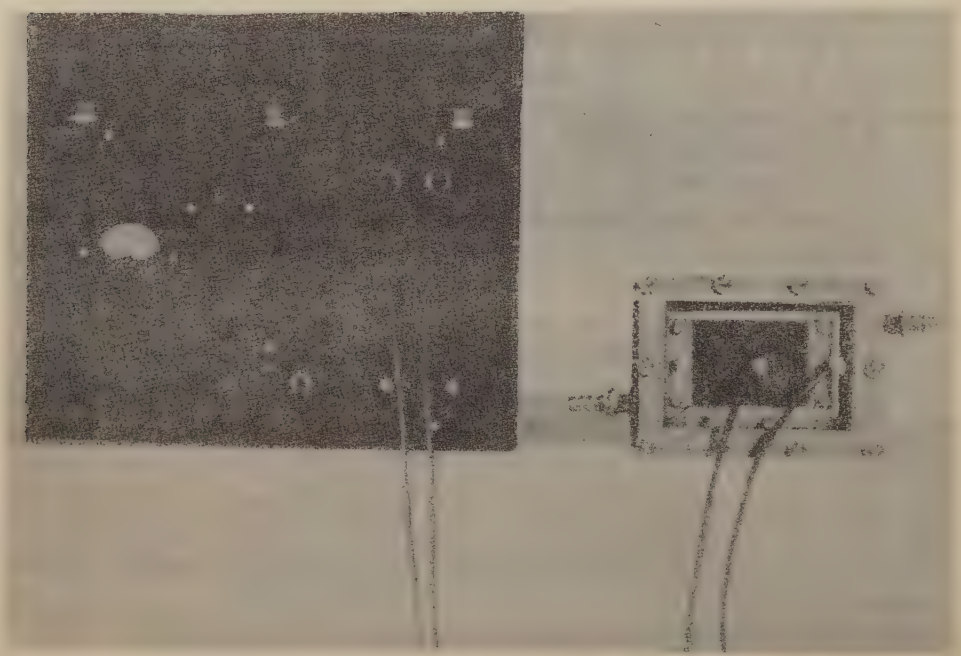

Fig. 5. View of spark counter together with electronic equipment.

4. Acknowledgment

The authors desire to express their gratitude to Professor H. Niewodniczański for his lively interest in the work connected with the designing and perfecting of the spark neutron counter as well as to A. Budzanowski for valuable discussions during course of the work. We thank F. Leś, who, employing an apparatus of his own design, sprayed the aluminium coating on the cathodes of the counters used in these experiments. We thank T. Waluga and A. Ostrowicz for the great creative skill shown during the assembly of the electronic equipment used with the counter. We also thank J. Bartke and S. Kraśnicki for the help given in determining the counter characteristics for various concentrations of CO_2 in air.

КРАТКОЕ СОДЕРЖАНИЕ

Г. Яник и А. Шкатула, *Двухсторонний искровый счётчик, с большой считающей поверхностью, для регистрации медленных нейтронов.*

В настоящей работе описан двухсторонний искровый счётчик для детектирования термических нейтронов с поверхностью катодов 7.5×11 cm_2, покрытой с обеих сторон слоем бора. Совокупная длина никелиновых проволок калибра 9,08 *m.*, составляющих анод счётчика, равняется около 3 метрам. Из приложенных характеристик, совершённых при разных концентрациях CO_2 в воздухе, составляющем атмосферу счёчика, видно, что, по мере возрастания концентрации CO_2, возрастает и эффективность счётчика, уменьшается однако длина плато́ и растёт наклон характеристики. В труде даны условия стабильной работы счётчика.

REFERENCES

Bella, F., Francinetti, C., *a) Nuovo Cimento* — **IX 10,** 1335 (1953) *b)* 1338 (1953); *c)* 1461 (1953).

Chang, W. Y. & Rosenblum, S., *Phys. Rev.* **67,** 222 (1945).

Connor, R. D., *a) Nature* **163,** 540 (1949; *b) Proc. Phys. Soc.* **B 64,** 30 (1951); *c) J. Sci. Instr.* **29,** 12 (1952).

Czownicka, A. & Janik, J. A., Zeszyty Naukowe Uniwersytetu Jagiellońskiego, Zeszyt 2 (1956)

Eichholz, G. C., *Nucleonics* **10,** 46 (1952).

Janik, J. & Szkatuła, A., *Inżynieria i Budownictwo* **12,** 349 (1955)

Madansky, L. & Pidd, R. W., *a) Phys. Rev.* **73,** 1250 (1948); *b)* **75,** 1175 (1949), *c) Rev. Sci. Instr.* **21,** 407 (1950).

Payne, R. M., *J. Sci. Instr.* **26,** 321 (1949)

Savel, P., *a) C. R.* **234,** 2596 (1952); *b)* **235,** 156 (1952); *c) J. Phys. Radium* **15,** 113 A (1954).

LETTERS TO THE EDITOR

SLOW NEUTRON DETECTION IN PRESENCE OF GAMMA RADIATION

By Tadeusz Domański

Institute of Nuclear Research of the Polish Academy of Sciences, Warsaw

(Received June 5, 1956)

I present a gamma-insensitive detector of slow neutrons consisting of: scintillator, 931—A type photomultiplier tube, amplifier and discriminator. Although this type of photomultiplier is disadvantageous in scintillation counting it had to be used for reasons of availability.

The scintillator consists of ZnS(Ag) used in form of a thin layer deposited on the glass bulb of the tube. The ZnS(Ag) layer is covered with a natural boron layer. The luminescence time of this luminophor amounts to a few microseconds.

The scintillations engendered by alpha particles from B 10 produce large electrical pulses on the multiplier tube output. Unfortunately, pulses produced in the tube itself by a strong gamma radiation are of the same order of magnitude. Gamma rays do not produce appreciable scintillations in the ZnS(Ag) layer but they expell electrons from the photocathode and the dynodes.

There is, however, a fundamental difference between both kinds of electrical pulses as the pulse duration is large for scintillation pulses and short for gamma pulses. In order to separate these two kinds of pulses a Miller integrator circuit followed by a simple amplitude discriminator was introduced in the discriminator stage. In this way gamma-ray background can be practically eliminated. The efficiency of this detector is close to 1%.

ROLE OF TRANSVERSE MAGNETIC FIELDS IN THE ELECTRODELESS GAS DISCHARGE AND IN THE JOSHI EFFECT

By S. R. Mohanty and T. R. Bhat

Physico-Chemical Laboratories Banaras Hindu University INDIA

(Received June 12, 1956)

The Joshi effect (Joshi 1943, 1945), *viz.*, the instantaneous and reversible photo-variation (mainly diminution — Δi and, under definite experimental conditions, enhancement + Δi) of the current i of the gas discharge, is of fundamental importance for theories of the behaviour of electrically excited media and the influence thereon of irradiation. It is observed in numerous gases and vapours, elemental and compound, over a wide range of the operative conditions, *e.g.*, the exciting potential V (and the attendent electric field E) (Mohanty, Jayaraman and Krishna Rao 1954), the gas pressure (Mohanty and Kamath 1948), etc., and is apparently a general property of the

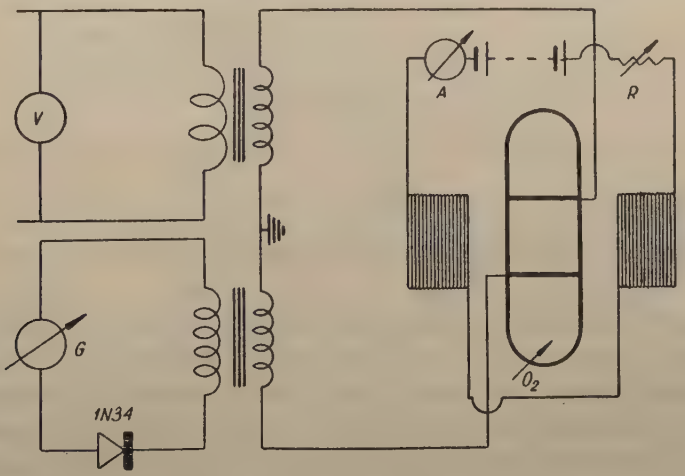

Fig. 1. Role of Transverse Magnetic Fields in the Electrodeless Gas Discharge

discharge phenomenon (Mohanty 1955). A transverse magnetic field H modifies electronic/ionic paths under E (Thomson and Thomson 1933, Townsend 1947). It was of interest therefore, to investigate in some detail the role of H in the electrodeless gas discharge and in the production of $\pm \Delta i$.

The electrical discharge was produced in a chemically cleaned soda glass tube (outer diam., 7.27 mm; inner diam., 5.57 mm) filled with pure oxygen at 26 mm Hg (26°C). Two external rings of untarnished copper foil (each 0.5 mm wide) separated through 2.8 cm constituted the electrodes. The gas was excited over 2–4 kV (rms) of 50 c/s frequency. The *effect* $\pm \Delta i$ ($= i_L - i_D$, where i_L and i_D are the values of i

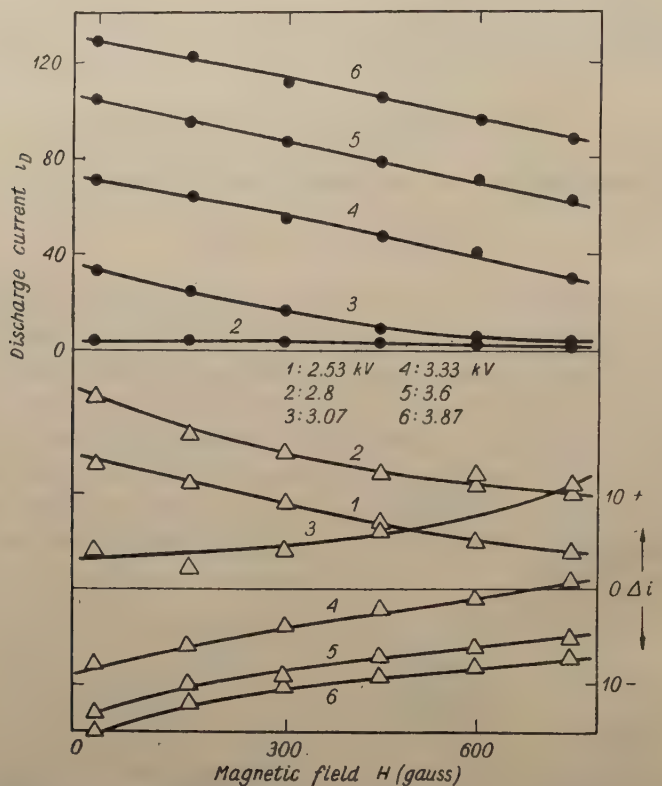

Fig. 2. Variation of the Discharge Current and the Joshi Effect with the Transverse Magnetic Field

under light and in dark respectively) was observed on a crystal (1N34, Sylvania) — galvanometer (G) system (Fig. 1) with light (3700 – 7800Å) from a 300 watt, 200 volt tungsten filament lamp placed at a distance of 26 cm from the discharge tube; heat radiations from the lamp were cut off with an appropriate filter. Magnetic fields H (0–750 gauss) of desired strengths were obtained by passing suitable currents through a solenoid consisting of 600 turns of enamelled copper wire (B. S. G. 24) per cm on a uniform glass tube (diam., 4 cm). The solenoid was branched into two equal parts, each on either side of the discharge tube, such that the produced H was at right angles to the normal electronic/ionic paths under E.

It is seen from Fig. 2 that i decreases progressively with H. Thus *e.g.*, i_D at 3.6 kV decreased from 104 to 62 for an increase in H from zero to 750 gauss. The threshold

potential V_m of the self-maintained discharge, characterized by a sudden increase in i (Fig. 3), on the other hand, is increased linearly (inset, Fig. 3), from 2.89 kV at $H = 0$ to 3.13 kV at 750 gauss.

The positive *effect* $+ \Delta i$ is small at low applied V and increases initially *ceteris paribus* with V (Fig. 4) to a maximum at $V_{+\Delta i \max}$. Above $V_{+\Delta i \max}$, $+ \Delta i$

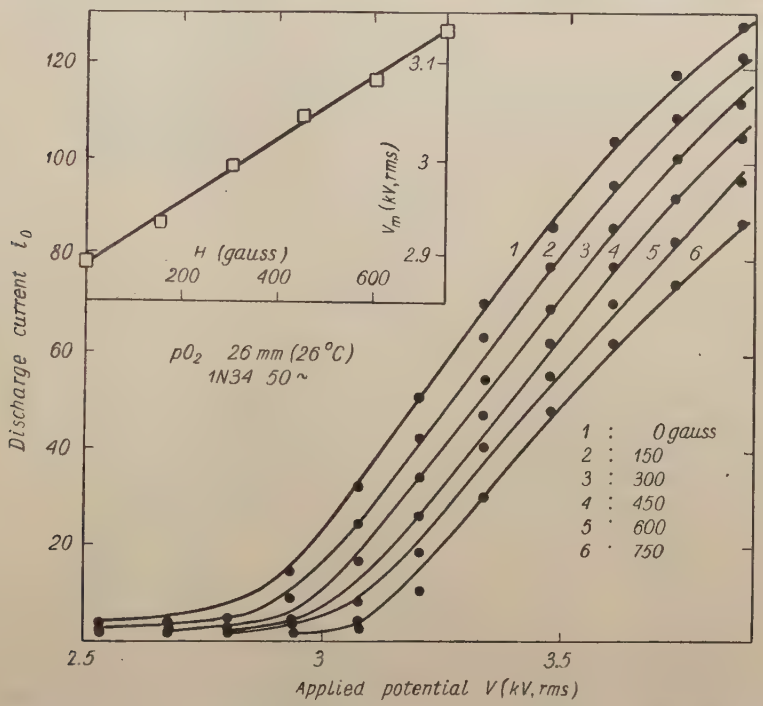

Fig. 3. The Breakdown Threshold Potential as a Function of the Transverse Magnetic Field

diminishes rapidly and changes sign (to the negative *effect* $- \Delta i$) at an inversion potential V_i^I. Beyond V_i^I, $- \Delta i$ increases with V in the range investigated. Whilst $+ \Delta i$ at $V < V_{+\Delta i \max}$ diminishes with H, that in the region $V_{+\Delta i \max} - V_i^I$ increases (Fig. 2). Furthermore, the maximum $+ \Delta i$ is smaller the higher the H (Fig. 4). Thus, $V_{+\Delta i \max}$ and V_i^I values for the tube ($H = 0$) were 2.75 and 3.11 kV respectively. At 2.53 kV, $+ \Delta i$ was 13 for zero, and diminished to 4 for 750 gauss. At 3.07 kV, on the other hand, $+ \Delta i$ values were 4, 6 and 10 for $H = 0$, 450 and 750 gauss respectively. The negative *effect* $- \Delta i$ at $V \geqslant V_i^I$ diminishes with, and inverts at higher, H. At higher V, $- \Delta i$ diminishes progressively, *e.g.*, at 3.6 kV, from 13 to 5 over 0 – 750 gauss. The potentials $V_{+\Delta i \max}$ and V_i^I are enhanced under H (Fig. 4), the former from 2.75 to 2.85 kV and the latter from 3.11 to 3.44 kV, in the range investigated.

For occurrence of $\pm \Delta i$, Joshi (1946, 1947a, 1947b) postulates that (1) an adsorption-like electrode layer consisting of electrons, ions and excited particles is formed

under discharge; (2) light releases electrons from this layer; (3) negative ion formation due to capture of the photoelectrons by excited neutral particles reduces i to give $-\Delta i$, mainly as a space charge effect; and (4) uncaptured photoelectrons, and their secondaries produced under E if appropriate, cause $+\Delta i$. The effect of H is to produce a drift of electrons/ions at right angles to both H and E. Consequently, the

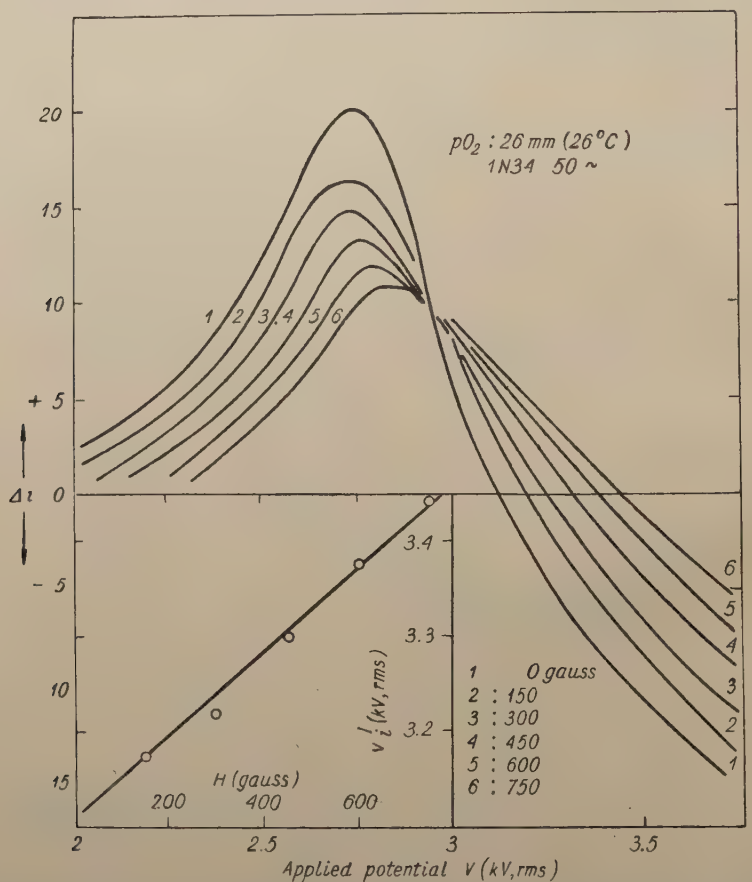

Fig. 4. Influence of Transverse Magnetic Fields on the Potential Dependence and Inversion of the Joshi Effect

removal of electrons by diffusion and wall recombination is accentuated (Loeb 1939). The observed diminution in i, as also in $\pm \Delta i$, with increase in H follows. In consequence of the electron/ion drift, an electric field E' is set up opposite to the original E. The observed diminution of $+\Delta i$ below $V_{+\Delta i\ \max}$, its enhancement in the range $V_{+\Delta i\ \max} - V_i^I$ and the diminution of $-\Delta i$ follow, as also the augmentation in V_m and V_i^I.

Grateful thanks of the authors are due to Professor S.S. Joshi for his kind interest in the work.

REFERENCES

Joshi, S. S., *Proc. Indian Sci. Congr., Chem. Sec.*, Presidential Address (1943); *Proc. Indian Acad. Sci.*, **A22,** 389 (1945); *Proc. Indian Sci. Congr., Phys. Sec.*, Part III, Abstr. 26 (1946), Abstr. 25 (1947a); *Current Sci.*, **16,** 19 (1947b).

Loeb L. B., *Fundamental Processes of Electrical Discharge in Gases*, John Wiley and Sons, Inc., New York (1939).

Mohanty S. R., *J. Chem. Phys.*, **23,** 1533 (1955).

Mohanty S. R., Jayaraman J. and Krishna Rao G. V. G., *J. Phys. Soc. Japan*, **9,** 576 (1954).

Mohanty S. R., and Kamath G. S., *J. Indian Chem. Soc.*, **25,** 405 (1948).

Thomson J. J. and Thomson G. P., *Conduction of Electricity through Gases*, Cambridge University Press, Cambridge, Vol. II (1933).

Townsend J. S. E., *Electrons in Gases*, Hutchinson's Scientific and Technical Publications, London (1947).

ERRATA

Acta Physica Polonica, **14**, 135 (1954):

Disintegration of the ^{9}Be Nucleus in Coulomb Field by J. Sawicki

Recently W. Czyż (Phys. Rev., **102**, 1185 (1956)) has noticed that Guth and Mullin (Phys. Rev., **76**, 254 (1949)) erroneously omitted the interference terms coming from the different $P \to S$ and $P \to D$ transitions in the ^{9}Be (γ, n) angular distribution. Here the interference terms in the angular distribution were also omitted after Guth and Mullin.

On including these terms the following corrections should be made: Eq. (13), p. 138, should read

$$| I_r (P \to D) |^2 f_{PD} (\Omega_r) = \frac{k^2}{9^3} \frac{1}{4\pi} (1 + 3 \cos^2 \hat{\gamma}) \; | R_{PD} |^2 \tag{13}$$

Eq. (17), p. 140, should read

$$d\sigma' = Z^2 \frac{e^4}{\hbar^2 v^2} \frac{32}{729} \left[(| R_{PS} |^2 + | R_{PD} |^2 + 2 R_{PS} R_{PD} \cos (\delta_2 - \delta_0)) \ln \Gamma + \right.$$

$$\left. + 3 \left(\frac{1}{2} | R_{PD} |^2 - R_{PS} R_{PD} \cos (\delta_2 - \delta_0) \right) \left(\frac{1}{2} (3 \cos^2 \theta_r - 1) (1 - \Gamma^{-2}) + \sin^2 \theta_r \ln \Gamma \right) \right] \tag{17}$$

Since the interference terms vanish after integration over Ω_{r_r} the cross-section $= d\sigma/dE_r$ (Eq. (18)) remains unchanged.

Acta Physica Polonica, **15**, 49 (1956):

Generalization of the Method of Supplementary Variables to Systems Composed of two Kinds of Particles by Z. Galasiewicz

On page 55 line 5, the expresion $\frac{4\pi e^2 N_1}{m}$ should read $\sqrt{\frac{4\pi e^2 N_1}{m}}$

„ 55 „ 6, „ „ $\frac{4\pi Z^2 e^2 N_2}{M}$ „ „ $\sqrt{\frac{4\pi Z^2 e^2 N_2}{M}}$

„ 56 „ 5 from the bottom „ (formula 34) $e^{-i(k_1+k_2)r_j}$ „ „ $e^{i(k_1+k_2)r_j}$

„ 59 line 9 from the bottom „ $-ih \frac{\partial}{\partial Q_k} (Q_k^{(i)})$ „ „ $-ih \frac{\partial}{\partial Q_k^{(i)}}$

„ 60 line 3 (formula 54) „ $\frac{e^2 N_1}{2m} \sum_{k,k \leqslant k_0} (k^2 P_k^{(1)} P_{-k...}^{(1)})$ „ „ $\sum_{k,k \leqslant k_0} \left(\frac{e^2 N_1}{2m} k^2 P_k^{(1)} P_{-k...}^{(1)} \right)$

„ line 4 „ $\frac{Z^2 e^2 N_2}{2M} \sum_{k,k \leqslant k_0} (k^2 P_k^{(2)} P_{-k...}^{(2)})$ „ „ $\sum_{k,k \leqslant k_0} \left(\frac{Z^2 e^2 N_2}{2M} k^2 P_k^{(2)} P_{-k...}^{(2)} \right)$

Volumen XV (1956) — Fasciculus 5

Laboratory equipment

Letters to the Editor